

COMPETITIVE MOLECULAR-ADSORPTION
ON ACTIVATED CARBON

BY

ROBERT HAROLD SPENCE

A DISSERTATION PRESENTED TO THE GRADUATE SCHOOL
OF THE UNIVERSITY OF FLORIDA
IN PARTIAL FULFILLMENT OF THE REQUIREMENTS FOR
THE DEGREE OF DOCTOR OF PHILOSOPHY

UNIVERSITY OF FLORIDA

1961

This work is dedicated to my wife, Regina. Our dreams could never have become a reality without you. You never doubted me or lost confidence in me, even when I lost confidence in myself. You gave steadfastness of yourself to accommodate my every whim, mood, and desire. You pushed me when I needed to be pushed and pulled me on the back when I needed that, too. You spent many hours visiting laboratory glassware and keeping me company through the many long nights in the lab. You spent long hours learning and performing lab assignments to free me to do other work. You found the time, usually late at night, to type my drafts. You helped me with many time-consuming tedious calculations. You were always there for me. There could never be adequate recompense for you for the minutes, the frustrations, the sufferings, and sacrifices you endured over the last three years. I can only begin by saying thank you for your unending patience, for always being there when I needed you, and for your love.

Acknowledgements

The word "acknowledgments" does not begin to repay the contributions made by those who have shared the high and low points with us during the past few years:

My advisor, Dr. John Lisch, who took me under his wing after the untimely death of my original advisor. Thank you for your constant motivation, your sage advice, your concern for us both professionally and personally, your confidence, your support of my laboratory work, and your friendship.

Dr. Joseph Gelfand, thank you for your excellence in teaching, your timely given support during my earlytime struggles, and your openness to students.

Dr. LARRY MILLER, thank you for your constant spiritual and moral support.

Dr. Benjamin Hopson and Dr. Dennis Wahl, thank you for your encouragement and interest in us as a student.

To Ann Hill, my graphic artist, thank you for your patient and generous support and especially for sharing your home with us.

To Don Chiriac, thank you for help with my computer problems and for your willingness to give of yourself.

To Joe Nagley, Lisa Brinkman, Boris Topp, John Hsieh, Rong Li Liu, Hu Liang, Chun Yiu Liu, Chang Yiu Kiu, and Rich Horton, thanks for many good conversations and friendship.

To Barbara Baroque, who converted my drafts to the final product. Thank you for your long and unconventional hours to accommodate my time schedule and for your confident support.

Finally, to my parents. Thank you for your many years of hard work and sacrifices to give us the tools to become what I am. Thank you for your unwavering confidence, your boundless love, and for always being there.

TABLE OF CONTENTS

ACKNOWLEDGMENTS	1440
LIST OF TABLES	1793
LIST OF FIGURES	18
ABSTRACT	85
COPYING	
1 INTRODUCTION	3
2 LITERATURE REVIEW	6
2.1 Introduction	8
2.2 The Nature of Adsorption	7
2.3 The Nature and Characterization of Adsorbed Gases	14
2.4 Effects of Adsorbate Properties on Adsorbed Gas Adsorption	48
2.5 Effects of Adsorbent Solvent System Properties on Adsorption	53
2.6 Descriptive Single-Stage Equilibrium Models	63
2.7 Approaches to Predictive Single-Stage Equilibrium Models	73
2.8 Multivariate Equilibrium Models	81
3 RESEARCH OBJECTIVES	102
4 MATERIALS AND METHODS	104
4.1 Adsorbent	106
4.2 Adsorbates	106
4.3 Equipment	109
4.4 Adsorbent Solubilities	130
4.5 Sample-weight Determination	131
4.6 Single-stage Adsorption	134
4.7 Analytical Procedures for Single-Stage Adsorption	134
4.8 Multivariate Adsorption Studies	134

4	RESULTS AND DISCUSSION.....	189
4.1	Single-solute Adsorption Studies.....	189
4.2	Single-solute Desorption Studies.....	192
4.3	Competition Adsorption.....	199
4.4	Sequential Solute Addition.....	201
5	SUMMARY AND CONCLUSIONS.....	199
7	ENGINEERING SIGNIFICANCE.....	191
APPENDICES		
A	SINGLE SOLUTE DESCRIPTION, ADSORPTION, AND SOLUBILITY DATA.....	194
B	SEQUENTIAL AND SIMULTANEOUS SOLUTE ADSORPTION DATA FOR THE D-CRESOL-PAHED, PHEHOL SOLUTE PAIR.....	197
C	SEQUENTIAL AND SIMULTANEOUS SOLUTE ADSORPTION DATA FOR 2,4-DICHLOROBIPHENYL- PHEHOL (OCP1/KLVL) PHEHOL SOLUTE PAIR....	199
D	SEQUENTIAL AND SIMULTANEOUS SOLUTE ADSORPTION DATA FOR D-CRESOL/2,4-DICHLOROT- NITROBIPHENYL (DAP) SOLUTE PAIR.....	199
E	MULTI-SOLUTE SIMULTANEOUS ADSORPTION DATA..	199
REFERENCES.....		200
BIBLIOGRAPHIC NOTES.....		204

W **B** **T**

TABLE		PAGE
I-1	Pore volumes and surface areas for various pore size distributions for one activated carbon ISO, DFO.....	179
I-2	New materials that have been used as porous activated carbons.....	186
I-3	Characterization of 12 x 80 mesh Calgon F.Diamond 100 granular activated carbon.....	189
I-4	Physical and chemical properties of organic compounds studied.....	197
I-5	Densimetric and concentration ranges for single-solute UV analysis.....	199
I-6	Method for sequential solute addition; Compound A is followed by compound B....	199
I-7	Comparison of Freundlich and Langmuir adsorption isotherm equations for single-solute studies.....	197
I-8	Experimental reliability data.....	196
I-9	Kelley-Kelly's adsorption irreversibility.....	199
I-10	Bidirectional addition equilibrium data for ALP/DFO solvent pair.....	199
I-11	Synthesonous addition equilibrium data for ALP/DFO solvent pairs.....	199
I-12	Simultaneous adding equilibrium data for OCHA solvent pairs.....	199
I-13	FREUNDLICH AND measured solid-phase equilibrium values for simultaneous additions of ALP/DFO solvent pairs.....	199

5-5a	Predicted and measured solid-phase equilibrium values for simultaneous addition of ALP/DMF solute pair (continued)	108
5-5	Predicted and measured solid-phase equilibrium values for simultaneous addition of ox/DMF solute pair (continued)	109
5-10	Competition tests for the liganded simplified IAS model (continued)	110
5-11	Multi-solute simultaneous addition equilibrium data and predicted values	120
5-12	Irreversible adsorption for binary systems at differing equilibrium concentrations versus $\log C^0/\text{mg/L}$. All values in mg/g .	126

LIST OF FIGURES

FIGURE	PAGE
1-1 Acidic oxygen surface functional groups.	18
1-2 Basic oxygen surface functional groups...	18
4-1 IR absorbance wavelength scan for aromatic...	118
4-2 IR absorbance wavelength scan for allyl phenyl...	119
4-3 IR absorbance wavelength for 2,4-dihydroxyacetophenone...	120
4-4 IR absorbance wavelength scan for orthogonol...	122
4-5 Schematic diagram of continuous flow carbon contact column system...	125
5-1 Single-solute adsorption isotherms for o-NITROL...	128
5-2 Single-solute adsorption isotherms for allyl phenol...	129
5-3 Single-solute adsorption isotherms for 2,4-dihydroxyacetophenone...	130
5-4 Single-solute adsorption isotherms for orthogonol...	141
5-5 Single-solute adsorption isotherms for all four solutes using 100 mesh carbon...	142
5-6 Single-solute adsorption isotherms for all four solutes using 120 & 150 mesh carbon...	143
5-7 Single-solute adsorption and desorption isotherms for o-NITROL...	144

3-4	Basic isolate absorption and Winklerian analysis for allpl. phase. (continued)	121
3-5	Correlation between the viability factor and the competition factor, $r_{j(1)(1)}$	122
3-6	Correlation between the viability factor and the competition factor, $r_{j(1)(2)}$	124

Abstract of Dissertation Presented to the Graduate School
of the University of Florida in Partial Fulfillment
of the Requirements for the Degree of
Doctor of Philosophy

COMPETITIVE SOLID-SOLUTE ADSORPTION
ON ACTIVATED CARBON

by

Robert Stanley Ryanak

December 1985

Chairman: John Sedick, Jr.
Major Department: Environmental Engineering Sciences

Fundamental to the successful development and use of dynamic, multi-solute sorption models is an accurate solid-solute equilibrium model. Current models often fail to adequately describe experimental data. Interest in describing and predicting the adsorption of specific organic solutes from dilute aqueous solutions has led to the need to better understand molecular mechanisms affecting adsorption. An experimental program was conducted to examine the effects of unequal competition and irreversible adsorption in bimolecular and solid-solute systems. Carbon particles were significantly affected under single-solute adsorption conditions, which are the most sensitive component of any multi-solute equilibrium model.

Single-solute systems indicated substantial irreversible adsorption for all four of the organic solutes studied. Unequal competition for adsorption sites due to carbon surface heterogeneity and solute affinity for carbon was observed in all binary combinations studied. Equilibrium irreversibility adsorption was also observed. The application of several current multi-solute equilibrium models failed to provide an accurate description of the data. A recently improved, simplified ideal adsorbed solution (IAS) theory model was superior to all other models tested when used with the unequal competition modification. The model is predicated through correlations between solute adsorption and competition factors. The model has not been expanded beyond binary systems. Much more work is needed to test, validate, and expand this improved model to account for unequal competition and irreversible adsorption in the ultimate design process.

CHAPTER I INTRODUCTION

The surface and ground water resources of today's industrialized societies were once a reliable source of supply for domestic and agricultural consumption. Ground water supplies were consistently of good quality and free of infectious contaminants that would threaten man's health. The large industrial expansion and rapid growth societies have experienced in the last 50 years have seen a concomitant increase in the variety and volume of chemicals manufactured, used, and disposed of in the environment. Many of these new chemicals were refractory and also capable of producing adverse health effects in man. A large number of these chemicals have exhibited toxic, carcinogenic, mutagenic, or teratogenic properties. Lack of awareness has resulted in the casual disposal of these chemicals into soil and water resources, often through industrial and municipal wastewater streams.

As knowledge of the potential adverse health effects of the chemicals grew, concern over uncontrolled exposure through water supplies also grew. National concern, reflected in a proliferation of federal, state, and local legislation, developed when improved analytical techniques

revealed the presence of numerous n. toxic chemicals in water supplies throughout the country. A list of hundreds of potentially hazardous compounds was promulgated by the Environmental Protection Agency (EPA). The EPA also placed maximum allowable limits on their concentrations in drinking waters and wastewaters.

Activated carbon adsorption has emerged as one of the most effective and dependable treatment technologies united to the task of removing the broad spectrum of dissolved organic compounds from waters and wastewaters. Empirical research has generally demonstrated the advantages and limitations of the many variations of applied adsorption technology. The broad applicability of activated carbon adsorption was most recently emphasized when numerous over-refinement was given to existing granular activated carbon treatment technology as a central strategy for organic precursors in trihalomethane formation.

The rapid development in empirical applications of activated carbon technology was not accompanied by a similar growth in understanding the fundamental principles underlying the technology. This imbalance is readily noticed in the design approach for activated carbon systems. Laboratory experimentation followed by laboratory pilot-scale testing prior to full-scale design is the norm for every activated carbon application in water and wastewater treatment. Little is known of the forces and mechanisms of

adsorption of organic compounds from aqueous solution by activated carbon.

National approaches to carbon system design have only just begun to emerge. Simple descriptive models for single-solid equilibrium adsorption systems have been developed. Some have a solid theoretical basis, and others are empirically formed. elucidation of the structure and nature of the activated carbon surface has begun but is incomplete. The interactions between solute, solvent, and adsorbent still remain to be clearly defined. A few studies of competitive adsorption in bimodal systems have resulted in descriptive, multi-solid equilibrium models. As basic knowledge of the adsorption process increased, descriptive equilibrium modeling has improved. Models are currently being studied which attempt to describe the fundamental thermodynamics of specific adsorption interactions. The crucial role played by equilibrium models lies in the development of predictive dynamic models for full-scale system design and analysis.

The ultimate goal of fundamental research into the nature of activated carbon adsorption is the development of a comprehensive, theoretically based design approach that can predict dynamic column behavior for individual solutes in the complex mixtures of the water and wastewater streams to be treated. The development of prediction models has generally been limited to simple mixtures of one or two compounds. Essential is the development of such dynamic

productive models is the inclusion of a general equilibrium positive model. Current mini-mini equilibrium models are limited by inadequate descriptions of adsorption mechanisms. The failure of existing models lies in the assumptions of equal competition and reversible adsorption. Such assumptions are based on a thermodynamically inert, homogeneous surface species. Adsorbed species is known to be heterogeneous with adsorption characteristics that vary with each chemically available species. Such assumptions have been made to simplify model development; however, progressively adsorbate and unequal competition can significantly influence final equilibrium conditions.

The consequences of surface surface heterogeneity are best observed in operating granular activated carbon adsorbents where influent and effluent concentrations usually vary considerably with time. Irreversible adsorption is especially highlighted in dynamic systems. For example, current productive models indicate that the introduction of a new solute should not compromise effluent quality. The new solute should be safely adsorbed with no detectable trace in the effluent. However, if significant irreversible adsorption had occurred with previous solutes, then the new compound would pass right through the adsorbent much quicker than predicted. Consequently, the usefulness of existing models to account for surface surface heterogeneity should improve predictive accuracy. This research was directed at

examining competitive and irreversible adoption in order to increase fundamental understanding of the adoption process, compare existing social performance, and test a model explicitly qualified to include staged competition.

CHAPTER 3 LITERATURE REVIEW

3-1. Introduction

The literature addressing adsorption and its application to the removal of organic solutes from aqueous systems by activated carbon is widely dispersed internationally among a variety of disciplines. Sources of the literature include many diverse and occasionally unconnected technical journals, a number of books, and many theses and dissertations. No single source of information describing the state-of-the-art of activated carbon adsorption exists. Little communication is evident in the literature among scientists and engineers studying and applying carbon adsorption. Summaries of the theory of adsorption from solution can be found in several basic references (1-3). General information on adsorption of organic compounds from aqueous solutions by activated carbon is presented in several books and review articles (4-10). More specific information can be found through the extensive lists of references in the above works.

This chapter begins with a brief summary of the nature and extent of adsorption. Activated carbon as a successful adsorbent is discussed in Section 3.2. The effects of the

nature of the adsorbate and solvent on carbon adsorption are reviewed in Sections 2.4 and 2.5. Several single-solute equilibrium models are reviewed in Section 2.6, and various multi-solute equilibrium models are discussed in Section 2.7. The development of predictive, multi-solute adsorption models is the goal of many current research efforts. The creation of activated carbon adsorption as an effective, dependable technology in the removal of a wide spectrum of organic contaminants from aqueous systems has stimulated efforts to improve the ability to describe and predict adsorption in multi-solute systems. Such ability is necessary in order to improve process modeling and design.

2.1 The Science of Adsorption

Adsorption has been defined as the accumulation of substances at a surface or interface, primarily as a result of forces active at or near the boundaries of the surface (3, 14, 26). The processes resulting in the adsorption of many organic solutes from aqueous solutions by activated carbon involve complex interactions of these physical and chemical forces. Much research has been conducted in an effort to understand and describe these surface chemistry phenomena. As the chemistry of carbon adsorption is better understood, the activation processes to produce activated carbon can be modified to increase carbon adsorption capacity and specificity. Subsequently, mathematical models describing

and partitioning adsorption phenomena can be greatly improved. Ultimately, pilot and full-scale plant design procedures can then be modified to optimize the adsorption process for particular applications.

The various forces existing between a solid surface and nearby solute molecules originate in the electrostatic interactions of nuclei and electrons. The forces of adsorption can be classified into four types: physical, chemical, ion exchange, and specific adsorption. The balancing of these surface forces minimizes the free energy of the surface and results in a state of dynamic equilibrium in which a solute is concentrated on the surface of a solid phase, such as activated carbon.

Physical adsorption results from the action of van der Waals forces and classical electrostatic forces (2, 3, 11). The van der Waals forces include London dispersion and repulsion forces and are always present. Electrostatic interactions involve polarization, dipole and quadrupole interactions and are significant only when the surface is ionic or polarizable. In physical adsorption, the electron distributions of both adsorbent and adsorbate experience some distortion, but there is no exchange or sharing of electrons (10). The net adsorption force, consequently, is weak, and adsorbate molecules are not fixed to a specific site on the surface but can move laterally from site to site or readily desorb. This type of reversible adsorption is

sometimes referred to as "ideal" adsorption." The heat of adsorption is low for physical adsorption, on the order of a few hundred calories per mole of adsorbate. Physical adsorption is nonselective, can occur in monolayer or multilayer configurations, is relatively rapid and reversible, and requires little or no activation energies [1]. Specific discrimination does not occur during physical adsorption.

The London dispersion-attraction forces are relatively weak, electrostatic forces which exert a relatively long-range influence compared to the very short-range, very substantial chemical bond forces (12). London forces account for the observed general attractions between atoms and molecules that are not charged and do not possess permanent dipole or quadrupole moments. The attractive potential arises from the coupling of instantaneously induced dipoles and quadrupoles. These arise from the fact that even neutral atoms consist of systems of oscillating charges due to the presence of positive nuclei and negative electrons. London theorized a quantum mechanical perturbation of electron distribution caused by the continuous action of electrons in atoms and molecules that was exhibited as rapidly fluctuating temporary dipole and quadrupole moments (13). These fluctuating moments in solute molecules near a solid surface can affect the electron distribution in surface molecules and induce temporary dipoles and quadrupoles. The surface can also induce such moments in nearby

alone molecules as well. The attractive potential arising from dispersion forces then is the sum of dipole-dipole, dipole-quadrupole, and quadrupole-quadrupole interactions (7). Dipole-dipole interactions are dominant with short-range effects inversely proportional to the sixth power of distance. Dipole-quadrupole and quadrupole-quadrupole interactions are inversely proportional to the eighth and tenth powers of distance, respectively. The short-range repulsive force is considered to be inversely proportional to the twelfth power of distance and, consequently, becomes significant only when the electron orbitals of the surface and adsorbate molecules interpenetrate. London forces are sometimes considered long-range forces since evaporating liquids are notably preoccupied between atoms and molecules. These forces operate between polar and nonpolar molecules and covalent, metallic, and ionic solid surfaces (20).

Classical electrostatic interactions of physical adsorption are more specific than London forces (2, 7). Several different surface-adsorbate interactions are possible. If the solid surface possesses an electrical field, an attractive potential can be developed by the polarization of molecules within the field's influence. These attractive potentials depend on the surface electric field strength and the polarizability of the solute molecules. Polar molecules possessing permanent dipoles or quadrupoles moments will also interact with the surface field to an extent dependent on

the solid characterization and the magnitude of the permanent moment. The surface and adsorbate molecules are also capable of hydrogen bond donor and acceptor groups (ii). For example, hydrogen bonding by phenolic proteins with oxygen as a surface functional group on activated carbon has been offered as one adsorption mechanism (iii). However, if bonding groups on the surface or adsorbate molecule have a strong affinity for water, hydrogen bond adsorption will not be significant (iv). Competition with water will prevent close approach by solute molecules, and existence of strongly ionized groups may screen hydrogen bonding groups. Weak electrostatic attractions are not significant where the solid surface is covalent and a strong enough electrical field does not exist and cannot be induced by polar molecules. However, the surfaces of activated carbon are sufficiently heterogeneous to participate in all of the discussed interactions.

Chemisorption, or chemisorption, is a much more specific adsorption mechanism than physical adsorption. Chemisorption occurs when atoms are exchanged or shared between adsorbate molecules and the surface of the adsorbent so that chemical reaction actually occurs. Consequently, chemisorption exhibits all the characteristics of a chemical bond. These characteristics include irreversibility, substantial activation energy requirements, isolated reactions at specific sites on the adsorbent surface, and bimodality

of adsorbed species. The chemisorption bond is very short and very strong, on the order of 50 to 100 kilocalories per mole compared to the few hundred calories per mole observed in physical adsorption (1). Chemisorption exhibits specificity for electron valencies while physical adsorption does not. Chemisorption results in only monolayer adsorption. Subsequent adsorbed layers may form but result from physical adsorption forces. Physical adsorption, a thermodynamically nonexothermic process, is usually the significant adsorption type at temperatures well below 0°C. Sufficient activation energies may not be available for any appreciable chemisorption to occur. As temperature is increased, physical adsorption decreases since the free energy driving force decreases. Chemisorption, however, becomes more significant as more energy is available to overcome activation barriers, and reaction rates increase. There will be a temperature, however, beyond which chemisorption decreases, since chemisorption is also a net endothermic process. Chemisorption occurs at the energetically most favored sites with the extent of binding dependent on the strength of adhesion and activation. The covalent bond thus formed can appear as ionic character to the adsorbed molecule and the overall surface. This ionic character depends on the relative electronegativities of the bonding atoms. A dipole moment is usually formed with the more-constant electric double layer also forming at the surface

the effect of the electric double layer is to reduce the strengths of subsequently formed bonds and to impede mass transfer across the surface film to the interior sites of the carbon surface. Chemisorption since the occupation of the surface and can affect the adsorption tendency of neighboring sites. When a surface is almost completely covered, lateral interactions among adsorbed species may become important.

Ion exchange adsorption results from charged functional groups on the adsorbent surface interacting especially charged adsorbate ions. An originally neutral adsorbent may also gain a surface electrical charge by adsorption of an ionic solute molecule (8). This process may result in the release, or exchange, of a different ion which passes into solution. In exchange adsorption the adsorbent remains electroneutral or retains the original charge. Spectroscopic adsorption, or the simultaneous adsorption of a hydrated proton with adsorption of an anion, may also occur (9). Salts such as sodium or calcium, which are normally negatively charged, readily adsorb anionic dyes and surfactants (11). Sometimes ions carrying the same charge as the surface are adsorbed through van der Waals and other forces. Such ion exchange adsorption is usually independent of temperature, since surface charge varies little with temperature. Ion exchange adsorption does occur by activated carbon but

is not thought to contribute as much as carbonyl to specific adsorption to the net adsorption result.

Specific adsorption describes the result of specific interactions between adsorbate molecules and surface functional groups on the activated carbon. These specific interactions can exhibit a wide range of adsorption energies from low-energy physical adsorption to high-energy chemisorption. An example of specific adsorption is the interaction of aromatic hydroxyl and nitro-substituted compounds with activated carbon (31). Adsorption of phenolic acetates through the formation of strong donor-acceptor complexes with surface carbonyl oxygen groups, in addition to hydrogen bonding. The oxygen group donor-acceptor interaction determines the strength of the donor-acceptor complex formed. The carbonyl oxygens of the carbon surface act as electron donors, and the aromatic rings of the adsorbate molecules act as acceptors. Such an adsorption interaction exhibits reversibility, and the adsorbate molecule adsorbs in a planar orientation. Even the surface carbonyl sites are exhausted, adsorption continues by complexation with the rings of the benzene planes of the carbon structure. Nitro group substitution enhances the donor-acceptor interaction by acting as an electron withdrawing group. Enhanced adsorption has also been observed for *p*-chlorophenol and *p*-cresol on activated carbon, further demonstrating specific adsorption interactions (32).

The preceding discussion described the nature of adsorption in terms of adsorbent-adsorbate affinity. However, adsorbate-solvent interactions also greatly influence the extent of adsorption. The reduction of interfacial tension through adsorption reduces the overall interfacial free energy. Surfactants have long been known to lower interfacial tensions significantly (1, 2). The reduction of interfacial free energy results from the loss of solvent-solid interfacial area which lowers that interfacial free energy. The creation of a solvent-solid interfacial area and a solvent-surfactant interfacial area through coagulation of a surfactant on the surface of the solid results in an increase in the system interfacial energy. However, the magnitude of the increase in the system's interfacial energy is less than the magnitude of the decrease, and the net result is an overall decrease in total interfacial free energy. Such an energy balance promotes the concentration of surfactant molecules at a surface or at a interface.

The extent of adsorption is also related to the degree of hydrophobicity of the solute, expressed as solubility. Increasing hydrophobicity decreases solubility and generally increases the extent of adsorption (38). Molecules' role states that the greater the solubility, the stronger the solute-solvent bond and the smaller the extent of adsorption. This qualitative relationship generally holds true.

However, there are many exceptions. A special case of Langmuir's rule is Traube's rule which states that adsorption from an aqueous solution increases as a homologous series is extended. As a homologous series is extended, the increasing number of carbons and chain length makes the solute less soluble. The removal of more hydrophobic solutes allows more water-water bonds to reform. Commonly, the greater the solubility, the stronger the solute-solvent bond and the smaller the extent of adsorption.

A general outline of the nature of the adsorption process has been presented. These general principles apply to most adsorption systems with various adsorbents, solvents, and adsorbates. Adsorption from aqueous solution by activated carbon is just one application of this separation process. To describe the nature and extent of adsorption with activated carbon, other relevant factors must be examined, including the nature of activated carbon and the effect on adsorption of varying carbon characteristics, the nature of the solute, and the effects of the solvent, water.

2. The Nature and Characterization of Activated Carbon

2-1-1 Surface Area

Activated carbon refers to a large group of carbonaceous materials prepared in a manner to exhibit extremely

large surface areas, high degrees of porosity, and unique surface reactivities. It can be envisioned as a solid foam. Such characteristics make activated carbons an effective adsorbent for a broad spectrum of organic solutes in water and wastewater. Activated carbon has a long history of use in hundreds of separation applications which consume hundreds of millions of pounds of the material annually (12, 13). Two general classes of activated carbon include gas-adsorbent carbon and liquid-phase carbon. Gas-adsorbent carbons for chemical recovery or impurity removal are characterized by a rather homogeneous system of 4.5 to 5.5 nm (5 to 55 Å) radius micropores and surface areas exceeding 1000 m²/g (14). Liquid phase carbons, in contrast, exhibit a wide variety of surface areas, pore sizes, and pore size distributions.

The surface area of activated carbon is essentially irreversible. Commercially available carbons for water and wastewater applications have specific surface areas ranging from 400 to 1000 m²/g (15). When specific surface areas exceed 1000 m²/g, the pore sizes become too small (less than 1 nm) to effectively adsorb aqueous organic solutes (16). Surface areas are determined through a variety of methods. Adsorption of nitrogen gas described by the Brunauer, Emmett, and Teller (1944) isotherm equation has been the most common method (7, 10). The surface areas reported by carbon manufacturers are determined by the N₂ BET method (1-12%).

Carbon dioxide adsorption at 25°C as described by the Polanyi-Dubinin surface equation is thought to be a better measure of the total surface area of microporous carbonaceous reversible regularly condensed films of N_2 at very low relative vapor pressures before monolayer adsorption is complete may yield erroneously high specific surface areas (13). Other methods to measure surface area in attempts to characterize and compare activated carbons have included adsorption of phenol, *p*-nitrophenol, methylene blue, rhodamine B, eosin, and succinic acids from aqueous solutions, adsorption of stearic acid from organic solvents, retention of ethylene glycol against vacuum after wetting with the liquid, and selective adsorption from phenol-benzene and ethylene glycol-water mixtures (14). Since only that portion of surface area and pore volume which is at the point of proper size will be available for adsorption, the use of surface area measurements or pore volumes is of little value in describing the possible effectiveness of a carbon. Equal weights of carbons prepared from different raw materials by different activation methods may have the same total N_2 , H_2 , or CO_2 Polanyi-Dubinin surface areas, yet will exhibit very different adsorption behavior in the same aqueous solution of organic compounds. Other carbons with significantly different total surface areas performed equally well when treating domestic wastewaters (14). An adsorption study of dyes with molecular weights from 100 to

1978 Salama indicated that the carbon with the lower surface area performed much better than another carbon with a higher surface area (24). The granular activated carbon's specific surface area as determined by the BET method with N_2 was 550 to 1000 m^2/g (21). Since this carbon was used in adsorption experiments with simple and complex phenol ethoxylates, a better measurement of available surface area was desired. Adsorption time was selected to better represent large organic molecules, and the specific surface area measured was 24.3 m^2/g for the same granular carbon. However, when compared to a sphericalsphericalsilicate clay with a methylene blue specific surface area of 111.5 m^2/g , the granular carbon was much more effective in removing the phenol ethoxylates (27). Consequently, it is the nature of the carbon surface and not the magnitude of the surface area which determines its adsorption characteristics.

3.3.3 Pore Size and Distribution

Pore sizes and their relative distribution within a carbon particle are two of the most significant factors determining adsorption capacities and kinetics. Pores are formed during the activation process and exhibit a bimodal distribution in activated carbon (8, 25, 26, 29). Table 3-1 lists two definitions of pore size distributions and corresponding pore volumes and surface areas for one activated carbon (18, 28). Approximately 40 percent of the

TABLE 3-1: Pore Volume and Surface Areas for Various pore size distributions for ore agglomerates (20, 24)

Pore Type and Diameter (nm)		Pore Volume (cm ³ /g)	Specific Surface Area (m ² /g)
Macropore	> 10	0.12	---
Mesopore	> 2-40	0.38	---
Microspore	< 2-40-2000	0.25	---
Total		0.81	954 (0.387)
Macropore	1.0-4	0.10-0.18	1000
Transitional:	0.2-200 nm wide	0.40-0.12	20-70
Developed			
Transitional:	0.2-200 nm wide	0.7	100-100
Microspore	< 2000-1000	0.2-0.8	0.5-2

Note: 1 nm = 10 Angstrom (Å).

total pore volume consists of micropores. The specific surface area contained in the micropores usually amounts to percent of the total S_{sp} BET surface area (8, 11, 19). The pore pattern in a carbon particle is thought to be arranged such that very few micropores actually lead directly to the outer surface (8, 18). The macropores are thought to lead from the particle surface into the interior. Transitional pores then branch off from the macropores, and the micropores, in turn, branch off from the transitional pores. The consequences of this structural arrangement on adsorption capacities and rates are clear. Exclusion of compounds due to physical size limitations, reduced pore diffusion rates due to steric hindrances, van der Waals forces, and also inevitable interactions in channels approaching molecular dimensions as well as pore blockage will all significantly influence the extent of site cooperation. Most of the adsorption occurs in the micropores, unless pore sizes or blocked transitional and macropores physically exclude a molecule. Adsorption can occur on the surfaces of transitional pores, although this size range primarily serves to connect micropores with the macropores. Transitional pore adsorption is thought to contribute to the adsorption-desorption hysteresis effect which many carbons exhibit (18). Macropores simply serve as bulk fluid phase regions where solute mass transport from the bulk phase to the interior surfaces of the carbon occurs. The surface under

has been used to measure adsorption surface areas while the surface number has been used for transitional pore surface area evaluation (11).

3.3.3 CARBON STRUCTURE

The molecular and crystalline structure of activated carbon is a major factor in determining the types of surface functional groups which can exist. These surface functional groups contribute significantly to the absorption behavior of an activated carbon. Although very little work has been done on activated carbon diversity, the structure of activated carbons has been described through studies of carbon black. Chemically there appears to be no difference between the two substances, the only physical difference appears to be in internal carbon areas (14). Two review articles on activated carbon surface chemistry list the usual references for the derivation of the structure of activated carbon from studies of graphite and carbon black (12, 13). Three forms of carbon have been defined: diamond, graphite, and amorphous carbon. Amorphous carbon has been assumed microcrystalline carbon to reflect a better understanding of that substance's structure. There are several forms of microcrystalline carbon including activated carbon, carbon blacks, carbon blacks, soots, and carbon electrodes. It is the starting materials, the preparation process, the very large specific surface area, and surface

functional groups that distinguish activated carbons from other microcrystalline forms.

The development of the structural model became clear from structures of ideal graphite (8, 18, 19): carbon atoms form flat hexagonal ring structures that are joined to form a two-dimensional layer. The combination of covalent and coexistent bonds gives each carbon-carbon bond a one-third double bond character. The ideal graphite crystal is completed by the addition of an infinite system of parallel layers of these fused hexagons. The layers are high parallel and approximately 0.33 nm apart by relatively weak van der Waals forces. Microcrystalline carbon differs from graphite by consisting of small, elementary crystallites instead of homogeneous, parallel, infinite two-dimensional planes. The crystallites are composed of layers of hexagonal carbon rings, but the layers are not perfectly parallel. The planes in a microcrystallite are believed to be 2-5 nm in diameter (8, 18). Most three of these planes form the microcrystallite, giving a height of about 0.8-1.12 nm, although as many as 18 planes can be present. The planes in the microcrystallites are regularly displaced in a random manner and overlap one another irregularly. This irregular geometry is accompanied by the formation of internal vacancies within the microcrystallites that, in activated carbon, are often filled with impurities, some of which are intentionally added to catalyze the carbonization

and nucleation steps in the activation process. In addition, the microcrystallites may contain "unsequenced" carbon that participates in tetrahedral bonding between tilted layers resulting in layer cross-linkage. The edges of the microcrystallites are high energy sites where substitution sites are always present in differing amounts. These foreign atoms may bond to the edge of the crystallite to form functional groups or may actually be incorporated into the fused ring structure to form "heterocyclic" ring systems.

The microcrystallites are interconnected to form the carbon matrix by tetrahedrally bonded carbon atoms, common hexagonal ring layers, cross-linked carbon hexagons, and functional groups at the edges of the crystallites. The microcrystallites are interconnected to form two types of structures: a graphitizing or a nongraphitizing structure. A graphitizing structure is generally considered to be a soft substance formed at temperatures exceeding 1500°C. That is, at high temperatures the unsequenced (amorphous) carbon is removed by expanding the microcrystallite graphite layers both in diameter and height and orienting the larger crystallites into a more ordered, or sequenced, graphite-like parallel arrangement. A nongraphitizing carbon does not form a three-dimensional graphite structure, even at temperatures higher than 1500°C (10). This implies considerable cross-linking between microcrystallites. Such strong cross-linking is promoted by the presence of oxygen or by a

lack of hydrogen in the raw material. Activated carbon is classified as a nongraphitizing material. There are some disordered fragments of graphite formed by the burning out of nonoxidized carbon, but throughout the entire volume of material activated carbon is considered to be structurally heterogeneous with a much greater pore volume and surface area than graphitizing carbons. The heterogeneity in the physical structure of activated carbon greatly influences adsorption capacities and adsorption kinetics.

1.3.4 Surface Chemistry

Adsorptive behavior in activated carbon is determined not only by its porous, physical structure but also by the chemical nature of its surface. The composition of the carbon surface are reflected in the diversity of adsorption reaction mechanisms for organic compounds in aqueous systems. The presence of edges on the broken graphite planes shifts electron distributions in the graphite ring structures (12). As a result, sp²-hybridized electrons and permanent and temporary dipole and quadrupole moments appear, altering adsorption properties for polar or polarizable substances. The presence of heteroatom atoms in the heterocyclic ring structures also shifts adsorption properties. Chemically bonded elements on the edges of the microcrystallites, such as hydrogen and oxygen, form reactive adsorption sites. Heteroatom adsorption, both on

the surface and its microspacelike structure, significantly influences the adsorption of electrophiles and nonelectrophiles from solution. All of the variations in the chemical nature of the carbon surface are, to a great degree, attributable by the choice of raw material as well as activation conditions, especially activation temperature (12). The details of the surface chemistry of activated carbon are presented in several specific and general review articles which also contain extensive lists of references (8, 9, 13, 15, 16, 24, 28, 31-33).

Most of the carbon surface can be described by two distinct regions (32). The first region includes the planar surfaces of the microcrystallites. Each portion of the surface appears to be relatively uniform in nature and not likely to contain any attached functional groups. This homogeneity is attributed to the involvement of carbon electrons in covalent bonding with neighboring carbon atoms. The vacancies in the ring structures are expected, and primarily van der Waals forces could be responsible for weak adsorption interactions. However, interactions between the π -bonds of the planar ring structures and certain organic solutes can also result in adsorption. Such a π -bond adsorption mechanism has been suggested for the adsorption of phenol (34). The bulk of the surface area of carbon particles is found in the micropores. Since they are formed in the activation process by the removal of

interplanar, unexposed surface; none of the total particle surface area is thought to be of the planar surface type (12).

The second major type of surface area is that provided by the edges of the microcrystallites and is quite different from the planar surface area. A wide variety of functional groups and vacancies characterize this type of surface. Since carbon atoms at the edges of the basal planes are not completely surrounded by other carbon atoms, the electronic distributions are not completely balanced by σ -bond interactions, and site reactivity is much higher. These "free valences" at the edges of the microcrystallite planes readily react with, or chemisorb, oxygen, hydrogen, and, to a lesser extent, sulfur, nitrogen, and chlorine (8). The relative amounts of noncarbonaceous material in an activated carbon varies significantly depending on the raw material selected and the activation process used. Oxygen constitutes 2 to 25 percent, by weight, of activated carbon. Hydrogen is present in amounts ranging from 1 to 14 times that of oxygen, on a molar basis, for carbons containing 0.54 to 2.25 percent oxygen by weight (11). Inorganic matter, both originating in the raw material and added during the activation process, can be present in amounts up to 4 to 5 percent, by weight, of the activated carbon (13). Although much of this matter is removed after activation by various acid-washing procedures, leaving less than 1 percent

ash is the commercial product, often small amounts of ash can significantly affect adsorption processes (24).

Surface compounds formed with oxygen are the most important determinants of the carbon surface chemistry because of the high reactivity of such compounds and their significant presence, evidenced by the oxygen weight fraction of carbon. Various surface oxide groups exhibit an acid-base chemistry that determines the classification of a carbon as acidic or basic (25). Acidic carbons are defined as carbons that lower the pH of neutral or alkaline distilled water and that are relatively hydrophilic. Basic carbons raise the pH of neutral or acidic distilled water and are relatively hydrophobic (26). Oxygen is added to carbon in four principal ways (27). Oxygen can be present in the raw material, as a carbonyl oxide, for example. Oxygen can be adsorbed on the surface of carbon during the activation process or chemisorbed on the activated carbon at room temperature. Finally, treatment of activated carbon with chemical oxidizing agents can also result in oxygen chemisorption. Oxygen complexes can be removed from the carbon surface by desorbing at very high temperatures. The form of the desorbed oxygen are carbon monoxide, carbon dioxide, and water. The form of the removed oxygen can indicate the type of surface oxides that were present on the carbon (25).

Acidic surface oxides develop when the carbon is exposed to oxygen at subcritical temperatures below 618-648°C or by the action of aqueous oxidizing solutions, such as acidified potassium permanganate, nitric acid, mixtures of nitric and sulfuric acids, hypochlorous acid, sodium hypochlorite, and ammonium persulfate (28, 29, 30, 31). Some of the known acidic surface oxides include quinoxaline-type groups, cycloperoxide, carboxylic anhydride groups, phenolic hydroxyl groups, normal lactone groups, carboxyl, and five-membered lactone groups (8, 28, 32, 33, 34). Figure 2-1 illustrates some of these groups as they might appear on the edges of the microcrystalline basal planes. Carboxylic, lactone, and phenolic groups are thought to be the most common (35). Such surface oxides result in a negative surface potential for the carbon.

The specific absorption mechanisms for each type of group with various classes of organics have not been clearly defined. A few studies have examined the effect of acidic surface oxides on the adsorption of a limited number of organic solutes in simple and bimolecular systems (31, 33, 34, 40). The lack of information on the chemical surface characteristics of each carbon studied poses great difficulty in mechanism definition. Aromatic compounds, especially phenol and its derivatives, are the most commonly studied class of organics for the effect of surface oxides on adsorption. An early study with six different commercial



FIGURE 2-1. Various copolymer structures (functional groups)

oxidized carbon (11) revealed that surface oxygen surface groups tended to reduce the capacity of the carbon surfaces for adsorption of methyl yellow from aqueous solution but did not affect the adsorption of methylene blue. The behavior was attributed to electrostatic repulsion between the anionic methyl yellow and the surface oxide groups.

Subsequent studies investigated the effect of acidic surface oxides on the adsorption of phenol, nitrobenzene, and sodium benzenesulfonate (12, 14, 15). The alteration of the carbon surface by chemical treatment, especially with respect to the formation and removal of surface oxides, significantly changed the adsorptive capacity of the carbons studied. In all of the experiments oxidation strongly reduced the adsorptive capacity for all adsorbates. Reduction of the oxidized carbon slightly increased the capacity, and high temperature outgassing of the oxidized carbon restored the original capacity. Two possible explanations for the observed inhibition of adsorption were the removal of electrons from the π -electron system of the carbon by the chemisorbed oxygen and the binding of water molecules to the acidic oxide functional groups. Since phenol was thought to adsorb through interaction of its π -electron system with the π bonds of the graphitic carbon planes, removal of available electrons would reduce phenol adsorption. The adsorption of water molecules would result in the formation of complexes of associated water within the carbon pores and would

promot mass transfer of organic molecules to a large portion of the active intraparticle surface area. These, and other studies (35, 36), suggest that exchangeable and isocyan-type surface oxides reduce the adsorption of aromatics. These are the two principal types of acidic surface oxides formed by chemical reactions or by activation temperatures below 400°C. Carboxyl groups in the form of quinone and hydroquinone are formed at activation temperatures above 400°C and improve the adsorption of aromatics through the formation of an electron donor-acceptor complex with the surface exchange group. Adsorption of aromatics can also occur, however, by π -bond interaction with the rings of the basal planes (38). The adsorption of nonpolar aliphatic compounds is also hindered by acidic surface oxides (39). These hydrophobic compounds preferentially adsorb on carbon free of acidic surface oxides. Again, the formation of water complexes through hydrogen bonding with the surface oxides blocks the surface from these hydrophobic aliphatics.

Basic surface oxides are formed when a carbon surface is first freed from all surface compounds by heating in a vacuum or an inert atmosphere to 100-1000°C and then brought into contact with oxygen after being cooled to temperatures as low as -80°C (20). Activated carbons with basic surface oxides as the predominant type of oxygen functional groups are not common. Basic surface oxides may only occur 2

percent of the surface, -OH or -OH₂⁺ whereas acidic surface oxides can cover as much as 18 percent (38). Both carbons exhibit a positive surface potential (39). The structures of basic surface oxides are not well defined. Some suggested structures and mechanisms to account for observed acid adsorption are illustrated in Figure 2-2 (18, 39). The formation of carboxylic acid, when carbon with oxides bound in chromene-like structures is oxidized in the presence of a strong acid, is the only concept able to explain all the observed acid adsorption phenomena (18).

In addition to specific adsorption mechanisms, the presence of both acidic and basic surface oxides impart a polar nature to the carbon surface (38). As a result, the surface will exhibit preferential adsorption for a more polar component of a binary mixture. For example, a carbon essentially free of oxides will preferentially adsorb benzene over methanol while a carbon with acidic surface oxides will preferentially adsorb the methanol (38). With increased surface polarity pore constriction or blockage can result from the adsorption of water through hydrogen bonding. For polar solutes, the surface oxide-solute interaction is stronger than for nonpolar solutes, compensating somewhat for the extra energy needed to desorb water (34).

This brief overview of the surface chemistry of activated carbon illustrates some of the many parameters and mechanisms involved in determining the adsorptive capacity

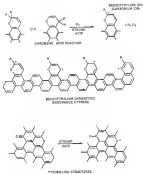


Figure 1-1: Basic copper surface functional groups

is an additional source for an organic compound. The specificity of mechanisms for certain classes of organics, the variety in type and relative abundance of surface functional groups among different carbons, and the lack of laboratory studies beyond single or bimolecular systems point out the complexity and difficulty in modeling carbon adsorption on a macro scale.

3-3-5 Particle Size

The effect of carbon particle size on adsorption capacity, especially equilibrium capacity, is not clear. Theoretically, grinding and sieving of an activated carbon to a particular size fraction should have no effect on adsorption capacity. Assuming that the carbon particle is a spherical cube, the outer surface area of the largest particle in a 1000 mesh carbon (0.04 mm x 0.0125 mm) would be 16.9 m^2 . Assuming a carbon density of 0.41 g/cm³, 1 gram of 1000 mesh carbon particles cubes would have an outer surface area of approximately 0.01 m². Grinding of this carbon to pass a 300 mesh sieve (0.054 mm) would produce a theoretical outer surface area of approximately 0.3 m². Further grinding to pass this gram of carbon through a 300 mesh sieve (0.054 mm) would result in a theoretical outer surface area of approximately 0.10 m². Compared to the 1000 m²/g surface area of a typical activated carbon, the outer surface area contributed less than 0.01 percent. Therefore,

grinding a larger mesh carbon into smaller-sized particles (100/200 mesh) should not affect total carbon surface area to any observable extent.

Several researchers have examined the effect of carbon particle size on adsorptive capacity and, for the specific carbons studied, observed little or no effect. In two separate studies a coconut-shell-based carbon exhibited no effect of carbon particle size in the adsorption of phenolic compounds for particle-size fractions ranging from 12 to 14 mesh to 100 to 120 mesh (43,44). The variation of adsorptive capacity with particle size for a coal-based carbon was examined for size fractions of mean particle diameters ranging from 0.875 to 1.501 mm (45). No effect on equilibrium capacities was observed. Other studies have produced similar results (46-47). Based on such results and theoretical considerations, a number of researchers using a particular size fraction of a ground and slanted sample have assumed that particle size did not affect carbon adsorption capacity (48-53).

Other researchers, however, have observed an increase in adsorption capacity with a decrease in carbon particle size. In one study, a coconut-shell-based carbon was crushed and slanted to produce two narrow-range particle-size fractions (54). In a second study a coconut-shell-based carbon was only slanted to produce the desired particle-size fractions and, in both studies, a significant

increase in capacity with decreasing particle size was observed (53). In both studies the times required to attain equilibrium were carefully determined. A bituminous-based carbon was studied in the development of a rapid method for determining surface adsorptive capacities (55). Carbon particle size again effected adsorption capacity for the specific carbon used. Adsorptive capacity for humic acid on a lignite-based carbon also varied with particle size (54). The recent study concluded that there was not enough information available to state with certainty that particle size will effect adsorption capacity for the carbon of interest (47).

Several phenomena have been postulated to explain the observed variations in adsorptive capacity. Available pore volume may increase as carbon particle size decreases due to the opening of previously sealed pores and channels. Pore increase in available pore volume may result in an increase in the adsorption capacity for smaller, low molecular weight solutes but may not effect the adsorptive capacity for larger, high molecular weight solutes. If blockage of large channels or constrictions is a mechanism affecting adsorptive capacity, then reducing carbon particle size by free-flowing along such channels may increase the total pore volume available to large organic molecules. It is also likely that the pore structure throughout a carbon particle is not uniform as a result of activation conditions. The

adsorption capacity can be greater in the outer regions of a carbon particle due to more extensive network of pores and channels, whereas the particle interior may consist only of a small volume of macropores and sealed channels. Grinding and sieving to achieve a particle size fraction may result in the retention of the low-capacity core and the discarding of the higher capacity outer shell. Further studies are needed to define the effect of available pore volume, pore distribution, molecular size of organic solute molecules, uniformity of activation, and pore blockage on adsorptive capacity as the diameter of a carbon particle is reduced by standard laboratory grinding and sieving techniques.

1.1.4 Manufacturing of Activated Carbon

The rapid development and use of activated carbon as an adsorbent was begun during World War I when a production unit was developed to shield soldiers from phosgene gas. Since that time the applications and varieties of activated carbons have expanded into a complex industry where many different activated carbons are available. The unique characteristics of specific surface area and surface functional groups are primarily determined by the raw material and the manufacturing, or activation, process. The importance of activation temperatures and contact with oxygen in the production process has already been mentioned. Continued improvement in raw material selection,

surface preparation, and surface activation promotes greater adsorption and more effectiveness in the removal of organics from the aqueous phase.

The selection of raw material is an important first step in manufacturing an activated carbon. Table 3-3 lists some of the raw materials that have been used in the production of activated carbon. Bituminous coal, lignite, and petroleum coke are the most common raw materials for water and wastewater treatment applications (14). The choice of raw materials determines the amount of tarry substances formed during carbonization, the subsequent development of pore structure, the amount of hydrogenation within to develop surface functional group and heterocyclic ring structures formation, and the amount of oxygen available to form surface functional groups.

The actual manufacturing process has two objectives. The first is to produce a very large surface volume ratio with a specific distribution of pore sizes. The second objective is the formation of specific types and quantities of surface functional groups. Two methods of manufacture are used. A previously charred carbonaceous substance is oxidized with steam and high temperatures, as the carbonaceous raw material is chemically delignified and modified at lower temperatures. Almost all of the activated carbon used in the United States for water and wastewater treatment applications is produced by the high

TABLE 3.2: Raw materials that have been used to produce activated carbons.

*Coal (bituminous)	Root sugar aldehydes	Graphitic material
Crack waste	Wood	Rubber
Cracked shells	Coffee beans	Waste tires
Spent	Cocoons and shells	Leather wastes
*Lignite	Gel shells	Woolen
Wood	Vegetable wastes	Pop will wastes
Waste	Fruit pits	Slack India
*Petroleum coke	Waste	Fish
Bone	Peat moss heavy oil	Coals

*Most common raw materials for water and wastewater applications.

temperature-steam process (38). The details of the process vary considerably among manufacturers with critical steps kept proprietary. The general process for manufacturing activated carbon consists of a dehydration step, a carbonization step, and an activation step. Descriptions of each step for a variety of raw materials are available in the literature (8, 18, 38).

The manufacture of granular activated carbon from a bituminous, subbituminous, or lignite coals generally is accomplished by the following operations (39): Pulverizing, screening, and crushing followed by sizing to a range of 2 to 40 mesh U.S. Standard Sieves begins the process. Dehydration is accomplished in air at temperatures ranging from 150 to 315°C for 4-5 to 18 hours. Dehydrating agents such as zinc chloride or phosphoric acid may be added. Depending on the oxygen content of the raw material, 1 to 5 percent by weight of oxygen may be added to the coal if the subsequent activation process occurs in a controlled oxygen atmosphere. Acid washing may precede the dehydration step to reduce the inorganic content of the raw material.

The second operation in the manufacturing process, carbonization, occurs in the absence of oxygen and at temperatures ranging from 450 to 850°C. Metallic chlorides can be added to increase the effectiveness of the carbonization process. During this phase, also called pyrolysis, a char suitable for steam activation is produced. Most of the

carboxylic alcohols as well as hydrogen and oxygen are removed as gases formed during this pyrolytic decomposition. Elementary microcrystallites are formed in irregular arrangements with many free interfaces that become filled or blocked by unorganized surface lamorphous from the decomposition of tarry substances. The resultant char has little adsorption capacity as a consequence.

The third essential operation, activation, determines the final characteristics of the carbon. Temperature is the most critical parameter and varies from 400 to 1600°C. The microcrystallites residues are oxidized, removing pure blocking materials. The pores are enlarged and cleaned. The microcrystallites grow and form the final rigid skeletal bone structure that determines the ultimate resistance, or breaking, of the carbon. Low-capacity carbons are partially activated by removing tarry products by heating them in a stream of inert gas or by extracting them with a solvent. High adsorption capacity carbons are activated under conditions where the activating agent (steam, carbon dioxide, or oxygen [air]) reacts with the carbon. Disordered carbon is first oxidized to open the pores between the microcrystallites. Then the crystallites themselves are partially oxidized to create a much greater pore volume. Micropores and transitional pores are formed at the expense of mesopores. A burn-off between 50 and 75 percent of the

crucial that results in the small pore structure typical of activated carbons used in water and wastewater treatment.

The activating agent reacts with the carbon at the edges of the microcrystallites to form surface functional groups. The type and density of groups are determined by activation temperatures and presence of activating agents. Since higher temperatures promote the formation of larger microcrystallite planes, some control over surface functional group density is exerted. The type and density of oxygen-containing surface functional groups are usually controlled by the temperature of the deoxygen step, which completes the activation process. The higher the temperature, the less oxygen remains on the carbon surface. As an example, activation temperatures of 400 to 800°C with low deoxygen temperatures will produce an abundance of acidic surface oxide groups which are best suited for adsorption of alkaline solutions. Activation temperatures of 800 to 1200°C and low deoxygen temperatures produce large quantities of basic surface oxides which readily adsorb acid. Deoxygen temperatures around 1800°C will remove almost all oxygen from the carbon surface producing a product suitable to remove trihalomethanes, such as chloroform, which do not adsorb well on carbons having a high density of surface oxide groups [24, 25].

Other treatments to increase surface area after activation have included deashing the carbon with hot

hydrofluoric or hydrochloric acid, burn-offs in oxygen under low oxygen partial pressures at 500°C, and exposure to steam at 18°C (21). Postactivation processes can include washing, grading, grinding, acid washing, water washing, drying, and packaging. Activated carbon is pulverized so that 95 to 100 percent pass a 100 mesh U.S. Standard Sieve (149 micron opening) and 10 to 20 percent pass a 105 mesh sieve (140 micron opening). Granular carbon is described by two sizes: one which passes the carbon and one which retains it. A typical commercial granular carbon is described as 12 x 40 mesh, where carbon would pass a 12 mesh sieve (1.48 mm) and be retained by a 40 mesh sieve (3.75 mm). Carbon is usually packaged in airtight containers to minimize oxygen adsorption and adsorption of volatile organics from the surrounding air.

3.3.9 Summary

The foregoing discussion has shown that activated carbon is a complex, highly heterogeneous adsorbent. The surface of activated carbon can be manipulated by manufacturing processes to exhibit a wide variety of adsorptive behavior. Adsorption energies can range from the very weak van der Waals physical adsorption energies to the very strong energies of the chemical bonds typical of chemisorptions. Adsorption mechanisms are also greatly affected by the physical structure of activated carbon, where pore

size distributions affect the rate and capacity of adsorption for solutes of various physical dimensions and charge characteristics. Consequently, activated carbon cannot be considered a relatively homogeneous material, with adsorption phenomena described by a few simple physical mechanisms.

3.4 Effects of Adsorbate Properties on Activated Carbon Adsorption

The effects of physical and chemical properties on the adsorption capacity for specific organic solutes in aqueous systems have been studied extensively in efforts to correlate such properties with observed adsorption behavior. The ultimate goal of such correlations was some degree of predictability in the adsorption process to improve the cost effectiveness of system design. Some adsorbate properties studied include molecular weight, functionality, polarity, hydrophobicity, dipole moment, aqueous solubility, molecular size, geometry, and surface area. Although these properties were studied individually, results indicated that few were independent of other properties in their effects on adsorption. However, all were shown to directly affect adsorption capacities under some set of well defined experimental conditions.

Adsorptive capacity was observed to increase with molecular weight in homologous series (31, 37, 38). The increase in molecular weight was due to the addition of hydrophobic complex groups to the basic molecular

MOLECULAR SIZE IS INVERSELY RELATED TO CHAIN LENGTH. As molecular weight increased in these studies, hydrophobicity increased, solubility decreased, molecular size increased, and molecular geometry and surface area changed. However, adsorption capacity studies using a series of n-alkyl-phenol ethoxylates indicated that adsorption capacity decreased with increase in molecular weight (31). The increase in molecular weight was due to the addition of ethylene oxide groups onto the n-alkyl chain. As molecular weight increased, hydrophobicity decreased while polarity, solubility, and molecular size increased. Consequently, the use of molecular weight as a predictive parameter for adsorption capacity is limited by interrelationships with other molecular properties.

Functionality has also been examined as an indicator of adsorption behavior. The addition and/or substitution of such functional groups as NH_2 , OH, CH_3OH , SO_2 , alkyl groups, and benzene rings to benzene and phenolic have been the most commonly studied functional systems (32, 33, 37-39, 40-42). Adsorption capacity for phenolic compounds increased as alkyl substituents were added to the phenol and as the alkyl chain length decreased. Polycyclic compounds adsorbed better than corresponding monocyclic compounds. The adverse effect of OH, CH_3OH , and SO_2 groups on adsorption has attributed to hydrogen bonding of these groups with water molecules rendering the species more hydrophilic. In the

enhances the introduction of the OH group enhanced, rather than hindered, adsorption even though the addition of OH resulted in an increase in aqueous solubility. The presence of neighboring CHO and OCH_3 groups was thought to result in intramolecular hydrogen bonding with the OH group. Neighboring groups, like OCH_3 , would also sterically hinder hydrogen bond formation between water and the OH group. Functionality appears to be a qualitative, rather than a quantitative, indicator of trends in adsorption capacity because of the many exceptions to the expected behavior and is not suitable as a general predictive parameter.

Polarity has also been examined as an indicator of adsorption capacities and for predicting adsorption characteristics of other organics. The dipole moment, as a measure of the polarity of a compound, exhibited no correlation with the carbon capacity for 46 organic compounds studied (31). Aniline and phenol possess the same dipole moment, yet exhibited different adsorption capacities on the same carbon. Nitrobenzene had the highest dipole moment of five organics, yet was the most favorably adsorbed. One review article described seven different polarity scales that have been used to classify organics (32). Predictability of adsorption capacities was limited to compounds of the same class as the representative compounds. Lack of knowledge concerning how each chemical in a class would react in a particular system also limits the usefulness of

non-polar,ly solutes). Again, the diversity of compounds as well as reactions involving more than just one type of base interaction do not allow any one classification scheme for organic and adaptive capabilities.

Aqueous solubility seems to provide the most widely applicable means of organic classification for adaptive purposes. All the previously described adaptive properties can be reflected in an aqueous solubility parameter. The semiquantitative Lundelius' rule described an inverse relationship between the extent of adsorption of a solute and its solubility in the solvent from which adsorption occurs (8). One interpretation postulated that the greater the solubility, the stronger the solute-solvent bond that must be broken and the smaller the extent of adsorption. The special case of Lundelius' rule is Traube's rule which relates the aqueous solubility of various organics in a homologous series inversely to the extent of adsorption (9). An investigation of 81 organic solutes representing 22 different functional groups commonly found in petrolechemical wastes showed, without exception, that as aqueous solubility decreased, adsorptive capacity increased (20). This relationship held true not only for decreasing solubility within a functional group but also for decreasing solubility between functional groups.

Further development of the solubility capacity-solubility relationship has resulted in the application of a solubility parameter, δ , to a macroscopic single solute equilibrium model for vapors in aqueous solutions (21, 43). This parameter attempts to relate the physical, chemical, and structural characteristics of neutral organic compounds as their potential to undergo a change from the liquid to a surface phase. The numerical value of the total solubility parameter consists of components which represent specific types of force interactions. The total parameter is a function of a dispersion component, the permanent dipole orientation and induced dipole component (lumped to form a polar component), and acidic and basic components (lumped to form a hydrogen bonding component). Assigning meaningful values to these components is difficult. In the study applying the total solubility parameter to the macroscopic single solute equilibrium model to calculate net adsorption energies, the dispersion, or nonpolar, component was calculated using refractive indices (43). The hydrogen bonding component was determined using aqueous solubility data. The calculation of the polar component was restricted to several homologous series and could not be calculated independently. The study reported good agreement among the four of five methods available to calculate the total solubility parameter. The calculated value was used together with values for the dispersion and hydrogen bonding

components to estimate the polar component values. This scheme of classification lacks a quantitative, theoretically justified basis and is limited by the lack of a simple method to calculate the component solubility parameters for all applications. However, the use of total solubility parameter values in the equilibrium model has resulted in correlations between amounts of compounds adsorbed by activated carbon and the calculated van der Waals adsorption energies for several organic compounds (82, 83).

The Polanyi adsorption potential theory has been applied to adsorption of organic solutes from aqueous solutions (84). A method was developed that takes as possible, given a calibrating isotherm for a specific carbon, to estimate the adsorption isotherms with that carbon for a wide variety of organic liquids from water over the adsorbate range from saturation to very low concentrations, given only their solubilities and densities. The discussion of the application of the Polanyi theory to adsorption from water solutions with activated carbon also provided a list of references describing the fundamental studies on liquid-phase adsorption onto activated carbon (85). The model assumes heterogeneity of adsorption energies over the adsorption space on surface and that any interactions between solute and solute and between different solutes in solution are reflected in their effects on solubilities. However, the solubilities that enter into the calculations for comparative adsorption

and the solubilities of each component in the presence of the other.

Absorption capacity, however, has not always correlated inversely with aqueous solubility. One study showed that the absorptive capacity for phenol on a specific carbon was the same as for benzyl alcohol and higher than that of salicylic acid, yet phenol is more soluble than either (81). Since phenol adsorbed just as well as cresol, yet has a solubility an order of magnitude less than cresol. The absorptive capacity for o-cresolphenol was greater than that for cresol or chlorophenol yet its solubility is lower. Similar observations were recorded for other organic solutes. The conclusion of the study was that no overall general tendency of increase in absorption with decrease in solubility was observed over the range of the 18 compounds studied.

Aqueous solubilities and single solute adsorption capacities have been used in kinetic systems to attempt to predict relative adsorbabilities (29, 31, 33-37). The adsorptive behavior of allyl phenols in two-component systems was better described by the Ideal Mixed Solution (18) equilibrium model than by the Langmuir model for competitive adsorption (38). The 18 model was selective and single solute isotherm constants. Another study used isotherm constants and solubilities to predict the preferentially adsorbed compound in 18 kinetic systems (39). Solubility was a successful predictive parameter for

10 out of 12 pairs tested. The Freundlich k constant, an indicator of the adsorptive capacity of a carbon for a solute, was a successful index in all 12 pairs tested. Those other adsorbate constants from the Langmuir and Freundlich models were not as successful. An improved calculation procedure for the IAS equilibrium model was used successfully in describing adsorption in binary and ternary systems containing similar and dissimilar components and mixtures containing different initial concentrations of solutes (18). However, another study showed that molecular weight was a more reliable indicator of multi-solute adsorption preferences than solubility when comparing polycyclic and aromatic compounds (19). The effect was attributed to stronger adsorptive forces due to greater surface area contact. Solubility was a reliable indicator of preference for homocyclic aromatic pairs.

There does not seem to be any one adsorbate property that is universally applicable for predicting relative single solute adsorption capacities. Table I listed considerations, adsorptive capacity generally increases with increasing molecular weight and with decreasing solubility. In multi-solute systems preferential adsorption appears to be proportional to some measure of single solute adsorption capacity, such as the Freundlich k , and to molecular weight. Such adsorption also appears to be inversely

proportional to solubility. Single active adsorption isotherm parameters have been used for attempting quantitative predictions of multi-solute adsorption while parameters describing the physical-chemical nature of the sorbent have been used qualitatively. However, the paucity of assumptions to all efforts at predicting performance and quantities of adsorption imply that no single adsorbate property is applicable for general use. The development of several useful multicomponent equilibrium models attempts to combine several of the more significant properties to improve overall predictability.

2.3 Effects of Aqueous Solution Systems Parameters on Adsorption

Aqueous system characteristics which exert influence on adsorbed carbon adsorption include temperature, pH, dissolved solids, and matrix complexity. Since adsorption is normally an endothermic process, adsorption capacity generally decreases with increasing temperature. Gas phase adsorption involves heats of adsorption on the order of several kilocalories per mole, and such systems are very temperature sensitive. However, adsorption on aqueous systems involves much smaller heats of adsorption, on the order of a few hundred calories per mole, due to the endothermic disruption of water when adsorption of a solute occurs on a carbon surface. Normal temperature variations experienced in

water and water-water adsorption processes have only a minor effect on adsorption capacities (8, 31, 32, 48, 52).

Received salts can significantly influence the adsorptive capacity of carbon for ionized organic molecules but exert little influence on neutral solutes. The adsorption of sodium benzenesulfonate was greatly increased when CaCl_2 was added to the solution (34). This was attributed to a decrease in the mutual repulsion between carboxylic acid groups through interaction with the divalent calcium ions. At pH 3.0 no significant differences in adsorptive capacity for p-nitrophenol were observed with NaCl concentrations up to 1 mole/liter. At pH 8.8 the p-nitrophenol exists solely as a neutral species. When the pH was raised to 11.8 where ionic species dominate a significant salt effect was observed at the higher NaCl concentrations (48). The explanation involved an ion pairing of the anion with the cationic p-nitrophenol, thereby reducing the electrical double layer. A second possible mechanism was a partial repulsive charge reduction between adsorbed anions by the salt. A study of the effect of phosphate buffer on 2,4-dichlorophenol and 2,4-dinitrophenol indicated no influence on adsorptive capacities for undissociated solutes, but an increase in adsorption of dissociated solutes as buffer concentration increased (49).

The effect of salts on the adsorption of ionic solids has received increasing attention as these substances have

was cited as precursor to trichloromethane formation. The concentrations of a phosphate buffer in solution had a significant effect on the adsorption of acid fulvic acids at pH 7.0 (89). Another study showed that the adsorptive capacity for dissociated dinitrophenol nearly doubled in the presence of a 0.01 M phosphate buffer (70). However, a later study demonstrated that enhanced adsorption of humic acid was due to various concentrations (sodium, magnesium, and sodium and that sodium concentrations, hydroxide, sulfide, bicarbonate, and phosphate) had little or no effect (11). All anions studied showed little additional effect on adsorption capacities beyond salt concentrations of 1 to 4 millimoles per liter. The effect of salts varied significantly with pH showing increased influence on adsorption as pH increased, confirming the effect of cations on the adsorption of dissociated fulvic acid species.

Available literature indicated that inorganic salts can influence the extent and rate of adsorption of anionic organic onto negatively charged surfaces. Two studies have attempted to define the mechanisms responsible for enhanced or hindered adsorption in the presence of salts. Specific-type mechanisms include solute-salt interactions to alter species distribution, salt-adsorbed organic interactions to alter surface packing, and salt-cation interactions to alter surface charge characteristics. Salts do not appear to significantly influence the adsorption of neutral compounds.

but few data are available. Available data are insufficient to draw general conclusions about the effects of co-ions, various salts, and salt concentrations on activated carbon adsorption of organics in aqueous solutions.

The effect of pH on adsorptive capacity has been widely studied. The two components of the adsorption mechanism thought to be affected by solution pH are the chemical characteristics of the carbon surface and the extent of molecule dissociation (11). Equilibrium capacities for sulfonated stybenzenes in pH regions far from the pH range for these compounds increased with increasing hydronium ion concentrations (12). Far from the pH range pH changes would not significantly affect the net ionic character of the adsorbing species. The increase in adsorption capacity was attributed to partial neutralization of the carbon surface's negative charge character, reducing resistance to pore diffusion. A study of the adsorption of phenol at pH's from 2.0 to 10.0 showed an unexpected reduction in adsorption capacity with decreasing pH (13). The interaction of hydronium ions with various methoxy groups competitively with phenol was postulated to explain the decreasing phenol capacity. The effect on nitrophenols was not as great and was attributed to stronger bonding energies through the phenolic acceptor-donor complex reaction. The adsorption of the hydronium ion as a competitive solute at low pH values has been supported by other work (10, 14, 15, 16).

The extent of desorption for Lollidox arises is greatly affected by pH, especially for weak organic acids like phenols. Observed changes in adsorptive capacities with pH for phenol and nitrophenols were attributed to changes in solubility (21). Adsorptive capacities for aromatic acids passed through a minimum at pH values near the pK_a points of the organic acids where both ions and molecules exist in comparable amounts in the bulk solution (22). This study also indicated that substantial amounts of ionic species were adsorbed as well as molecular species. In a study involving chloro-substituted phenols the adsorptive capacity for trichlorophenol increased substantially as pH decreased (23). Dichlorophenol adsorption was significantly less affected by pH changes. Adsorption capacity was observed to reach a maximum near $pH = pK_a$. The neutral species of both isomers adsorbed more strongly than the ionic species. The effect of pH on adsorption from a mixture of the two substituted phenols was large but could not be described by existing competitive models. Adsorption capacities for 2-methylpyridine and α -naphthol decreased as pH was lowered from 9.5 to 3.5. The effect of α -naphthol was much less than that for 2-methylpyridine. In the pH range of 4.5 to 5.5 the amount of ionic species of α -naphthol increased and of 2-methylpyridine decreased, yet adsorption capacities were unaffected. This indicated that both ionic and neutral species were adsorbed on the carbon.

The decrease in adsorptive capacity of the two compounds was attributed to competitive adsorption or spinosine loss. Substantial increases in the adsorption of fabric acid were reported as pH values decreased in a study that attributed the enhanced adsorption to a decrease in fabric acid solubility (10).

The effects of pH on adsorption capacity in aqueous solutions are not well understood. Observed pH effects depend on the nature of the surface surface, especially the functional groups thereof, the nature and concentration of the organic solutes, temperature, and ionic strength. The effects of pH are not well described by existing competitive equilibrium models outside narrow and well-defined experimental conditions. Differences in solubility between neutral and ionic species contribute to observed changes in adsorption capacities. Development of repulsive forces between the solute and the surface as between ionic species is also significant. Changes in the surface charge of the surface due to hydroxyl or hydronium ion adsorption or ionization of surface molecules or weakly acidic surface functional groups could substantially affect adsorption equilibria. In water treatment processes the adsorption of neutral organic compounds is probably not greatly affected by solution pH changes as the cations encountered are the weak acids used in most of the studies reported in the literature (11). Much of the organic of health

complexes are not neutral compounds. However, in the case of organics susceptible to ionization, pH conditions yielding the highest undissociated state seem to provide the best conditions for adsorption.

Matrix complexity is the final major characteristic of an aqueous system which influences adsorption capacities. Matrix effects are particularly significant in wastewater treatment applications. The presence of other organics in the solution usually reduces the adsorptive capacity of a particular system for each organic solute, although the total adsorptive capacity of the system is usually increased. Mutual inhibition can be predicted to occur if adsorption is restricted to one or two molecular layers. Two additional criteria for predicting mutual inhibition are that the adsorption affinities of the solutes do not differ significantly and that there are no strong interactions among solutes (7). Since the fixed equilibrium positions are dictated by thermodynamics, many multi-solute equilibrium models have been developed in attempts to provide some predictability in multi-solute systems.

The bulk of the data available in the literature on competitive adsorption involve bisolute studies. In a phenol-tetracycline system (28) the presence of the DTC reduced the single solute adsorptive capacity of phenol by approximately 20 percent (34). Although the phenol was a much smaller molecule and had a higher

effective rate of diffusion, pore blockage by ads was thought to reduce the surface area and pore volume available to phenol. A study of competitive adsorption between dichloro- and tri-chlorophenol showed that, as the equilibrium concentration of one solute increased relative to the second solute, the adsorption of the second solute decreased (74). In a study of competitive adsorption with binuclear mixtures of organic bases and neutral species, similar results were seen for some mixtures but not for others (75). Some adsorbents with substantial competitive effects while others showed little competition. In some cases, electrostatic repulsive forces were significant. Little competition was expected where there was a large difference in solute molecular sizes because of pore size distributions on the carbon. Mutual suppression of single solute adsorption capacities was also observed in a study of six fatty acids and four phenolic compounds (76). In competitive adsorption from binuclear mixtures of a fatty acid and a phenolic solute reduction in the adsorptive capacity for fatty acids was substantial but was not so extensive for phenol. Other binuclear studies are also available (77-79). Additional binnuclear data will be discussed in the presentation of solute-solute equilibrium results.

More recent interest are data from solute-solute studies involving three or more compounds. In a mixture of three fatty acids the adsorptive capacity was reduced for acetie

and substantially $\frac{1}{2}$ slightly $\frac{1}{2}$ proportion were kept over, the capacity for butyric acid actually increased somewhat (78). In a study of competitive adsorption in binary phenolic mixtures, the equilibrium capacities were successfully predicted by the Ideal Adsorbed Solution Model with a modified calculation procedure (89). A three-component mixture of glucose, alkyl benzoate sulfonate, an amino acid, and lactic acid was studied as a column reactor to validate a dynamic packed bed column model. Some calculations were also made for a four-component influent (90). Adsorption equilibria of individual solutes in binary mixtures of varying initial concentrations showed decreases in single solute adsorptive capacities (91). The most strongly adsorbed solute was described by a Freundlich isotherm, but the more weakly adsorbed solutes had curved isotherms on a log-log scale. The curved isotherms of individual solutes adsorbed from a mixture were typical if one or more of the competing solutes had higher adsorption capacities as a single solute than the remaining solutes. However, all solutes showed decreased adsorptive capacities in mixtures. These observations were also confirmed by equilibrium data in mixtures of up to six components.

The previously discussed research all described or postulated factors determining interactions among competing solutes. The relative size of adsorbates seemed to primarily affect adsorption processes by pore blockage. The

relative affinities of competing solutes, if sufficiently different, can result in the displacement of previously adsorbed solutes. A very strongly adsorbed solute can even cause an otherwise adsorbable compound to appear to be nonadsorbable. In column studies of mixtures of solutes, effluent concentrations of a solute exceeding influent concentrations in a steady state system are commonly observed. The relative concentration of solutes can also play a major role in site competition. A solute can adsorb more successfully when its concentration relative to other competing solutes is increased. Solute-solute interactions such as electrostatic repulsion/attraction between ions, dipoles, and π -electron clouds can be significant. The heterogeneity of the carbon surface can include adsorption sites so specific as to preclude any competition. Such noncompetitive adsorption is believed to be limited to ionic species and, therefore, determined by solution pH and carbon surface characteristics. The increase in reduced adsorption capacity with multi-solute systems is thought to reflect these phenomena. Site specificity can also result from limited accessibility due to pore size restrictions in addition to reaction specificity of certain surface functional groups. The unprecedented increase in mechanistic complexity in competitive adsorption renders mathematical description extremely difficult beyond binolute systems. Current efforts to develop predictive models consequently

most rely on such techniques as lumped isotherm parameters, surface homogeneity, total organic carbon isotherm analysis, and other approximations to reduce a multi-solute adsorption problem to a two- or three-component system.

2.4 Equilibrium Single-Solute Adsorption Models

Adsorption results in the accumulation of a solute from a solution onto a surface of a solid until a state of dynamic equilibrium is reached in the system at a fixed temperature. At such equilibrium there is defined distribution of solute between solid and liquid phases. Mathematically descriptions of this equilibrium are referred to as adsorption isotherms and attempt to express the solid phase concentration of solute as a function of the liquid phase concentration at equilibrium. Single-solute adsorption systems are generally described by one or two of several isotherm equations. Some apply solely to monolayer adsorption while others can describe multilayer adsorption.

2.4.1 Henry's Law

Henry's law is the simplest of the single-solute equilibrium models. This linear isotherm is valid only at very low concentrations and assumes that all molecules are isolated from their nearest neighbors. This linear relationship is analogous to the limiting behavior of solubility of gases in liquids and the constant of proportionality

referred to as the Henry constant. This linear partitioning model is thermodynamically based and is the lower boundary condition for any adsorption equilibrium model (8, 11). It is expressed as

$$q_g = K_h c_g \quad (8-1)$$

where q_g is the equilibrium solid phase concentration, c_g is the equilibrium liquid phase concentration, and K_h is the Henry constant or the partition coefficient. The thermodynamically based Langmuir equation reduces to Henry's law at small solute concentrations. Several other single and multi-solute equilibrium models have been modified to reduce to Henry's law as dilute solution conditions are approached. A three-parameter isotherm equation was developed to describe the adsorption equilibria of five organic compounds over a concentration range of 10^{-5} to 10^{-1} M (12). Three of the isolates (propionitrile, *n*-propylal, and acetone) exhibited isotherm slopes near unity at the lower concentration ranges, and the slopes approached unity even closer as temperature rose. Such behavior is Henry's law was typical of poorly-soluble isolates. The remaining isolates (prochlorophenol and *p*-nitroal) did not exhibit the same behavior, which indicated that the phenol-ester surface interactions were much greater than those of the first three isolates. The proposed three-parameter isotherm reduced to Henry's law at low concentrations and was

successful for describing the adsorption of the solutes studied.

Linear partitioning behavior was also observed for polychlorinated biphenyls (PCBs) when adsorbed as a river sediment (20). At higher solution concentrations the adsorption equilibrium was nonlinear. Deviance to Henry's law was observed for the adsorption of phenol and several other phenols at concentrations in the 10^{-3} M range (21). Numerous data for many different types of organic compounds over a concentration range of 10^{-5} to 10^{-2} M showed compliance with Henry's law at equilibrium concentrations below 10^{-3} M (22). The more poorly adsorbed compounds, such as urea, showed linearity at higher equilibrium concentration values (10^{-3} to 10^{-2} M), whereas more strongly adsorbed compounds did not exhibit linearity. For example, the isotherm for 2,4,6-trichlorophenol over a range of 10^{-5} to 10^{-2} M had a maximum slope of only 0.183 at 10^{-5} M. Three other three-parameter isotherms not commonly used in water and wastewater studies also reduced to Henry's law at low concentrations (23).

The importance of Henry's law in equilibrium modeling has been rather neglected since organic solutes of interest in adsorption studies were in the mg/L range; however, with analytical techniques available today to analyze for organics at the nanogram per liter range and with the presence of almost 100 compounds of toxic concern in water

surface at the monogram level, the ability of any equilibrium model to reduce to Henry's law has become much more significant.

1-4 : The Langmuir Equation

The Langmuir equation has been one of the most popular adsorption equilibrium models because of its theoretical basis, accuracy, and simplicity. The model can be derived from statistical thermodynamics as well as kinetically (4, 5). The kinetic derivation is based on the following assumptions:

1. Molecules are adsorbed at a fixed number of well-defined localized sites;
2. Each site can hold only one adsorbate molecule;
3. All sites are energetically equivalent;
4. There is no interaction between adsorbed and gaseous phases;
5. Adsorption is reversible.

The adsorbed layer, therefore, can only be a monolayer if the model is to successfully describe the equilibrium. The Langmuir equation is commonly written as follows (6).

$$q_e = \frac{Q \cdot q_s}{1 + Q/q_s} \quad (2-2)$$

where q_e is the equilibrium solid phase concentration, Q is the equilibrium liquid phase concentration, Q is the units

plate concentration when a complete monolayer is formed on the surface, and b is related to the net enthalpy of adsorption. If b is proportional to $e^{(-E/RT)}$, where E is the universal gas constant and T is absolute temperature, the Langmuir equation will reduce to Henry's law when $bC_0 \ll 1$. The two Langmuir constants are determined by best fitting the following linearized form of equation 3-2 to experimental data:

$$\frac{1}{q_{\infty}} = \frac{1}{Q} + \left(\frac{1}{bQ} \right) \left(\frac{1}{C_0} \right) \quad (3-3)$$

The basic assumptions of the Langmuir equation are never met in activated carbon adsorption systems treating water or wastewater because of the heterogeneity of the carbon surface. Adsorption data have been successfully described by the Langmuir equation for very narrow concentration ranges, but it usually does not fare well when compared to other isotherm equations.

3.4.2 The Brunauer, Emmet, and Teller (BET) Equation

The BET model was an extension of the Langmuir equation to describe multilayer adsorption (4, 7). Consequently, this equation also assumes a surface composed of uniform, isolated sites and that adsorption at one site does not affect adsorption at neighboring sites. The model development is based on the same kinetic picture as the Langmuir

equation has resulted that layers of molecules adsorb on top of the previously adsorbed monolayer. The BET model also assumes that the Langmuir equation applies to each successive layer. The first layer's heat of adsorption may have a unique value, but in all succeeding layers the heat of adsorption is equal to the heat of condensation of the liquid adsorbate. The BET equation is commonly written as follows:

$$\frac{C_a}{(C_a - C_g)P/P_0} = \frac{1}{(1 - P/P_0)} + \frac{1}{(1 - P/P_0)} \frac{C_a}{C_g} \quad (2-4)$$

where k is a constant reflecting an energy of interaction with the surface, C_a is the adsorption concentration of the solute in the liquid phase, and the remaining symbols are as defined for equations 2-3. Equation 2-4 is usually rearranged to a linear form for application with experimental data.

$$\frac{C_a}{(C_a - C_g)P/P_0} = \frac{1}{1 - P/P_0} + \frac{1}{1 - P/P_0} \frac{C_a}{C_g} \quad (2-5)$$

The BET equation has become the standard one for surface area determinations, usually with nitrogen at 77°K as the adsorbate (4). However, the equation has not enjoyed wide use in the field of environmental engineering because of difficulties in obtaining appropriate values for C_a and also because at the concentrations found in most water and

estimated applications $C_{\text{eq}} \gg C_0$ and the BET equation reduces to the Langmuir equation. The saturation concentration, C_{eq} , can only be estimated in practice by an iterative procedure to fit the model to experimental data (24). The model is also restricted by the same limitations of the Langmuir equation.

2.4.4 The Freundlich Equation

This simplification equilibrium model is one of the most widely used in the water and wastewater treatment field. The equation was developed to experimentally describe adsorption and therefore has its greatest weakness. This equation was meant to describe that portion of the isotherm beyond the dilute solution region of Henry's law (25). The development of the equation was based on the assumption that the adsorbent had a heterogeneous surface composed of different classes of adsorption sites, with adsorption on each class of sites conforming to the Langmuir equation (26). The development of the Freundlich equation begins with the Langmuir constant, b , which is related to the net enthalpy of adsorption. On heterogeneous surfaces b will not be a constant but rather a distribution function of energies that can be related to fractions of occupied surfaces. The new adsorption isotherm is the integration of each adsorption isotherm function for each value of b as its distribution function. This integral equation is the experimentally

observed adsorption isotherms. One particular solution of this integral equation assumes the Langmuir model to be the isotherm function and attributes the deviation to a solubility in the heat of adsorption. The solution to the integral equation, in this case, has the form

$$q_a = K C_a^{1/n} \quad (12-6)$$

and is known as the Freundlich adsorption isotherm (4), where K and n are statistically determined, least fit parameters. The equation does not become linear at low concentrations and does not show a saturation or limiting value. Although the derivation is somewhat theoretically based, it is considered an empirical equation limited in its usefulness to its ability to fit data. The limitations of the Freundlich equation are often ignored by many investigators who increasingly extend the model beyond the valid experimental range of derivation (41). However, the model has successfully correlated experimental data for adsorption on activated carbon from aqueous systems over a wide range of concentrations, and the model has been incorporated into several multi-phase adsorption equilibrium partitioning models.

3.3.3 Three-Parameter Equations

The lack of fit of the Langmuir equation over a wide concentration range and the empirical limitations of the Freundlich equation have led researchers to propose several other equations to describe experimental single-phase adsorption data. One study compared the Toth, Redlich-Peterson, and Rosen (three-parameter) equations with a new three-parameter equation (21). Six dilute aqueous binary systems were examined. The Toth and the study's equations best described the data, although all four had absolute relative percent deviations less than 18 percent and, for most of the eight compounds studied, less than 5 percent. The Toth equation is little known in the West, having been published in east European literature. Its derivation follows a similar line as the Freundlich isotherm but specifies the dependence of the integral enthalpy of adsorption as a function of the solid phase concentration of a particular solute. This dependence is quantified through a dimensionless quantity that was defined for ease in obtaining experimental data. It described experimental data well as the above study. The isotherm equation developed in the study incorporated the concept that highest energy sites are filled first so that the rate of adsorption declines rapidly with increased surface coverage. The equation had the form

$$q_{\infty} = \left(\frac{q_0}{K} \right)^{1/n} \frac{K_0 P}{K}$$

(11-12)

where K and K_0 are functions of temperature and p is a constant (11). Both isotherm equations were used with the Ideal Adsorbed Solution (IAS) multi-phase equilibrium model successfully in predicting adsorption for six bisolute systems at 25°C.

A modified, three-parameter Freundlich model was developed to correct for the crossover from Freundlich-like adsorbed behavior to Henry's law behavior (12). The equation was successfully used to predict adsorption on several bisolute mixtures and one ternary mixture using the Ideal Adsorbed Solution (IAS) multi-phase model. A similar expanded set of Freundlich equations was used to describe single solute adsorption isotherms for the prediction of multi-solute adsorption using the IAS theory in five dilute, aqueous, binary systems (13). The binary solute isotherms were divided into five segments, each with a different set of Freundlich constants. This approach was chosen over existing three- and five-parameter isotherm equations to minimize computational time and expense. Another three-parameter model was developed to combine Henry's Law and the Freundlich equation to describe adsorption data over a wider range of concentrations (14). This equation takes the form

$$q_{\infty} = \frac{K_0 P}{1 + K_0 P} \frac{K_0}{K} \quad (11-13)$$

where a , b , and c are determined by minimizing fit of experimental data to the equation. At low solute concentrations the equation reduces to Henry's law. At high solute concentrations the equation is equivalent to the Freundlich model, and when $c = 1$, the equation becomes the Langmuir equation. This equation has generally described adsorption data well. Unfortunately, this equation does not readily adapt to multi-site equilibrium models.

There are several other single-site descriptive equilibrium models using a variety of parameters that treat adsorption data effectively. Some of these are listed and described elsewhere in a brief review of single-site equilibrium models (87).

2.7 Approaches to Predictive Single-site Equilibrium Models

2.7.1 Thermodynamic Approach

Physical adsorption has been described by classical thermodynamics applied in a microscopic approach to two- and three-dimensional models (1, 2, 6-7, 78, 88). The fundamental expression of the thermodynamics of adsorption is the Gibbs equation which, for dilute solutions of one solute, may be approximated by

$$\Gamma = \frac{1}{RT} \left(\Gamma \frac{RT}{V_s} \frac{1}{C_s} \right) \quad (2-10)$$

where Γ is the amount of solute adsorbed per unit area of surface at equilibrium, in terms of the bulk concentration (also termed the surface excess). If γ is defined as the interfacial tension, then a solute which reduces γ will adsorb at the surface (2).

The development of surface form of the Gibbs adsorption equation for the solid-liquid interface remains in the form

$$\int_1^n n_i^R ds_i = \Delta \sigma = 0 \quad (2-18)$$

at constant temperature and where Δ is the molar surface area of the adsorbent, n_i^R is an adsorbed adsorption term approximated by Γn_i in dilute solutions, σ_i is the chemical potential of component i , P is the spreading pressure, V is solution volume, and $\Delta \sigma_i$ is the change in concentration caused by adsorption (18).

The development of the Gibbs equation requires a thermodynamically inert solid with an available specific surface area identical for all adsorbates (19). Given the heterogeneous nature of the activated carbon surface, such assumptions are limitations to the use of the equation. However, this approach is incorporated in other methods of describing adsorptive behavior in multi-solute systems

3.1.2 Energy Balance Approach

This Approach takes a microscopic view of the adsorption process at the surface of a solid phase and applies an energy balance to the adsorption. Two models under investigation which take this approach include an application of the solvophobic theory and the net adsorption energy approach. These two models emphasize the importance of solute, solvent, and adsorbent interactions in the adsorption process.

The solvophobic theory was developed to estimate the effect of solvents on several types of reactions involving molecules common in biology, including denaturation, aggregation, and conformational changes (8). The application of the theory to adsorption in aqueous systems gave the net solvent effect as a summation of six free energy terms (9, 10). Although the terms could be calculated from the physicochemical properties of the system, the calculations were very complicated. If the solute molecules were much larger than the water molecules, then the equation simplified to one needing only the total solute molecular surface area to predict adsorption capacity. The solvophobic theory, while finding excellent application in noncrystalline liquid chromatography, has several limitations in its use in aqueous systems with heterogeneous sorbents (11). So far, its application is restricted to non-ionic, nonpolar solutes. The noted

assumes a uniform, nonpolar, noninteractive carbon surface and does not describe adsorbate adsorption of each solvent. Characteristics as pH and ionic strength. Such predictions would require microscopic details not yet available, such as adsorbate hydrophobicity. It also does not provide information on the shape or type of adsorption isotherm for a particular solute. The theory also produces only a single adsorption capacity value, rather than a broad-range isotherm.

The net adsorption energy model was developed to include the solvent effect in aqueous phase adsorption by relating a calculated net adsorption energy to adsorption capacity at specific solution concentrations (32, 43). The model uses the solubility parameter concept, which was discussed earlier in Section 2.4, to determine the net adsorption energy. The calculated energy is a function of a compound's aqueous solubility, molecular weight, density, a dispersion component of the solubility parameter for the organic compound, and a dispersion component of the solubility parameter for the activated carbon surface. The net adsorption energy (E_p) is calculated by combining the solute's affinity for both the adsorbent (E_{pa}) and the solvent (E_{ps}) and the interaction between solvent and adsorbent (E_{sa}). The E values are in calories per mole, and the subscripts a , s , and a refer to adsorbent, solvent, and adsorbent, respectively. The equation is of the form

$$E_{\text{D}} = E_{\text{D}0} = (E_{\text{D}1} + E_{\text{D}2})$$

(11)

Each of the energy terms is calculated using component values of the solubility parameter, δ , for the organic compounds. The application of the net adsorption energy concept to available adsorption data for medium-polarity to high-polarity organic compounds showed that measured adsorption capacities increased as calculated net adsorption energies increased (11).

The application of this concept has shown several limitations to its usefulness. The compounds that have been tested were qualitatively ranked. The model assumes a uniformly spherical activated carbon surface. Quantitative determinations of the components of the solubility parameter are not well developed. Application of the theory to predict the adsorption capacities of neutral organic compounds is not clearly understood. A comparison of this theory with the Polanyi theory found that the relationship between adsorptive capacity and net adsorption energy was predictive only if separate relationships were defined for branched and linear alcohols (11). If the model is to be generally predictive of adsorption capacities of organic solutes, a single relationship is needed. As adsorption energy increased, the study showed greater deviation from linearity for the alcohols. The model was not able to predict adsorption isotherms accurately, although rough

estimates were obtained using only the adsorptive index, the molar volume, and a rough estimate of solubility. The model is relatively new and untested but shows promise in elucidating the importance of volume, solubility, and adsorbent characteristics and roughly estimating relative adsorption capacities for different organic compounds.

1.1.3 Adsorption Potential Approach

This approach is multilayer adsorption postulates a potential field at the surface of a solid body which attracts molecules "fall" (4). The adsorbed layer resembles a planetary atmosphere being most compressed at the surface and growing less dense as the distance from the surface increases. This concept of a changing adsorption potential in the adsorption process was incorporated into the Polanyi adsorption potential theory, one of the best known of the potential theories (4, 14). The development of this theory is described and well documented in several studies that applied the theory to adsorption from aqueous solution onto activated carbon (44, 51, 53).

The Polanyi theory postulates a fixed volume close to the solid surface where the adsorption process occurs. For carbon this volume essentially consists of micropores of varying size and shape. The adsorption potential is defined as the work required to remove a molecule from the location in the micropore to infinity. The magnitude of this

potential depends on the nature of the surface and the distance of the solute molecule from the surface. The potential will be greatest for micropores whose values approximate that of the solute molecules close surface area contact will be a minimum as well as the van der Waals forces of interaction.

One important consequence of this theory is that for any single solute species using the same carbon all of the single-solute isotherms from trace concentrations to saturation may be readily calculated from the isotherm of any one solute (18). That is, the theory postulates a single characteristic curve from a single-solute isotherm at any temperature. For a different solute, an absolute scale correction factor will produce the same characteristic curve. To produce the unique characteristic curve of a carbon, it is possible to transform the isotherm to the characteristic curve by the conversion of q_m and C_m to a value of adsorbate adsorbed and an adsorption potential. Dividing q_m by the liquid density results in the volume/mass isotherm ordinate. The adsorption potential is calculated by

$$\epsilon = RTM \left(\frac{C}{C_m} \right)^{1/n} \quad (12-12)$$

where ϵ is the adsorption potential and q_m is solute adsorbability. From this characteristic curve, the isotherm for any temperature can be calculated for the single solute.

A plot of adsorbate volume per unit weight of carbon against the adsorption potential per unit liquid volume is approximately the same for a series of similar compounds, such as a homologous series of hydrocarbons (64). An electron correlation factor will give the same correlation curve for a wide variety of compounds. Consequently, it should be possible, given one single volume isotherm, to predict single isotherm isotherms for a wide variety of organic solutes across a wide concentration range. One study correlated experimentally determined Freundlich K constants for nine alcohols and plotted K against calculated net adsorption energies (81). The resultant correlation line was used to predict K values for 12 additional compounds. The net adsorption energy concept predicted K values well, better than the Polanyi with which it was being compared. Both methods deteriorated for compounds with loadings greater than one millimole per gram. The model also had difficulty with branched-to-linear alcohol relationships. The adsorbate volume also had to be empirically adjusted for variations in the various adsorption at all states even when on a volume basis.

The Polanyi model assumes heterogeneity of adsorption energies over the adsorption surface which contrasts with the Langmuir assumption of equal energies everywhere. This allows better accommodation of competition and noncompetitive adsorption than the Langmuir noncompetitive model.

Any interactions between solute and solvent are reflected schematically as solubility effects. The model has several limitations. One is the assumption that all pores are accessible to the adsorbate. The model also assumes that only physical adsorption occurs and does not include chemisorption. However, this method is useful and somewhat easy to apply.

1.4 Sink-Source Equilibrium Models

Several models have been developed to describe competitive adsorption of organic solutes in aqueous solutions. Most are extensions of simple-solute descriptive and predictive models. Two different approaches to modeling are currently being developed as activated carbon adsorption. Modeling the equilibrium distribution between solid and solution phases in descriptive and predictive ways has been the thrust of this review of the literature. A different modeling approach which takes into account the dynamics of adsorption has been pursued by several investigators as a basis of a rational carbon column design. The interrelationship between these two approaches lies in the thermodynamics driving a carbon adsorption system toward mass equilibrium. All dynamic models must incorporate these thermodynamic equilibrium considerations in order to link thermodynamics with mass transport limitations adsorption processes.

Although each of the classical adsorption equilibrium models adequately describes or predicts equilibrium under certain specified conditions, one limitation shared by all is the failure to include the nature of the adsorbent. All the models assume that there are no specific adsorptive interactions or that chemisorption, if it occurs at all, is too small to affect overall equilibrium as the models describe them. The interaction of organic substances and surface functional groups can markedly change the pattern of distribution of adsorption isotherms for different solutes. Molecular sieving effect due to diffusing pore size distribution in various adsorbents and pore blockage can be more significant than physical adsorption forces reflected as adsorbability effects in determining adsorption behavior (10). Limitations of predictive and descriptive models, thus, can be attributed to assumptions made during their development. Assumptions common to almost all models are a homogeneous, thermodynamically inert surface, equal competition for sites, and adsorption determined by physical forces only, that is, complete reversibility.

3.4.1 Descriptive Models

Two descriptive models include a model proposed by Fritz and Schulerer and an extension of the Langmuir-Freundlich three-parameter model (11, 12). The Fritz and

Schneider model involves a general empirical equation of the form

$$q_{e,i,j} = \frac{a_{10} C_{e,i,j}^{b_{10}}}{a_{10} + \sum_{j=1}^n a_{1j} C_{e,i,j}^{b_{1j}}} \quad (2-24)$$

where i and j refer to different solutes, n is the total number of solutes, and a_{10} , a_{1j} , b_{10} , and b_{1j} are constants determined by the best fit of multi-solute experimental adsorption data (27). The equation includes the Langmuir competitive adsorption equation, the Jaeger and Bohlen relationship, a Redlich and Peterson equation, the Freundlich equation, and the Langmuir single-solute equation when the empirical constants are assigned certain values. The model is not predictive because multi-solute adsorption data are required to estimate model parameters.

An extension of a previously described single-solute three-parameter model was tested for multi-solute data predictability (28). The model is described by

$$q_{e,i,j} = \frac{C_{e,i,j}^{1/2} (K_{1,i,j} / K_{2,i,j})}{1 + \sum_{j=1}^n \left[\frac{K_{1,j}}{K_{2,j}} (C_{e,i,j} / K_{2,j})^{1/2} \right]} \quad (2-25)$$

where A , B , and C are parameters determined from single-solute isotherms, and the interaction terms, γ_{12} and γ_{21} , are determined from multi-solute system data.

Both these models adequately describe multi-solute equilibrium data for the concentration ranges of the specific solutes studied. The extended three-parameter model has been used as the dynamic solute simulation model [14]. However, because of the need for multi-solute data in order to estimate certain model parameters, these equations are valid only for the data sets to which they were applied. The model parameters are not readily associated to any solute properties. Consequently, the models are not applicable, in a general way, to a wide variety of solute types.

1.3.1 Langmuir-Competitive model

This model extends the Langmuir single-solute equation to a competitive, multi-solute model in the form

$$q_{i,j} = \frac{Q_i b_i C_{i,j}}{1 + \sum_{j=1}^N b_j C_{j,j}} \quad (10-12)$$

where i and j refer to the solutes in solution and the remaining terms are as defined previously for the Langmuir isotherm. The constants, Q and b , are determined from single-solute data. The model assumes equal competition

for sites, complete reversibility, and no interaction among adsorbed solutes. This model was applied to the adsorption of alkyl phenols on bisolite systems (28). Single-solute adsorption data were described by the Langmuir equation, but the competitive model did not adequately describe the bisolite data. Other studies also showed that the Langmuir competitive model did not perform as well as several other models (29, 34-36). The thermodynamic basis of the model was valid only when the constant, Q , was identical for all solutes (equal competition):

3.3.3 Noncompetitive Langmuir Model

The Langmuir competitive model was modified to describe adsorption from a bisolite system when a portion of the adsorption occurs without competition (75). The modification was based on the hypothesis that such adsorption occurs when the constant, Q , in the competitive model was NOT the same for both solutes. The model was expected to be valid only when a fraction of the adsorption occurs without competition, such as when the larger of the two solutes is unable to enter the smaller pores of the carbon or when a site is unavailable to one solute due to the chemical nature of the site. The number of adsorption sites where noncompetitive adsorption would occur was assumed to be equal to $Q_1 - Q_2$ in a bisolite system. The modified Langmuir competitive equation became, for $Q_1 > Q_2$:

$$q_{e,i} = \frac{(Q_1 - Q_2) \frac{b_1 C_{e,i}}{1 + b_1 C_{e,i}}}{1 + \frac{b_2 C_{e,i}}{1 + b_2 C_{e,i}}} + \frac{Q_2 \frac{b_1 C_{e,i}}{1 + b_1 C_{e,i}}}{1 + \frac{b_2 C_{e,i}}{1 + b_2 C_{e,i}}} \quad (2-14)$$

$$q_{e,i} = \frac{Q_1 \frac{b_1 C_{e,i}}{1 + b_1 C_{e,i}}}{1 + \frac{b_2 C_{e,i}}{1 + b_2 C_{e,i}}} \quad (2-15)$$

where the terms are as defined for the single-site Langmuir equation. The noncompetitive term is the first term on the right side of equation 2-14.

In the study that developed this modification (71), the noncompetitive model gave a much better description of adsorption data for four out of five bivalent pairs than the original competitive model when $Q_1 \neq Q_2$. When $Q_1 \approx Q_2$ as one pair, the two models were almost identical. This was taken as evidence of noncompetitive adsorption due to surface heterogeneity on the carbon. Noncompetitive adsorption has been applied by other research (74, 75). In a study of competitive adsorption between selected heavy metals and phenolic substances, the noncompetitive model was significantly better in describing adsorption data compared to the competitive model (76).

The most significant limitation to that model is its restriction to bivalent systems. The model also assumes that unequal competition occurs only when $Q_1 \neq Q_2$. However, unequal competition has been observed when $Q_1 = Q_2$ (47).

The model is limited by the validity of the single-site Langmuir equation to describe ion-exchange data. Other limiting phenomena of the Langmuir development also apply. The model does illustrate the occurrence of unequal competition due to the heterogeneous nature of the exchanger medium.

1.4.4 Competitive Polyelectrolyte Interaction Theory

The Polyelectrolyte Interaction Theory discussed as a single-site predictive modeling approach is being studied for application in multi-site systems (26, 27). The approach is based on the application of several physicochemical parameters (the inferred [18] shift parameter, a polarity parameter, and a steric parameter) with the polyelectrolyte theory to predict the adsorption of organic molecules in multi-site systems.

The 18 shift parameter is used to measure a solute's hydrogen bonding ability. It is determined by collecting boiling and melting 18 shift values (using an enthalpy scale) for various organics and then multiplying these values by the ratio of their molecular weight to percent aqueous solubility. This composite 18 shift parameter is then normalized with respect to phenol. As the value of this normalized parameter increases, observed single-site adsorbability also increases. From this it was concluded that solute adsorbability is proportional to boiling and

molecular weight and inversely proportional to solubility (21).

The polarity parameter describes the polar effect of the addition of a substituent group to a solute in a class of compounds when the parameter is correlated with conjugation, maximum absorption capacities. The Hammett equation is used to produce a parameter that reflects polar effects of meta- and para-substituted derivatives of benzene. For reactions involving aromatic ether-substituents and aliphatic compounds, the Taft equation provides the polarity parameter. Both parameters are tabulated in the literature for organic solvents normally found in natural waters (22). In general, as these parameters increase, the polarity effect of the substituent decreases and conjugation increases. This agrees with solubility correlations since a decrease in polarity generally results in a decrease in solubility.

Steric effects usually become important for aromatic substituents and a modified Taft equation is used to define a steric parameter. Values for this parameter are also available in the literature. Generally, as the steric effect of a substituent group increases, conjugation solubility increases, and there is a decrease in the polarity parameter. Therefore, polarity and steric parameters correlate inversely with conjugation adsorption.

This approach to multi-solute equilibrium predictability has not yet been well defined. Parameter data for a wide variety of organic solutes are limited. Comparisons of parameters are also restricted to classes of compounds. The approach also assumes reversible adsorption due to van der Waals forces only, which limit its potential use in adsorption systems where chemisorption is frequently encountered.

3.2.3 The Polanyi Adsorption Model

The Polanyi adsorption potential theory has been applied to adsorption from aqueous solutions of single organic liquids and single and multiple organic acids (8), and the references listed therein). Given the correlation curves for two individual solutes in water, the effective molar volumes, and the solubilities of each solute in the presence of the other, the competitive correlation curves may be constructed for the same strongly adsorbing solute. From the competitive correlation curves the competitive isotherm may be constructed. Its application to multi-solute systems of organic liquids partially miscible in water and completely miscible in each other led to a successful comparison with the Ideal Adsorbed Solution model (10). Binary and ternary solute systems were examined in this study.

All work developing this approach has been done on one type of carbon. The limitations of the Polanyi model still

apply will prove accessible to the community, (except for adsorption only, effect of carbon ash content not included and limitations on predicting otherwise main factors and adsorbate dissimilar). Some problems may be encountered with group functionality and steric effects.

The Polanyi Competitive Model requires molar volumes, refractive indices, aqueous solubilities, and the characteristic curve of the carbon as the data base. Not all of these parameters are readily available, especially aqueous solubilities. The development and application of the theory are in terms comfortable to physical chemists' point of view, and correspondence with other competitive models, such as the IAB model, are not well understood. The model promises to provide more insight into adsorption mechanisms and better predictability for multi-solute competitive adsorption equilibria. However, more testing is required using different carbons and solutes commonly encountered in water and wastewater treatment.

1.4.4 Ideal Adsorbed Solution (IAS) Theory

The IAS theory was developed originally to calculate the adsorption equilibria for components in a gaseous mixture, using only data for pure component adsorption equilibria at the same temperature and with the same adsorbent (18). The theory was based on the concept of an ideal adsorbed solution, and the resultant expression was

derived using classical surface thermodynamics. The expansion of the theory involved the application of the thermodynamics of ideal dilute solutions to developing a method to calculate multi-solute equilibria, again using only data for single-solute adsorption (74). The central concept is that in an ideal solution, the concentration of a solute in a mixture is given by the product of the mole fraction of that solute in the adsorbed phase and the concentration of that solute which would exist in a single-solute system at the same temperature and spreading pressure as the mixture. This equation has the form

$$C_i = (R_i) (C_i^0) \quad (4-18)$$

where C_i is the concentration of solute i in the mixture, C_i^0 is the corresponding single solute concentration, and R_i is the mole fraction of solute i in the adsorbed phase.

The thermodynamic basis for this theory assumes an inert solid with a specific surface area identical for all adsorbates. At equilibrium the chemical potentials of adsorbed and liquid phases are identical, and the application of the Gibbs-Duhem equation results in the Gibbs adsorption isotherm presented earlier (Equation 2-28). In this relationship the work of adsorption, represented as ΔG° , is a function of the mass of solute adsorbed and the solute's chemical potential at constant temperature. The

spreading pressure, π , is defined as the difference between the interfacial tension (γ) of the pure solvent-solid interface and that of the solution-solid interface at the same temperature:

$$\pi = \gamma_{\text{pure solvent-solid}} - \gamma_{\text{solution-solid}} \quad (11-10)$$

The details of the thermodynamic developments are found in the original references [7], [8].

The spreading pressure of a solute can be related to the single-solute adsorption equilibria according to

$$\pi_1 = \frac{RT}{A} \left[\frac{C_1}{B} - q_1^s \right] \frac{dq_1^s}{dC_1^s} \quad (11-11)$$

where q_1^s is the single-solute solid phase concentration of solute 1, A is the specific surface area (surface area per unit weight), B is the unimodal gas constant, and T is absolute temperature. Since

$$q_1^s = f(C_1^s) \quad (11-12)$$

through the mathematical representation of the single-solute isotherm (Freundlich, Langmuir, three-parameter models, etc.), then spreading pressure becomes a function of C_1^s :

When solute species adsorb simultaneously from dilute solutions at constant temperature and spreading pressure, the

theory proposes that the adsorbed phase forms an ideal solution. Combining this theory with the Langmuir equation for isothermal adsorption (the Charneymanian basis) results in

$$\frac{1}{q_T} = \left(\frac{1}{q_s} \right) \quad (2-22)$$

where q_T is the total amount adsorbed from the mixture. The other relationships needed for the IAG calculation are

$$\sum_i q_i = 1 \quad (2-23)$$

and

$$q_i = (q_T)(\theta_i) \quad (2-24)$$

The calculation procedure begins with equations 2-18, 2-20, and 2-23 and a set of experimental values for $C_{i,0}$, the multi-phase equilibrium concentration for solute i (20). With an initial guess for K_i , an iterative procedure is used on a computer to solve this set of simultaneous equations. The iterative procedure results in K_i and $C_{i,0}$ values that allow all spreading pressures to be equal, as required by the IAG theory. That is,

$$P_1 = P_2 = \dots = P_n = P \quad (2-25)$$

Using the single-solute isotherm equation, q_1^m can be determined (Equation 2-11). The total amount adsorbed from solution is then calculated from Equation 2-22. The amount adsorbed of each solute in the mixture can next be calculated using Equation 2-23.

The difficulty in calculating multi-solute equilibria lies in the analytical solutions for the spreading pressure calculations (98). For accuracy in spreading pressure values, experimental data must be available over the loading range from zero to q_1^m . Consequently, although analytical solutions for Equations 2-22 exist for Langmuir and Freundlich equations, unless Henry's law is used, as the concentration approaches zero errors in π will occur. Limitations of the Langmuir and Freundlich equations in representing wide concentration ranges have already been discussed. Some improvement in determining π can be achieved by using the following form of the spreading pressure equation (100):

$$\pi = \frac{RT}{k} \int_0^{q_1} \frac{d \log Q}{d \log q_1} dq_1 \quad (2-24)$$

A study of several three-parameter, single-solute models for use in the IAS model showed that use of the Toth equation, as well as a three-parameter model proposed in the study, in the IAS calculations represented experimental data well in several binary systems (101). However, when

soluble species were present, large deviations were observed between predicted and experimental values. Another three-parameter, single-solute isotherm equation was used with the IAS theory to qualitatively predict breakthrough concentrations in continuous column studies (18). Single-solute data were represented by a set of Freundlich adsorption isotherm equations to simplify the application of the IAS theory (19). The method was tested with first, dilute, aqueous benzene solutions on four different activated carbons with good success. The intent of the study was to provide an easier way to calculate spreading pressure rapidly and accurately for predicting solid-solute equilibria.

A modified calculation procedure for the IAS model used solid phase solute concentrations instead of the original parameter based on an undefined weight of adsorbent. The procedure also included equations 2-11 for spreading pressure calculations; a modified three-parameter Freundlich model for single solute isotherm input; a new equation to allow prediction of equilibrium concentrations without using experimental data, and a numerical method to solve the simultaneous set of (3n+1) equations, where n is the number of solutes in the mixture (20). This procedure was tested with 16 sets of binary and ternary phenolic mixtures. The Langmuir competitive model in the IAS calculations was used as a comparison. The modified calculation procedure was

successful and superior to the Langmuir isotherm model in describing the competitive adsorption of the bisolute systems studied. The IAS theory was also superior to the competitive Langmuir equation in predicting multi-solute equilibria for the calculation of multi-solute adsorption on fixed beds (142). The complexity of calculations for the two isotherm models varied with the interparticle diffusion models used. Although the IAS theory required greater computational effort, it proved more successful in predicting breakthrough curves for the single and bisolute systems studied.

The IAS model is the most theoretically sound of the multicomponent adsorption models. It was theoretically extended to any number of competing components, and good agreement between experimental and predicted results has been shown. However, the model poses a formidable computational barrier, even using a computer, which increases exponentially as the number of components increases. The iterative solution procedures contribute to the model's complexity. The model exhibited increasing deficiencies when low solute concentrations were studied or where low surface doses were used (144). The model assumes an inert carbon surface with all sites equally available for competition and assumes complete reversibility. The accuracy of the model depends on the accuracy of the single-solute isotherm

data and the activity model, used to estimate spreading pressures.

3.4.3 Simplified SAM Model

A simplified calculation approach as the SAM model was suggested to reduce or remove the difficulties in determining spreading pressure curves for pure solutes in gas equilibrium systems (188). The development of the simplification was described in an article reporting on the relationship of the simplified model to the original theory (89). In the model development, when all competing solutes have identical isotherms, the total loading in the mixture is the same as that in each single-solute system, providing the spreading pressure is also the same. Under these conditions, single-solute concentrations are equal to the total concentration of the mixture. For the case when solutes have different isotherms, hypothetical solutes are defined in such a way that all have the same isotherm equation and, thus, the same spreading pressure dependence. In the development of the model these hypothetical solute concentrations are defined in terms of actual concentrations. For multi-solute systems the individual solid phase loadings are represented by

$$q_i = K \frac{(p_i^s)^{1/n_i} - 1}{n_i} \quad \left[\frac{p_i^s}{C_i} \right]^{1/n_i} \quad \left[\sum_{i=1}^N \left(\frac{p_i^s}{C_i} \right)^{1/n_i} \right]^{1/n_i} \quad (1-13)$$

20-10

K_1 = the single-site Freundlich constant, n_1

n_1 = the single-site Freundlich constant, n_1

K' = average value K_1 .

n' = average value n_1 .

The simplified model is identical to the ISE model when single-site isotherms are identical and for unequal isotherms when the isotherms are described by one Freundlich equation and n values are equal. When n and K values are unequal, the model can only approximate the ISE model (cf. 19). The simplified model was in good agreement with the ISE model in the concentration range of 0.01-0.1 M but began to diverge at higher concentrations (19). The simplified model can also be extended to include any number of competing solutes. The model can be used to find adsorption beds because calculations of concentrations are just as possible as calculating loadings. However, the inability to account for chemisorption and unequal competition also limit this model, especially in systems with varying solvent conditions. But, the great reduction in the number of computations while still maintaining ISE theoretical assumptions has made the simplified model very appealing.

3.1.4 Improved Langmuir-IR Model

One of the deficiencies of all multi-site models is the inability to account for irreversible adsorption and unequal competition. Such phenomena arise from the heterogeneity of the carbon surface, especially varying pore sizes and specific surface functional groups. The simplified IR model was chosen for modification because of the fundamental soundness of the model's development and the ease with which terms could be added to account for irreversibility and unequal competition for adsorption sites (16).

Irreversible adsorption is most often observed as dynamic fixed-bed adsorbents where changes in influent concentrations can produce a pronounced hysteresis effect. Experiments performed to determine the degree of reversible adsorption of phenol on various carbons showed only about 30 percent reversible adsorption, even with long equilibrium times (17). Similar behavior has been observed for adsorption of gases by porous solids (18). Postulated mechanisms for the observed irreversibility of phenol included: irreversible chemical reaction after sorption on the surface and desorption of the phenol through π -bond donor-acceptor complexes. Another study compared a rapid adsorption/desorption procedure to a slow equilibration technique with p-dimethylols (21). No hysteresis was observed in the rapid method, but significant irreversibility was observed in the slower technique. A discussion of

adsorption-desorption hysteresis in organic chemical-solid systems reviewed the many examples of hysteresis in adsorption and desorption experiments and proposed a model to account for this anomaly (1951). A study of adsorption irreversibility of five low molecular weight substituted phenols showed significant irreversible adsorption (1951). The irreversibility was influenced by surface functional group type and position. The study discussed and referenced several literature citations that showed that multi-site adsorption equilibrium models fail to accurately predict solid-phase loadings on activated carbon for various system conditions. Temporal competition and irreversible adsorption due to a heterogeneous carbon surface were not accounted for in existing models and were postulated as the cause of much of observed multi-site model inaccuracies.

Modification of the simplified model resulted in the inclusion of a competition factor that improved model performance in several simultaneous adsorption studies (1961). The competition factor was found to be significant only for the solute with a higher adsorbility. This competition factor was correlated with a solubility term for several solute pairs and gave the improved model a predictability capability. The competition factor was determined by using nonlinear RAS programming for each set of data.

Modification of the simplified model to account for multi-site irreversibility resulted in the evaluation of

two irreversibility parameters in bivalve systems. Due to a lack of multivariate irreversibility data in the literature, the study was limited in its evaluation of the two added parameters. Within the limited confines of the study, some improvement in describing sequential solute addition data was shown. A limited correlation of the irreversibility parameters with a solubility term also gave some degree of predictability to the improved model.

The model was developed from bivalve adsorption data, and, therefore, its application to more complex systems has yet to be tested. However, the model and its development do provide an increased understanding of the adsorption process with heterogeneous solidified matrix surfaces as well as the causes and effects of irreversible adsorption and unequal competition.

CHAPTER 3 RESEARCH OBJECTIVES

The review of the literature has shown that the surface of activated carbon is heterogeneous. Carbon surfaces exhibit a wide variety in the distribution of pore sizes and surface energies. The heterogeneity in the physical structure of activated carbon greatly influences adsorption capacities and kinetics. Adsorption behavior is also determined by intricate surface chemistries which reflect solute and solvent interactions with surface functional groups.

The literature has also shown that existing multi-solute equilibrium models fail to account for carbon surface heterogeneity. The unequal competitive adsorption and irreversible adsorption arising from surface characteristics can be significant and cause these models to fail. When these equilibrium models do not accurately describe, or predict, observed equilibria, then the dynamic production models using these equilibrium models will also fail.

The overall objective of this research was to contribute to the state of the art for predicting multi-solute equilibria. Four organic solutes representative of an existing contaminated ground water aquifer at a hazardous

male rats were subjected to study competitive adsorption. The specific objectives of this research were to

1. Determine the extent of irreversible adsorption to improve understanding of the effects of irreversibility on existing models.
2. Determine the extent of unequal competition for adsorption sites and the effect of such competition on existing models.
3. To compare several multi-site equilibrium adsorption models.
4. To test a modified model which attempts to include unequal competition in a predictive approach.

To pursue these objectives, several phases of experimental work were conducted. Single-site isotherms were developed, and the equilibrium model best fitting the observed data selected. Single-site desorption studies were next begun to determine the extent of single-site irreversible adsorption. Basic studies with sequential and simultaneous adsorptive variations were conducted to evaluate competitive adsorption and compare existing models. Limited multi-site experiments were also completed to examine model effectiveness in describing and predicting observed equilibria. Finally, the results of the basic equilibrium studies were used to test a model and its predictability potential.

CHAPTER 4 MATERIALS AND METHODS

4.1 Adsorbent

The adsorbent used in this work was Calgon Fulcrum 402, manufactured by the Calgon Corporation, Pittsburgh, Pennsylvania. This bituminous coal-based activated carbon is commonly used for removal of organic contaminants from industrial and municipal wastewaters. The manufacturer's specifications are provided in Table 4-1. The carbon was supplied by the manufacturer as a 12 x 40 mesh size (0.425mm x 0.425mm).

Two different carbon particle sizes were used in this work. Batch sorption experiments for single-solute systems were initially conducted using a carbon particle size of less than 100 mesh (average opening, 0.475mm). Subsequent continuous flow column experiments and other batch studies were conducted with a 120 x 140 mesh carbon size (0.425mm x 0.354mm). The preferred carbon was used to minimize equilibration times in batch experiments. The 120 x 140 mesh carbon was chosen for use in continuous flow column studies to minimize carbon losses while allowing reasonable equilibration times.

TABLE 4-1. Characteristics of 12 x 40 mesh Calgon Filtrasorb 300 granular activated carbon.

Parameter	Value
Total surface area, m^2/g (H_2 , BET procedure)	810-820
Effective size, mm	2.50-2.60
Mean particle diameter, mm	0.5-1.1
Iodine number	1000
Bulk density, $1000/g$ g/cm^3	30-31 0.40-0.41
Water soluble ash, percent	0.1
Total pore volume, cm^3/g	0.28
Micro-pore volume, cm^3/g (pore radius < 2 nm)	0.20
Transitional pore volume, cm^3/g (2 nm < pore radius < 10 nm)	0.05
Meso-pore volume, cm^3/g (pore radius > 10 nm)	0.03

Note: 1 mm = 10 Angstroms (\AA)




The powdered carbon was prepared by pulverizing a quantity of the 12 x 40 mesh virgin carbon in a laboratory blender and sifting with a 100 mesh U.S. standard sieve. Carbon retained by the sieve was repulverized and sieved until more than 90 percent of the original carbon volume had passed through the 100 mesh sieve. The powdered carbon was washed with distilled, deionized water that had been passed through a bed of granular activated carbon. Washed carbon was dried in porcelain dishes in a 105°C convection oven, cooled, and stored in a screw-cap glass bottle in a desiccator until used.

The 100 x 100 mesh carbon was prepared by pulverizing and sieving 12 x 40 mesh carbon in a similar manner. Carbon which passed the 100 mesh sieve and was retained by the 140 mesh sieve was washed, dried, and stored. Approximately 20 percent of the original 12 x 40 mesh carbon volume was actually retained as 100 x 100 mesh carbon after pulverizing. The remainder passed the 100 mesh sieve. Washing, drying, and storage procedures were identical to those used for the < 100 mesh carbon.

4-2 Aldehydes

The four organic compounds used in this investigation are listed in Table 4-1 and were chosen for several reasons. Three different classes of aldehyde chemicals are represented by the selection: alcohols (n-heptanol),

Table 4. Reported and observed properties of organic compounds studied.

Property	Compound	Formula	Calcd	Found	Alkyl- substituted
Molecular weight	$\text{CH}_3\text{C}_6\text{H}_4\text{CO}_2\text{H}$	$\text{C}_7\text{H}_6\text{O}_2$	134.10	134.10	$\text{CH}_3\text{C}_6\text{H}_4\text{C}(\text{CH}_3)_2\text{CO}_2\text{H}$
Structure					
Density	1.010	1.020	1.010	1.010	
Fusion, 25°C	solid	liquid	solid	solid	
Boiling point $^\circ\text{C}$, 740 mm	181	200	—	180.5	
Boiling point $^\circ\text{C}$, 740 mm	—	—	—	—	
Aqueous solubility g/100 g	26.5 (20 $^\circ\text{C}$) 25.5 (25 $^\circ\text{C}$) 30.5 (30 $^\circ\text{C}$)	—	—	—	
Alkylate notes	2-hydroxyethyl ester 2-methylpropyl ester 2-ethylhexyl ester	observed	—	3,4-dihydroxy- methylphenyl ketone	2-hydroxy- ethyl ketone

benzene (2,4-dihydroxybenzophenone), and phenols (*o*-cresol and allyl phenol). All four are relatively small, neutral molecules with varying degrees of polar character and solubilities. Consequently, equilibrium with carbon should be reached rather quickly. All four are aromatic and, thus, are readily analyzable using a UV spectrophotometer for single-solute systems and high performance liquid chromatography (also a UV technique) for mixtures. All four are also present in a hazardous waste site currently on the Environmental Protection Agency's national priority list (20). The accidental spill at the site has been characterized with leachate from wastes left in and on the ground by a no longer operating wood preserving plant. Studies are currently underway to determine a permanent site recovery scheme. The use of simulated activated carbon is one of several alternative technologies being considered. These four compounds are also representative of the waste streams of several industries including wood preservation, wood pulping mills, and coal gasification plants.

The organic compounds used in this research were prepared from Aldrich Chemical Company, Milwaukee, Wisconsin. The 2,4-dihydroxybenzophenone, *p*-allylphenol, and *o*-cresol were available at 99 percent purity. The *o*-cresol was available at 95 percent purity. The physical and chemical properties of the solutes are listed in Table 4-1, as well as the symbols chosen to represent them.

throughout the remainder of this work. Stock solutions of 500 mg/L were prepared using a reagent grade, buffered dilution water (described below). Stock solutions were stored at 5°C until needed. Solutions for analytical standard curves and solute quantitation were prepared by diluting aliquots of the stock solutions with more buffered dilution water. Feed solutions for continuous flow studies were prepared by transferring aliquots of stock solutions to volumetric flasks and diluting to volume with buffered dilution water.

4.1 Dilutions

A high purity, reagent grade, buffered dilution water was used for all experimental work. The pH of the buffered dilution water was adjusted to 6.8 ± 0.2 for all experiments. The pH of 6.8 was chosen because it is below the pK values of the solutes studied and is more typical of contaminated groundwater and dilute industrial waste streams. At pH of 6.8 the solutes are predominantly neutral species in aqueous solutions. Consequently, adsorption resulting from force interactions between the carbon surface and dissociated, ionic species are avoided, as are solubility effects and neutral-ionic species interactions.

The buffered dilution water was prepared by passing distilled water through a Milli-Q water purification system manufactured by the Millipore Corporation, Bedford,

ANALYTICALS. The treatment sequence consisted of activated carbon adsorption followed by acid-aid desorption. The buffered dilution water was made as 10.5 l batches. The reagent grade water was collected in a 25 l glass bottle and 40 ml of a stock 1.13 M phosphate buffer solution and 13 ml of approximately 1.5 M hydrochloric acid were added and mixed. The resulting solution was approximately 0.004 M with phosphate buffer and had a pH of 6.8 ± 0.2 . The 1.13 M phosphate buffer was made by adding 97.75 g of dibasic potassium phosphate (K_2HPO_4) and 186.8 g of monobasic potassium phosphate (KH_2PO_4) to reagent grade water and diluting to 1.0 l in a volumetric flask. All stock solutions were stored in amber colored glass bottles widely used for these reagents. A pH 10.5 \pm 0.2 buffered dilution water was prepared by adding 2.980 g of sodium bicarbonate ($NaHCO_3$) and 2.44 g of sodium carbonate (Na_2CO_3) to reagent grade water and diluting to volume in a 1.0 l volumetric flask. The resulting buffered dilution water was 0.012 M in bicarbonate and 0.005 M in carbonate.

4.4 Aqueous Solubilities

The difficulty of obtaining aqueous solubility data from the literature resulted in the determination of approximate solubilities during this investigation. The method used was similar to the method reported in a study of the solubility of organic esters in water (1981). To seven

10 ml. ampoules glass tubes were added 1.00-1.005 g of allyl phenol. Five 10 ml tubes were used for each of the remaining compounds, with approximately the same weight of compound added to the tubes. Approximately 10 ml. of reagent grade water were added to each tube and a loose screw cap installed. Distilled deionized water was added to two tubes of allyl phenol to determine if a measurable change in solubility would occur in the presence of the 0.01M buffer. The tightened caps were sealed with wax film and placed inside a double layer of wetted cook bags. The bags, with the tubes sealed inside, were submerged in a temperature-controlled, mixing water bath and maintained for 97 hours at $25 \pm 0.5^\circ\text{C}$. After removal from the bath the tubes sat for 48 hours to allow phase separation to occur. Aliquots of the extracted solutions were withdrawn and diluted in volumetric flasks to a concentration range convenient for analysis.

4.5 Equilibrium Isotherms

4.5-1 Glassware

All isotherm studies were conducted with 125 ml. Brlenmeyer flasks. All work with solutions was done with glassware only. All glassware was soaked in a chromic acid wash at the start of the experimental program. The glassware was rinsed, washed with hot, soapy water, triple rinsed with hot water followed by a distilled water triple rinse,

methanol and acetylac chloride excess prior to air drying. The chromic acid wash was performed only once at the beginning of the study. However, all of the subsequent cleaning steps were used as all glassware between runs throughout the remainder of the study. As soon as the flasks were dry, an aluminum foil cover was placed on each for storage until next use.

4.5.1 Isotopes Preparation

Single-isotope equilibration studies were conducted using a bottle leach procedure where volume was constant and surface area was varied. Various amounts of radiolabeled carbon were weighed on weighing paper using an analytical balance and transferred to labeled 125 ml flasks with aluminum foil covers. Sodium acetate was prepared by diluting aliquots from previously made stock solutions in volumetric flasks. To determine if different initial sulfate concentrations affected single-isotope equilibria, several concentrations were used for each sulfate and for both carbon particle sizes. Appendix A contains the single isotope leachware data and lists the initial concentrations used for each sulfate-carbon combination. Initial sulfate concentrations varied from approximately 10-100 mg/L with most data points collected at 10, 100 and 100 mg/L levels. Aliquots of 100 mL of the acetate solution were then transferred to each carbon-containing flask using volumetric pipettes. Three additional

flasks received 100 ml. of methanol solution, but no carbon, and were used as blanks to check for leaks losses due to volatilization and/or adsorption on flask walls. Two other sets of replicates were set up for each isotherm. Each set consisted of three flasks containing the same carbon mass. The carbon masses chosen for these two replicate sets represented a low and a high volatile fossil equilibration concentration over the range of the experimental data. The flasks were tightly sealed by the use of a wax file over the aluminum foil cover. The isotherm flask sets, including blanks and replicates, were placed on a rotary shaker and agitated at 140 rpm for the selected equilibrium time of 14 days.

Isotherms for all volatiles on both carbon particle sizes were determined at $25.0 \pm 0.5^\circ\text{C}$ in a constant temperature room (the room was in use for other, unrelated research as well). Isotherms for SO, AIP, and GGP using 100 x 140 mesh carbon were measured at room temperature ($23 \pm 1^\circ\text{C}$) as well to determine if temperature significantly altered the single-solute equilibria.

4.3.3 Equilibration Times

One of the most common criticisms of single-solute equilibrium adsorption data is inadequate equilibrium contact time. A review of attainment of equilibrium in adsorbed carbon isotherm studies with phenol (187) revealed

"equilibrium" times from a few hours to several weeks. Significant differences in adsorption capacities were reported, in some of what was expected due to variations in carbon properties and environmental conditions. The study showed that granular-activated carbon took up to 2 weeks to reach equilibrium with phenol and up to 3 weeks for o-chlorophenol. Powdered carbon adsorbents took from 3 to 5 days to reach equilibrium. Up to 40 percent of equilibrium values were reached in the first few hours, but the capacity for capacity was utilized very slowly.

The contact time required to reach equilibrium varies with the type and size of adsorbent carbon used, the nature and concentration of the solute, and mixing conditions. The potential for microbial activity which can interfere with adsorption equilibrium studies must also be considered for extended contact times. Preliminary tests were run to determine the appropriate equilibrium contact time for this study. A series of 125 ml. flasks were used with identical masses of carbon and initial solute concentrations. Two or three flasks were withdrawn for replicate analysis at various times into the equilibrium study. Flasks were also analyzed throughout the run. For the 100 x 160 mesh carbon DAP and AP reached equilibrium in less than 3 days, AT in less than 3 days, and OC in less than 3 days. A 10-day equilibrium period was chosen to allow a safety factor.

4.1.1 Sample Analysis

Samples for analysis were prepared by filtration using an all-glass, multipore filtration unit and 47 mm filters. Glass fiber or 0.45 μ m pore-size filters are commonly used. Whatman GFA glass fiber filters (1.6 μ m nominal diameter of retained particles) were selected for this study because of successful use of similar glass fiber filters in previous studies with phenolic compounds after testing for solute adsorption and carbon particle retention (19, 2015). Two filters were used for each sample to prevent any carbon particles from passing into the filtrate. Whatman GF/F filters (0.7 μ m nominal diameter of retained particles) were also available but were about four times the cost of the GFA filters, and since the smallest carbon particle size in the 100 x 140 mesh carbon was theoretically 100 μ m, the additional expense was deemed unnecessary. No carbon was ever visually observed in any filtrate although some fines were captured on the second filter. Filtration was accomplished with only a slight vacuum from a faucet separator at a low flow of water to minimize any volatilization of solute during passage through the filters and glass frit. About half of the 100 ml suspension was passed through the filter unitably to cross the frit and glass walls. Then a 50 ml screw-cap glass tube was inserted into the filter flask under the filter down spout, and the remainder of the carbon suspension was filtered. This

eliminated the need to clean the filter flask between every sample and flushed the flask and filters with approximately 10 to 40 full void volumes of sample prior to any sample actually being collected. The first portion of the fulvic suspension was discarded prior to insertion of the 20 ml collection tube. New filters were used for each sample; fulvic samples were sealed by tightened, lined screw caps until analysis;

4.4 Single-solute Adsorption

Experiments were conducted to determine the extent of single-solute irreversible adsorption for each of the four organic compounds used in this study. A 1.48 L glass screw-cap bottle was used as the batch adsorption reactor for each of the four solutes. The mass of carbon added to each reactor was 5.888 ± 0.001 g. The corresponding single-solute isotherm was used to estimate the initial solute concentration at which to equilibrate the carbon in order to start with a solid phase loading on the upper end of the luminescence data range. The surface solution was made by diluting an aliquot of a stock concentrated solution to 1.4 L in a volumetric flask. The entire 1.4 L solution was added to the reactor and carbon. The reactor was closed with a lined screw cap and a wax film seal. All four reactors were placed inside a round drum which was rotated

in a ball mill drive for a 15-day equilibration period in the constant temperature zone $21.0 \pm 0.05^\circ\text{C}$.

After the 15-day equilibrium period the canisters were removed from the rotating drive. The contents of each bottle were filtered in a similar manner to that described earlier for the adsorption isotherm flasks. After a sample of the filtrate was collected, as before, the carbon on the filter and on the funnel walls was carefully rinsed back into the reactor with a portion of the 1.0 L of acetate-free buffered dilution water that would be added to begin the next desorption extraction. After the carbon was returned to the reactor, the remainder of 1.0 L was added and the reactor resealed. When all four reactors were resealed, they were placed again in the rotating drum for another 15 days, after which the filtration, filtrate sample collection, and carbon rinse procedures were repeated. Thus batchwise extraction, as desorption process, was continued until the liquid-phase solute concentration was less than the detectable limit of approximately 0.5 $\mu\text{g/L}$. It was assumed that the equilibration time for desorption would not be longer than that for adsorption. The mass of solute irreversibly adsorbed was calculated by, first, calculating the mass of solute adsorbed during initial equilibration, second, summing the masses desorbed in all the extractions, third, subtracting the total mass desorbed from the mass initially adsorbed.

4.1 Analytical Procedures for Single-Solute Analysis

Each of the compounds studied exhibited UV radiation, therefore, solute concentrations were analyzed by UV spectroscopy. All single-solute analyses were performed with a Beckman-Elmer Model DU HP-8100A Spectrophotometer. All samples were measured at a 2.5 cm slit width using 1.0 cm standard fused quartz rectangular cells in a dual beam arrangement. Wavelength scans were conducted for each solute between 180 and 320 nm in order that the most useful wavelengths for each solute could be selected. A representative of the wavelength scan results are shown in Figures 4-1 through 4-4. The solute concentrations for all four scans were approximately 10 mg/L.

The wavelengths selected for the analyses were chosen by setting an arbitrary upper limit on concentrations to be measured and scanning for wavelengths at which absorbance conformed to Beer's Law throughout the desired concentration range. The concentration ranges and wavelengths used in this study are listed in Table 4-3.

A series of nine standards covering the analytical concentration ranges for each solute were prepared before each set of sample analysis. The absorbance of each standard was determined and a least squares linear regression analysis performed to generate the standard curve by which sample concentrations were calculated from sample absorbance values. No standard curve regression equations

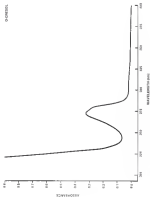


FIGURE 4. UV absorption spectra of poly(4-vinylpyridine) in benzene.

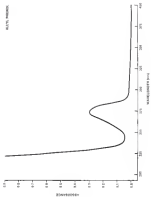
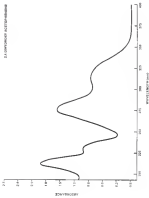


Figure 4-1 IR absorbance versus wavelength (nm) for allyl phenyl.



IR spectrum of 2,4-dichlorophenyl isocyanate. The spectrum shows characteristic absorption bands for the isocyanate group and aromatic ring.

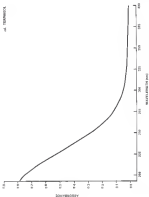


FIGURE 4-6. IR absorbance versus wavelength for *n*-tetradecane.

TABLE 4-1. Wavelengths and absorbance ranges for single-wavelength UV analysis.

Compound	Wavelength (nm)	Concentration Range (mg/l)
o-cresol	211.0	0-50
o-chlorophenol	211.0	0-50
m-terphenol	193.0	0-50
2,4-dihydroxy-acetophenone	217.1	0-50

showed an R^2 value (coefficient of determination) less than 0.910. The equilibrium solute concentrations, C_{eq} , were then used to calculate solid-phase concentrations, q_{eq} , by using the equation

$$C_{eq} = \frac{C_o - C}{R} \quad (4-1)$$

where C_o is the initial solute concentration and R is the mass of carbon. These values, C_{eq} and q_{eq} , were then used to calculate the adsorption isotherms.

4.4. Batch-Solids Adsorption Studies

4.4.1 Continuous-Flow Studies

A dual, continuous flow carbon contact system was used for all batch-solids studies. A schematic of the carbon contact system is presented in Figure 4-1. The dual system was designed to allow two independent experiments to be conducted simultaneously using only one pump drive. The feed container for each system was a 48 L glass bottle. Feed from the bottle was pumped through glass tubing to the top of the column by a dual stainless-steel peristaltic dosing pump system. The pumping rate was adjusted by a variable voltage motor speed control. The only nonglass segment of the feed transmission lines was the tubing used in the pump heads. The tubing was Tygon F-4040-A, a tubing designed to be resistant to the adsorption of organics. Two total 7000

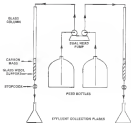


FIGURE 4-5 Schematic diagram of continuous flow carbon contact column system.

pump heads were used with this tubing. Glass tubing transmitted the feed to the top of each contacting column. Taking into an account of 500 hours of operation at the chosen pump speed.

The columns were 20 ml. graduated glass burets (1.2 cm i.d.) with glass stopcocks. The supporting base for the column was inside the column was a Pyrex-bond glass wool. Inlet tubes carried the column effluent a short distance to glass effluent manometers. Effluent was collected in a variety of condensers ranging in volume from 25 ml volumetric flasks to 1 l. glass bottles.

All glassware used in the multi-column studies was silanized. Unsilanized glass contains surface OH groups which form hydrogen bonds with oxygen atoms in solute molecules and can result in high adsorption, especially when the unsilanized glass has a large surface area, as does glass wool (111). An silanized material the adsorption of solute molecules is much weaker, since the hydroxyl groups are replaced by much less active siloxane groups. The silanization process was accomplished by soaking the glass wool in toluene containing 1 percent, by volume, of dimethyldichlorosilane (DCD incorporated) for 2 hours followed by a methanol rinse and a hexane chloroform rinse.

To prepare for a column experiment the columns were first cleaned according to the standard procedure described earlier. A glass wool plug was retained in a beaker of

buffered distilled water. When the air bubbles had been removed, the plug was inserted into the buret, which was filled with buffered dilution water. The glass wash plug was steady and lightly compressed in the bottom of the buret with a piece of glass tubing. In this manner all air was removed from the plug. Buffered dilution water was pumped through the system to insure that the plug was packed loosely enough to allow adequate flow with minimum head loss.

The carbon mass collected weighed 8.4488 ± 0.0002 g for all multi-column experiments. Previous work found that this size of carbon allowed satisfactory equilibrium times while minimizing the effect of carbon loss and weighing errors (104). It was also found that less than 5 g of carbon resulted in decreased amounts of cobalt that are to be accurately measured. The carbon was measured on weighing paper with an analytical balance and transferred to a 10 ml beaker for wetting. The slurry was then rinsed out of the beaker and into the column using a small glass funnel. Buffered dilution water was pumped through the column to check the head loss across the carbon and glass wool and, if the head loss was small, continued to be pumped overnight to equilibrate the carbon with the solvent.

Pump rates were maintained at 15.5 ± 1.5 milliliters per minute. The long glass burets used for the columns allowed head losses to increase while maintaining a constant

flow through the carbon bed. The approach was used to reduce head loss if the reduced loss due to the partially open valve, glass plug, and carbon threatened to overlie the level.

4.2.2 Simultaneous Addition

Two different methods of solute addition to the sorbing system were used. Simultaneous addition allowed the examination of competitive effects in twelve combinations of 3 solute pairs, four combinations of 3 solutes, and two combinations of 4 solutes. Sequential addition provided information regarding irreversible adsorption for solute pairs. Concentration ratios (mg/lmg/l) of approximately 18:30, 30:120, 120:30, and 18:18 were used for both methods of addition for OC/OC, NAP/NAP, and OC/NAP solute pairs. Concentration ratios of approximately 18:18:180, 18:120:30, 120:18:18, and 18:18:30 were used in simultaneous addition of NAP/OC/NAP combinations and ratios of 18:18:18:18 and 18:120:18:30 were used in simultaneous addition of all four compounds. The observed adsorption equilibria, together with single-solute isotherms and physicochemical data, provided information regarding mixed competition and irreversible adsorption for a group of small, low molecular weight, neutral organic compounds

3.2.1 Simultaneous Solute Addition

A 20 L feed solution was prepared as the desired concentration ratio by weighing amounts of pure solutes in a 20 mL glass beaker and dissolving the solutes in 1.0 L volumetric flask with buffered dilution water. After the first 1.0 L solution was added to the feed bottle, the same flask was used to measure the remaining volume of buffered dilution water. This minimized the amount of solute that may have remained on the walls of the flask initially. The buffered dilution water in the column was drawn down almost to the level of the carbon. The feed bottle was connected to the pump and the flow started. A stopwatch timed the experiment for efficient sample collection. At timed intervals different sample volumes were recorded and a portion of that volume added to 10 mL serum amp tubes with buffer-lined caps until analysis. Depending on the initial concentrations of solutes and time into the experiment, sample volumes collected and time intervals ranged from 25 mL and about 2 minutes to 10 L and 15 hours. Data tables for each experiment are found in Appendices B through E and contain the time intervals of sampling and sample volumes used for each solute combination and concentration ratio. If sample analysis could not be completed concurrently with the experiment to determine when equilibrium had been achieved, then the experiment was continued well beyond previously observed equilibrium times. Upon completion of

and experiments. The column containing water was washed, rinsed with buffered dilution water, 1.0 N Hydrochloric acid, and then buffered dilution water. The carbon and the glass wool support were discarded, and the burner, feed bottle, and effluent containers were cleaned with the standard washing method described earlier.

4.5.4 SEQUENTIAL SOLUTE ADDITION

Each set of equilibrium experiments at the concentration levels listed above was performed twice in order to reverse the order of solute addition. For example, for the solute pair OC/ALP, OC was the first solute added to the column, and when it had reached equilibrium, ALP was then added to the feed. The experiment was repeated at the same concentration ratios, except that ALP was the first solute added, then OC.

After equilibrating the column and fresh carbon with water overnight, the carbon was exposed to the first solute of the selected pair. The feed preparation procedure was the same as for simultaneous addition. Effluent collection, valve management, and sample preservation were also conducted with the same procedures.

After the first solute reached equilibrium, a new feed solution was prepared containing both solutes in the selected concentration ratio. The feed was initiated and sample collection began immediately. Since the carbon had

depth was as short, desorption of the first solute began almost immediately. Consequently, many samples were collected in the first few hours of the run. The same procedures were used for efficient collection, volume measurement, and sample storage as for the simultaneous addition experiments. The run continued until solvent and effluent solutes were within the approximate error of the analysis.

Finally, the concentration of the second solute was increased to the next desired concentration while that of the first solute remained the same. The feed preparation, sample collection, and volume measurements were repeated to generate a new set of equilibrium data at the new concentration ratio. A summary of the sequential addition process is given in Table 4-4 for compound A followed by compound B. The two experimental runs were repeated for A followed by A.

4.3.4 Soluto-solute Analysis

High Performance Liquid Chromatography (HPLC) was selected to analyze for individual compounds in solute mixtures. A Perkin-Elmer HPLC system, including a Series 3 high pressure pump, a constant temperature oven for the column, a Model LC-7B UV spectrophotometer, and a recorder, was used for all soluto-solute sample analysis. An Alltech 008 reverse phase HPLC column provided solute separation at a constant column temperature of 30°C. The mobile phase

TABLE 1-1. Method for sequential solute addition.
Compound A is followed by compound B.

Concentration for A = 10 mg/L	Concentration for A = 100 mg/L
Carbon equilibrated with A alone	Carbon equilibrated with A alone
New feed--B added at 10 mg/L and carbon equilibrated with A + B	New feed--B added at 10 mg/L and carbon equilibrated with A + B
New feed--B added at 100 mg/L and carbon equilibrated with A + B	New feed--B added at 100 mg/L and carbon equilibrated with A + B
End of experimental run	End of experimental run

selected was a 400- μ l volume of water and acetonitrile. Several ratios were tested during preliminary work to determine the optimum ratio. All separations were performed isocratically and were generally clean and sharp. Flow rates were varied between 1.2 and 1.8 ml/min to minimize analytical time while maintaining good peak separation. The flow rates selected resulted in column pressures less than 2000 psi. Sample volume was 100 μ l, determined by the loop injection system on the instrument.

A series of standards of known concentrations was analyzed during each run to produce a standard curve for each solute. A linear regression analysis was used to determine the equation of the linear standard concentration-time/peak height relationship. Solute concentrations were calculated by substituting the sample peak heights into the appropriate standard curve equation.

Wavelengths for each analysis were determined through a trial and error process and with the help of the single-solute absorbance versus wavelength scans presented earlier. Where possible, wavelengths were selected to enable the analysis of two solutes at the same wavelength, reducing the number of times a set of multi-solute samples had to be analyzed in order to quantify all solute concentrations. The full-scan absorbance values on the spectrophotometer were also saved for each analytical run to allow the peak height of the maximum expected concentration to

near about 85 percent of full scale. This allowed constant sensitivity for the expected range of compressions.

CHAPTER 3 RESULTS AND DISCUSSION

3.1. SINGLE-SOLUTE ADSORPTION STUDIES

The desired partitioning of a solute between liquid and solid phases is functionally expressed as an adsorption isotherm. The isotherm relates the solid-phase concentration of a solute to the equilibrium concentration of that solute in solution at a given temperature. Experimental isotherms have a variety of uses. They describe the capacity of an activated carbon to adsorb organic solutes from water or wastewater solutions. They provide information on the feasibility of adsorption for chosen solutes, for estimating carbon requirements, and for evaluating the performance of a variety of carbons under various loading conditions. More recently, adsorption isotherms have played an essential part in the development of predictive models and procedures for carbon system design and performance analysis.

3.1.1. Single-Solute Isotherm Data

Single-solute equilibrium studies in batch systems were conducted for all three solutes as discussed earlier. The data are presented in Tables A1-A3, Appendix A. Two single-solute equilibrium models, the Freundlich and the

Langmuir isotherms, Equations 1-6 and 1-21 were fit to the data using the least squares method in a linear regression analysis. The experimentally determined constants for the two models and the coefficients of determination are presented in Table 3-1. The Freundlich model best described the data for all four solutes and both carbon particle sizes. The Langmuirs are presented on log-log plots in Figures 3-1 through 3-4 as linear traces of the failed Freundlich equation.

Each of the traces shown in the figures represents several initial solute concentrations. (Appendix A contains the actual solute concentrations used for each compound.) The results indicate that the initial concentration had no detectable influence on the resulting isotherm for the solutes studied. This agrees with other researchers who evaluated the attainment of equilibrium in activated carbon isotherm studies (18,19). Their researchers cited several examples where previous work showed lower capacities for higher initial concentrations. However, it was concluded that incomplete attainment of equilibrium would subvert this effect and that no difference in adsorptive capacities would be observed if true equilibrium were reached. The lack of any observed effect on capacity with varying initial concentrations in this study supports the assumption that equilibrium was attained in the batch isotherm experiments.

TABLE 1.1. Comparison of forward-fit and backward-acceptance reduction equations for single-vehicle crashes.

Compound	Number of observations	Backward-acceptance		Forward-acceptance	
		$\hat{\theta}$	$1/\hat{\theta}$	$\hat{\theta}$	$1/\hat{\theta}$
				$\ln(\hat{\theta}/\hat{\theta}_0)$	$\ln(\hat{\theta}_0/\hat{\theta})$
forward					
2000-2010 north	13	105.1	0.009	1.013	0.098
2000-2010 north (10-1)	10	156.0	0.006	0.006	0.006
CRSS north	13	153.9	0.007	0.008	0.008
backward					
2000-2010 north	42	125.3	0.007	0.007	0.007
CRSS north	31	877.1	0.001	0.001	0.001
backward					
2000-2010 north	48	107.0	0.009	0.009	0.009
CRSS north	39	106.0	0.009	0.009	0.009
unimodal					
2000-2010 north	42	119.0	0.008	0.008	0.008
CRSS north	31	205.1	0.005	0.005	0.005

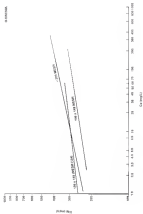
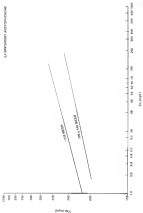


Figure 3-1. Sample-adsorbate isotherms for p-cresol.



FIGURE 1.2 Binding-volume absorption isotherms for a ligand.



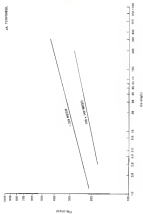


FIGURE 3-4. Sample-to-sample absorption coefficient (unitless) per unit length.

The relative adsorptive capacities with two different mesh sizes for various equilibrium solution concentrations of the solutes are shown in Figures 3-3 and 3-4. The observed trend in capacities did not correspond to trends in relative molecular weights or solubilities. Table 3-3 contains the experimentally determined solubilities for all four compounds. From the solubility data, OC would be expected to have the lowest adsorptive capacity and DAF and AF the highest. The solubilities did decrease as molecular weight increased, but neither parameter could be used to explain or anticipate the observed relative adsorptive capacities. Allig phenol exhibited the highest capacity over the entire 3 day equilibrium concentration range for both mesh particle sizes. For the powdered carbon isotherms (Figure 3-13 DAF adsorptive capacity was least, whereas for the 100/40 mesh carbon (Figure 3-4) AF was least adsorbed. The relative adsorptive capacities also changed as equilibrium solute concentrations increased. With the powdered carbon the order of increasing adsorption was DAF, OC, AF, and RLF, with AF and OC having very similar adsorptive capacities. However, at the upper end of the equilibrium concentration range the order was OC, DAF, RLF, and AF. In the upper concentration range both OC and DAF exhibited similar capacities as did AF and RLF. For the 100/40 mesh carbon only OC and DAF reversed relative capacities over the equilibrium concentration range and

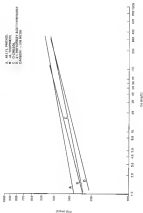


FIGURE 1-1 Benzene-vapor adsorption isotherms for 100 gram activated carbon, 25°C.

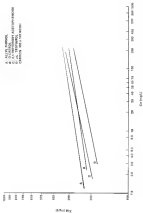


Figure 14. Benzene vapor adsorption isotherms for all four samples using 100 x 140 mesh carbon

Table 3-5. Experimental solubility data.

Compound	Solubility/g		Standard deviation (g/L)
	g/L	mg/L	
o-chlorol (OC)	34.84	149.9	0.33
4-(p) phenol (HAP)	4.317	43.9	0.050
2,4-dihydroxy- acetophenone (HAP)	2.298	23.1	0.016
o-terphenol (HAP)	3.383	33.9	0.034

showed similar behavior in the three most significant available concentration range.

The relative adsorption behavior observed in this study illustrates the difficulty in predictive modeling efforts for neutral, low molecular weight organic solutes representing different classes of compounds. The adsorption mechanisms for such compounds are a complex combination of physical and chemical force interactions that are the result of surface surface heterogeneity, molecular physical and chemical characteristics and solvent-solute interactions. Hydrophobic compounds adsorb on a much more predictive manner and correlate fairly well with simple characteristics such as molecular weight or solubility. This is because physical forces alone drive the adsorption to equilibrium. Similar success in predictability is also expected for ionic solutes where classical electrostatics determine the extent of adsorption. But the combinations of mechanisms for neutral, low molecular weight solutes of varying polarity provide any rational explanation of relative adsorptive capacities, such as those observed in this work.

The reported isotherm describes a set of adsorption conditions that also include an organic loading factor. This carbon loading is expressed in terms of limited acetone concentrations or milligrams of solute per milligram of carbon. Preliminary studies indicated that organic loadings greater than 1:1, in general, resulted in the onset of

multilayer adsorption and a rapid increase in solid phase solute concentrations over a very short range of equilibrium solution concentrations. This rapid deviation from the Freundlich model could be induced at any equilibrium concentration and was typical of Type II isotherms for the cases of multilayer adsorption in the Brunauer classification of isotherms (7). Organic loadings for all experiments were kept below the critical organic loading and provided an upper boundary for the adsorption systems studied.

The Freundlich model was found to give a good fit to the data throughout the concentration ranges studied. Deviations at the lower end of the equilibrium concentration ranges corresponding to dilute solution theory and Henry's law were not observed. However, the Freundlich model will not reduce to Henry's law when solute concentrations become low enough. From the deviation points for the isotherms in this study were not determined, the Langmuir equations have, as a lower boundary condition, the lowest measured equilibrium solute concentrations. The traces of the isotherms in Figures 3-1 through 3-4 represent the entire range of applicability of the Freundlich model parameters reported here. Extrapolations above and below these ranges may or may not conform to the model. At some point below the lowest equilibrium solution concentration conforming to Henry's law will occur, the Freundlich model can be modified to include a Henry's law term of lower equilibrium

representations are expected. A three-parameter model, such as the Toth equation discussed earlier in Section 3.4.3, could also be used, but the constants must be determined from the data by a nonlinear regression analysis.

3.4.3 Effect of Carbon Particle Size

The initial experimental approach for this work was to use powdered carbon for single-adsorbate isotherm studies and 180 μ m mesh carbon for single-adsorbate desorption and all multi-adsorbate studies. The use of powdered carbon results in rapid attainment of equilibrium, the larger carbon particle size facilitated desorption studies where recovery of the carbon mass was required after each extraction. The larger particle size also minimized carbon losses through the glass wool support in column studies. However, calculated solid phase loadings from powdered carbon isotherm equations did not agree with observed loadings of the 180 μ m mesh carbon in desorption experiments. Several flasks were prepared for each adsorbate using the 180 μ m mesh carbon to compare solid phase loadings with those observed for the powdered carbon. These flasks were equilibrated by the same method used to develop the powdered carbon isotherm data. In all cases the 180 μ m mesh carbon exhibited linear adsorption capacities that the powdered carbon over the entire equilibrium concentration range. Consequently, all single-adsorbate isotherm studies were reported using the 180 μ m mesh carbon.

The results of the additional isotherm determinations indicate that smaller particles also significantly affected equilibrium adsorption capacities. The isotherm data for both particle sizes for each solute are included in Appendix A. Figures 5-1 through 5-4 illustrate the observed effect of different particle sizes. In all four figures the adsorption capacities are lower for the larger particle size; however, the isotherm slopes changed only slightly. Since isotherm slope values are related to adsorption energies, the effect of particle size as to alter the number of sites and/or the surface area available to the sorbate.

The effect of smaller particle size on adsorption capacities could be a result of several factors. Solutes to which low equilibrium will show the same trend of reduced capacity with increasing particle size. However, successive isotherms for a series of particle sizes will also show increasing slopes as particle size decreases. This reflects the more rapid attainment of equilibrium for smaller particles at the larger concentration gradients at higher "equilibrium" concentrations. In this study preliminary experiments were completed to determine when equilibrium was reached for each compound in batch adsorption experiments. A ten-day safety factor was added to the equilibrium time of the slowest solute. Yet, all four solutes exhibited the same behavior. The absence of any observed effect by different initial solute concentrations

suggests the attainment of equilibrium in this study. In a previous work with lithium metal halogen salt systems, equilibrium was obtained in less than eight days for 90 and 100 mesh low molecular weight neutral phenolic compounds (104). Therefore, failure to obtain equilibrium is not considered to have caused the observed particle size effects.

A second cause of observed particle size effects on adsorption capacities involves significant differences in particle molecular dimensions and weight and a change in the pore size distribution caused by the grinding process. Would the micropore volume fraction increase and the transitional pore volume fraction decrease, that a powdered carbon would show increased capacities for the small, low molecular weight compounds and a reduced capacity for high molecular weight compounds. All four samples used in this study were small, low molecular weight compounds very similar in dimensions and molecular weight. Consequently, some other factor caused the observed capacity reduction.

The nature of the carbon particle may result in significant variations in activity as the particle is ground and moved into size fractions. Activation conditions may have been such that the inner cores of the lithium metal system were not completely activated and possessed a lower pore volume than the outer shells of the particles. Grinding away the outer shell and retaining only the inner core would then

result in lower adsorption capacities for larger particles since containing the less active inner cores. The smaller particles sizes would contain the more active outer shell fragments and exhibit higher adsorptive capacities than, otherwise, particles size would result in an increase in adsorptive capacity. The larger fraction of micropore and transitional pore volume would be lost in the water pump-out step past the 140 mesh screen. The inner cores retained by the 140 mesh screen would contain significantly less micropore volume, some of which may exist in voided, unutilizable channels. The effects of particle size on adsorption capacities observed in this study are probably due to such an uneven pore volume distribution with particle edges created by activation conditions. However, further work is required before definitive conclusions can be drawn.

The isotherm curves for CO in Figure 3-1 indicate a trend like a previous study (1964). This isotherm was developed under very similar conditions to those used in this study. Carbon particle size and preparation, CO concentration, equilibrium times, and isotherm procedures were similar. Since the referenced isotherm was conducted at 25°C and this study's isotherm at 54.5°C, the referenced isotherm should have shown lower capacities, not higher, if temperature affected the results. Selected points on the 54.5°C isotherm in this study were also determined at 25°C, and no effect of temperature was observed. The most

reasonable explanation may involve the means of grinding used. Both carbons were prepared as high speed blenders, but differences in blender configurations, blade design, and speeds could have resulted in particle splitting in the referenced study and particle shearing in this study. If the particles were split, then outer and inner pore volume distributions would be retained. A shearing process would leave behind a lower capacity carbon particle.

The effect of carbon particle size should be examined in any study where a particle size fraction does not include at least 75 percent of the original starting material. Cautionary about the commercially available carbon particle size, such as 1000 mesh carbon, cannot be made when laboratory studies use smaller selected size fractions without determining the effect of particle size. The evaluation and comparison of equilibrium methods, however, can be accomplished without knowing the effect of particle size on capacities, since the carbon's unique characteristics are held constant throughout each studies.

3.2 Single-Phase Adsorption Studies

Adsorption studies were conducted to determine the extent of irreversible adsorption of each of the four organic solvents using the 1000 mesh carbon. The carbon was first equilibrated with a solvent concentration calculated from literature data. The carbon concentration

corresponded to the expected equilibrium concentration measured during the isotherm experiments. The desorption/ extraction procedure should release the adsorption isotherm, if the adsorption were truly ideal and reversible. Two of the four desorption experiments were terminated prior to completion of the extraction because of equipment failure. The desorption data for all four columns are listed in Table 3-1, Appendix B. Figures 3-7 and 3-8 illustrate the desorption isotherms compared with the adsorption isotherms for two of the four columns. A clear hysteresis effect is evident indicating significant irreversible adsorption. Table 3-2 lists the weight percent of each molecule that was irreversibly adsorbed.

The hysteresis effect is well known in the adsorption of gases whose molecular and pore sizes are of similar dimensions. The resulting large surface area of contact can exhibit strong bonding energies, even though the forces are physical, not chemical, in nature. Consequently, long equilibrium times are required to allow for the slow diffusional process to remove the adsorbed molecule. When the equilibrium relative concentrations in this study were below the analytical detection limit of 5.1 mg/L for *o*-cresol and ethyl phenol, equilibration continued for 30 days. No detectable desorption was observed following this extended contact time. This indicated that failure to attain equilibrium was not a significant factor in the study. The



FIGURE 3-7. Adsorption-desorption and desorption-desorption isotherms for benzene, chloroform, and carbon tetrachloride.



Figure 10. Langmuir adsorption and desorption isotherm for ally phos.

TABLE 3-3. *Alkyl-alkene adsorption (unpublished)*

Compound	Percent Irreversibly adsorbed
<i>n</i> -decane	87.8
allyl alcohol	84.7
1,4-dioxane	70.8*
1-hexene	65.3*

*Desorption experiments terminated before reaching lower detection limits in liquid phase equilibrium concentration. Completion of the extraction would have resulted in slightly lower percent irreversible adsorption.

observations that initial solute concentration did not affect solid phase loadings during isotherm determinations also supports the assumption of equilibrium in the 18-day contact time. These results agree with other studies in which initial solute concentration and different procedures for isotherm development have developed as experimental biases in explaining observed hysteresis (113, 114).

The differences in the amount of irreversible adsorption among the solutes could be caused by several factors. The interaction of benzene π -electrons with partial positive charges on carbonyl or quaternary surface functional groups as a chelation mechanism has already been discussed. Amongst these basic physisic binding mechanism are the type and position of solute molecule functional groups. These structural variations may intensify site binding energies through inductive effects; however, much work is needed to substantiate such a hypothesis. Steric interference may not permit sufficient solute-surface contact to allow the π -bond, charge transfer mechanism to function. Hydrogen bonding on a solute like HAP may form a large hydration layer and may hinder the solute from close approach to a surface site. The extent of irreversible adsorption will also vary from surface to surface since no two surfaces have identical surface structure or chemistry.

Results of previous research on desorption using single-solute batch systems have been conflicting. In a

study of eight commercially available cations the amount of irreversibly adsorbed phenol equaled only 3-4 percent of the total adsorbed [84]. Irreversible adsorption for p-nitrophenol was less than 5 percent of the total observed adsorption. However, in another study, irreversible adsorption of phenol was approximately 50 percent of total adsorption [77]. In studies where short equilibration times were used for initial adsorption (on the order of hours), little or no irreversible adsorption was observed. However, in studies where equilibration times were much longer and the second, slow, diffusion-controlled phase of adsorption allowed to reach equilibrium, there is evidence of significant irreversible adsorption. To improve predictive models by accounting for irreversible adsorption, a more complete understanding of single-site irreversibility is needed. Currently only one model has been modified in an effort to account for the results of surface heterogeneity. The level of understanding of the mechanisms behind irreversible and competitive adsorption is rudimentary, at best. The approach used in the model modification was to add parameters and estimate their values by statistical curve-fitting analysis to produce a best fit of existing multi-site data. The development of a mechanistically fundamental model on statistically existing large amounts of multi-site data to some physicochemical properties are beyond existing capabilities.

4.2 Competitive Adsorption

4.2.1 Kinetic Simultaneous Adsorption

All natural solid-liquid equilibrium systems involve a heterogeneous surface and equal competition for adsorption sites on that surface. Activated carbon, however, has been shown to be heterogeneous. The nature of the surface functional groups, especially those containing oxygen, has already been discussed. The single-solute desorption results in this study imply that adsorption to such specific functional groups was the principal mechanism of adsorption for the four chosen solutes.

The results of the kinetic simultaneous adsorption studies are found in Tables 3-4 through 3-6. The results in Table 3-4 show that RLP adsorbed to a much greater extent than OC. The relative adsorptions observed are consistent with relative molecular weights and solubility. Alkyl phenol has a higher molecular weight, lower solubility, and greater hydrophobicity from the larger alkyl group on the benzene ring. Single-solute isotherm data reflect the expected relative surface concentrations. However, the large differences in adsorption of each solute at similar equilibrium solution concentrations were not expected. Adsorptive capacities for each solute in single-solute systems differed by less than 50 percent at equilibrium concentrations of 10 and 100 mg/L. In the kinetic system

TABLE 1. Simultaneous solution equilibrium data for the ACP/OC system (a).

Experiment	ACP		OC	
	C_0	R_0/R	C_0	R_0/R
	(mg/L)	(mg/g)	(mg/L)	(mg/g)
1	8.5	110	8.8	28
2	18.8	43	18.5	144
3	83.8	214	8.8	8
4	18.5	248	28.5	52

the separation for ALP and DC differed by more than 31 percent. Such results could be explained by adsorption rates observed during preliminary equilibrium studies in which RBP adsorbed much faster than DC, which adsorbed at a rate slower than any of the remaining three solutes. The higher affinity for carbon exhibited by ALP with a much faster mass transfer rate would result in significant sorption competition for sites between ALP and DC. The high degree of cross-solubility discussed earlier would preclude any significant adsorption of ALP and adsorption of DC over the DC molecule created the viscosity of the adsorption sites.

The results for the ALP/RBP heptane pair are included in Table 3-5. In this binuclear system RBP outcompeted ALP for adsorption sites. The RBP molecule has a higher molecular weight and a lower viscosity than does the ALP molecule. However, single-solute isotherm data show ALP to have a much greater affinity for the carbon than RBP (see Figures 3-4). Based on the isotherm data, ALP would be expected to out-compete RBP for adsorption sites. A possible explanation for this apparent anomaly may be a difference in mass transfer rates (bulk transport) that would allow the RBP molecule to reach available sites faster than AL molecules. No mass transfer rates were measured during this study, but the results from the preliminary single-solute equilibrium time determination indicated that RBP has the highest rate

TABLE I-4. Simultaneous adsorption equilibrium data for AgP/NaP solute pairs—

Experiment	AgP		NaP	
	C_0	x/y	C_0	x/y
	(mg/l)	(mg/g)	(mg/l)	(mg/g)
1	8.8	42	8.7	149
2	10.1	18	10.2	249
3	91.0	147	9.1	58
4	100.5	175	10.5	174

or adsorption of all four solutes. The combination of greater hydrophobicity, higher mass transport rates, and irreversible adsorption would allow DAP to outcompete AIP. Since the adsorption mechanisms for AIP and AI are not known, it is difficult to assess the effect of type and density of carbon surface functional groups that may be specific or preferential for DAP and AIP.

The results for the OC/AIP solute pair are found in Table 1-4. The DAP molecule outcompeted the OC molecule for sites. Based on molecular weight and solubility considerations, such a result could be anticipated. The single-solute isotherms for DAP and OC are almost identical (see Figure 1-11, especially near 18 mg/L, one of the kinetic initial concentrations). At 100 mg/L DAP showed a slightly higher capacity (less than 3 percent). Consequently, given similar mass transport rates, the two solutes should have exhibited similar separation. However, since OC showed the slowest rate of adsorption and DAP the highest rate in equilibrium time determinations, DAP successfully outcompeted OC for sites by occupying them first. Little displacement would occur since significantly irreversible adsorption has been shown for both solutes in the carbon used in this research. Again, the type, density, and specificity/ preferences of carbon surface functional groups are unknown, and their effect on unequal competition cannot be defined without further research.

TABLE 3-4. Benzenehexa addition equilibrium data for OC/DAP solvent pair.

Experiment	OC		DAP	
	C_{OC}	C_{OC}^0	C_{DAP}	C_{DAP}^0
	(mg/L)	(mg/g)	(mg/L)	(mg/g)
1	18.3	25	8.8	120
2	9.4	4	16.2	120
3	222.8	183	18.3	120
4	105.8	51	94.8	54

In all the bimolar experiments, the total adsorptive capacity for both solutes together did not exceed the single-solute adsorptive capacity of the carbon for the solute with the highest capacity of the pair. This is consistent with an earlier study of a four-component system where only about 60 percent of the anticipated carbon adsorptive capacity from single-solute capacities was realized (57). However, others have reported an overall increase in the total carbon adsorptive capacity for multi-solute mixtures (51). The equilibrium capacity for each solute on the activated carbon was adversely affected by the presence of another solute. The explanation of the slight decrease in total adsorptive capacity lies in the use of available surface area. If the total surface area of the activated carbon available for the adsorption of two solutes was not more than the area available for one solute, then adding that area with a less effectively adsorbed compound would result in a less efficient use of the available area. Since all four solutes are fairly similar in molecular weight and size, such an assumption is reasonable.

The above results confirm the heterogeneous nature of activated carbon with respect to adsorption sites and the physicochemical nature of the solutes. These effects, such as unequal competition, are not included in existing multi-solute equilibrium models.

The structural nature of the solutes can increase or decrease adsorption effectiveness. The addition of functional groups to the benzene ring of the phenol molecule affects polarity and steric hindrance and, consequently, adsorbability. The decrease in polarity of OC by the addition of the alkyl group in RA and the other groups for RBP and RP have obviously affected adsorbability. Increases in steric hindrance also increase hydrophobicity, improving adsorption effectiveness. Polar and steric effects may partially explain the more effective adsorption of RBP over OC even though their single-point isotherms are very similar. Assuming a perpendicular orientation with adsorption occurring at the hydroxyl end of the molecule, the hydroxyl and alkyl group hydrogen atoms interface with each other. The resulting atomic arrangement is spatially expanded and relatively inflexible and would reduce intraparticle diffusion. However, the meta and para groups on the RBP molecule could form an intramolecular hydrogen bonding arrangement reducing the molecule's steric hindrance and improving adsorption efficiency.

5.1.3 Multicomponent Equilibrium Model Application

Several existing multi-solute equilibrium models were tested using the previously discussed results. The Competitive Langmuir model and the Uncompetitive Langmuir model require single-solute isotherm determinations and the

calculations of the Langmuir isotherm describing these isotherms. The simplified IAD model also requires single-solute isotherm data but uses constants from the Freundlich model describing the isotherms. Because experimentally derived constants from single-solute data are required, the models are difficult to use in a truly predictive manner. The models also assume equal competition and reversible adsorption in the adsorption process. Since the results of IADs, and other recent work, indicate significant irreversibility and unequal competition for the systems studied, the above models would not be expected to adequately describe the data. The results of the application of these three models are presented in Tables 3-3 through 3-5 for the zinc/cadmium solution of the ALP/OL, ALP/OLP, and OL/OLP solute pairs. The experimental results are included for comparison.

The simplified IAD model was recently modified in an attempt to include the effects of unequal competition and irreversible adsorption (184). The simplified IAD model was selected for empirical verification for several reasons. This model uses the Freundlich parameters, which often yield very accurate descriptions of single-solute data. The model, when modified by placement of empirical terms, proved to describe multi-solute equilibria even when unequal competition and irreversible adsorption are not significant.

TABLE 3-7. Predicted and measured solid-phase equilibrium values for simulated solution of barite from data.

Model	Concentrations ratios (mg/L/mg/L)							
	T = 25°C		25-125		25-25		25-100	
	$\frac{a_{\text{Ba}}}{a_{\text{H}_2\text{O}}}$	$\frac{a_{\text{SO}_4}}{a_{\text{H}_2\text{O}}}$	$\frac{a_{\text{Ba}}}{a_{\text{H}_2\text{O}}}$	$\frac{a_{\text{SO}_4}}{a_{\text{H}_2\text{O}}}$	$\frac{a_{\text{Ba}}}{a_{\text{H}_2\text{O}}}$	$\frac{a_{\text{SO}_4}}{a_{\text{H}_2\text{O}}}$	$\frac{a_{\text{Ba}}}{a_{\text{H}_2\text{O}}}$	$\frac{a_{\text{SO}_4}}{a_{\text{H}_2\text{O}}}$
Experimental data	1.00	50	60	140	120	1	140	60
Concentrations (average)	250	420	140	5	1550	60	900	170
From temperature	1812	420	641	3	1812	60	3210	470
Sampled (145)	200	45	90	170	311	10	270	70
Integrated Sampled (145)	140	10	60	150	150	5	200	60

Notes: Values for $\frac{a_{\text{SO}_4}}{a_{\text{H}_2\text{O}}}$ are mg/g .

TABLE 1-8. Predicted and measured solid-phase equilibrium values for simultaneous sorption of benzene and ethyl acetate.

Model	Concentration ratios (mg/kg dry TOS)							
	0.0017		0.0184-1		0.0184-1		0.0184-1	
	X/Y_{exp}	X/Y_{calc}	X/Y_{exp}	X/Y_{calc}	X/Y_{exp}	X/Y_{calc}	X/Y_{exp}	X/Y_{calc}
Experimental data	61	140	13	100	100	94	130	1000
Competition Unimodal	780	340	170	160	1000	75	210	170
Good competitive isopropyl	1000	300	200	160	1000	75	1000	400
Simplified isopropyl	110	61	40	200	100	13	200	100
Unimodal simplified isopropyl	50	100	13	200	100	40	70	100

Note: Values for X/Y are mg^2/g^2 .

Table 5-4 Predicted and measured solid-phase equilibrium values for maximum addition of bicarbonate per kg.

Model	Concentration ratios (mg/kg/L)							
	20:10:4		1:1:0.5		10:1:0.5		10:1:0.5:0	
	$\frac{X_{\text{OC}}}{X_{\text{DOC}}}$	$\frac{X_{\text{DOC}}}{X_{\text{DOC}}}$	$\frac{X_{\text{OC}}}{X_{\text{DOC}}}$	$\frac{X_{\text{DOC}}}{X_{\text{DOC}}}$	$\frac{X_{\text{OC}}}{X_{\text{DOC}}}$	$\frac{X_{\text{DOC}}}{X_{\text{DOC}}}$	$\frac{X_{\text{OC}}}{X_{\text{DOC}}}$	$\frac{X_{\text{DOC}}}{X_{\text{DOC}}}$
Experimental data	15	170	4	250	140	100	50	40
Competitive Langmuir	470	370	20	200	400	10	517	400
Binary competitive Langmuir	400	370	100	200	400	40	100	400
Regulated log	200	100	40	515	100	33	200	200
Empirical Regulated log	41	140	5	204	100	40	10	200

Note: Values for DOC are mg/L.

Original competition for absorption sites was modified in the simplified IAF model by adding α_1 terms as shown below,

$$Q_2 = R' \left(\frac{R_1 - 1}{R'} \right) \left[\frac{R_1}{\alpha_1} C_1^{-1/\alpha_1} \right] \left[\frac{R_1}{R} \left(\frac{R_1}{R} \right)^{1/\alpha_1} C_1^{-R/\alpha_1} \right]^{1/\alpha_1} \quad (3.1)$$

where

$$R' = \left[\frac{(R_1/\alpha_1)}{R} \right] \quad \text{and} \quad R = \left[\frac{R_1}{R} \right]$$

The Freundlich constant, R_1 , was modified to allow adjustment of R values of individual solutes such that the solute with a larger R would not outcompete a solute with a lower R. The term R is proportional to the magnitude of a amphiprotic leathorn. The largest R results in an leathorn that is higher than a lower R-value leathorn. All multi-solute models predict the solute with the larger R to outcompete the solute with the smaller R. In this work GAP outcompeted ALP even though ALP had a significantly higher Freundlich R value. The GAP molecule also outcompeted the OC molecule even though the R for OC was higher. A reduction in the R values for ALP and OC would result in improved model performance.

The values for the competition term were determined by nonlinear Statistical Analysis System (SAS) programming which provided the best fit of the model to the data. The values for the competition terms for each solute pair are

linear in $\ln(\text{solid phase})$. From the magnitude of the values it is apparent that both terms are significant in the model development. The results of the application of the improved Simplified IAB model are also included in Tables 3-7 through 3-9. In all three solute pair simultaneous adsorption studies the improved Simplified IAB model gave, by far, the best description of the experimental data. All models predicted RfP to outcompete SC. The two Langmuir-based models failed to predict the relative effectiveness of adsorption. This is not surprising since the single-solute Langmuir model failed to describe that data. The Simplified IAB model based better, primarily because it used Freundlich parameters. The Freundlich model accurately described the single-solute adsorption data in this work. It is interesting to note that the Semi-competitive Langmuir model gave predictions that are in greater error than those of the Competitive Langmuir model. The Semi-competitive Langmuir model is intended to account for adsorption on sites that are not subject to competition. However, the model assumes that unequal competition occurs only for the solute with the larger solid-phase capacity. When solutes with equal or lower solid-phase capacities outcompete the solute with the larger solid-phase capacity, the model fails. The results in Tables 3-8 and 3-9 describe just such situations, and the Langmuir models both fail even to predict the more effectively adsorbed solute. The Simplified IAB model predicted

TABLE 5-10 Comparison between the two approved simplified
140 model.

Initial Rate (1/2)	"1"	"2"
ALL/00	1.343	1.340
ALL/00P	1.345	1.346
NO/00P	1.318	1.319

the more extensively adsorbed solute in all cases except three. The improved Simplified IAS model provided a much more accurate description of the order of effectiveness and the magnitude of the equilibrium solid-phase loadings.

3.3.3 Model Predictability

The modification of the Simplified IAS model required parameters from multi-solute data. This provided an improved description of the data but did not result in any model predictability. If the model is to be applied to multi-solute mixtures, some predictability is desired to avoid excessive and extensive laboratory analyses. In the work which initially improved the Simplified IAS model (16), the competition factors were correlated with a solubility term. Solubility was chosen because, of all the solute physicochemical parameters, solubility best correlated with adsorbability as discussed earlier. The form of the solubility factor is

$$\frac{(S_1 - S_2)}{S_1} \quad (3-21)$$

where S is solubility and $S_1 > S_2$. This allows for discrimination between equal $(S_1 - S_2)$ values when S_1 and S_2 are different.

Plots of the solubility factors are shown in Figures 3-7 and 3-14. The trend of increasing competition factor

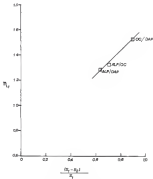


FIGURE 5-5. Correlation between the reliability factor and the competition factor, R_1 .

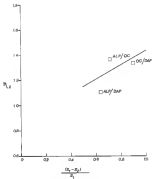


FIGURE 9-10: Correlation between the solubility factor and the composition factor, x_2^s .

with literature solubility data across eight systems used to test proposed model modifications.

In this work, both competition factors are significant. In the previous work only the competition factor associated with the higher solubility systems was found to be significant. Although much more work is needed to verify the correlation and determine the effects of different factors on such a correlation, the results provide some measure of predictability to the model. Thus, knowing what monomers are present, what the single-volume Flory-Huggins interaction parameters are for those constituents, and the constituent solubilities, improved predictions of multi-volume equilibria are possible. The extension of this predictive model to multi-volume systems may require the development of a lumped solubility parameter and combined Flory-Huggins parameters to represent the combined effects of all solutes in the mixtures.

3.3.4 Monomeric Equilibrium Solubility

Four tri-volume and two four-volume simultaneous solubility experiments were conducted to demonstrate the effect of unequal competition on more complex mixtures. The absorption data are tabulated in Appendix A, Tables B-1 through B-4. The final equilibrium solid and fluid phase concentrations are presented in Table 3-1.

TABLE 3-11: Multi-solute simultaneous addition equilibration data and predicted values.

	NAP	OC	ATP	AT
C_{eq}	9.4	10.1	24.0	—
C_o -observed	14	1.8	274	—
-predicted	13	16	206	—
C_{eq}	8.8	142.0	9.8	—
C_o -observed	19	117	47	—
-predicted	10	318	75	—
C_{eq}	80.8	8.8	10.2	—
C_o -observed	271	4.5	15	—
-predicted	248	17	28	—
C_{eq}	18.3	10.4	8.8	—
C_o -observed	148	53	71	—
-predicted	58	84	125	—
C_{eq}	9.8	18.3	10.0	10.0
C_o -observed	181	18	—	—
-predicted	85	72	185	12
C_{eq}	10.0	101.1	10.0	10.0
C_o -observed	73	82	—	—
-predicted	24	208	78	4

Notes: C_{eq} is the dilution feed concentration in mg/l
 C_o is the equilibrium solid phase loading in mg/g.

In the third tri-solute experiment, the same concentration ratios of DMP:OC:KLP were 1:1.12:1.04.2 mg/L. The effect of the higher concentration of KLP agrees with what would be expected from the relative surface plots in Figure 7-8. KLP alone had the highest single-solute capacity of the three compounds in this experiment. The remaining solutes showed very similar increases in equilibrium concentrations around 10.8 mg/L. The large difference in the solid phase loadings between the two demonstrates the effect of significant unequal competition. Differences in mass transfer rates, surface specificity/preference, and irreversible adsorption all probably contributed to the observed unequal competition. The combined adsorption of all three solutes (123 mg/g) was only slightly more than the single-solute capacity (114 mg/g) of the most effectively adsorbed solute, KLP. This indicates that the available surface area for KLP was essentially the same area available for OC and DMP. This implies that the density of surface-specific surface functional groups was low, and all three solutes were competing for the same sites.

In the second tri-solute experiment, the final concentration ratios of DMP:OC:KLP were 1:1.10:0.93.4 mg/L. The total adsorption for all solutes (123 mg/g) was slightly less than the OC single-solute capacity (125 mg/g). This again implies that most sites were active adsorption sites for all three solutes, although not of equal adsorption

adsorption. The NAP molecule, at less than 50 percent of the OC feed concentration, showed an almost equivalent solid phase equilibrium concentration. This demonstrates again the unequal competition between two solutes whose single solute isotherms nearly coincide.

The success of NAP in out-competing OC and ALP for adsorption sites is evident in the results of the third tri-solute experiment. In this experiment the NAP-OC:ALP feed ratios were 57.0:59.5 50:50 mg/L. The total adsorption for all three solutes (120 mg/g) was only slightly less than the single-solute solid phase capacity for NAP (100 mg/g) at 57.0 mg/L feed concentration. Over 50 percent of the total solid phase sorption loading consisted of NAP. If equal competition occurred, the ALP fraction should have been much higher, based on relative single-solute adsorptive effectiveness (see Figure 3-6).

In the fourth tri-solute experiment the feed concentration ratios of NAP:OC:ALP were 5 : 113.2 : 10.0 mg/L. The most effective adsorption was exhibited by NAP. If equal competition had occurred, then the NAP and OC solid phase loadings should have been much closer, based on single-solute capacities. The ALP molecule should have been the least effectively adsorbed solute in this experiment, assuming equal competition. The effects of unequal competition were again clearly evident. The argument that such an order in adsorption effectiveness could have been expected based

or relative solubilities fails when compared with the single-solute isotherm data. The two solutes with almost identical single-solute isotherm curves (OC and OAP) had very different solubilities (OAP: 3.3 percent, OC: 3.2 percent).

Results from the two experiments using four solutes each confirm the previously observed trends. The solid phase equilibrium concentrations of AOP and OT were not measured because peak separation in the liquid chromatograph did not occur with the column (OC) used. Solid mobile phase and mobile phase concentrations as well as another column (ICL) failed to separate the two solutes.

Overall competition was further demonstrated by the time varying concentrations of the experiments as they approached equilibrium. In all four of the two-solute experiments significant amounts of OC were initially adsorbed, then desorbed as the slower adsorbing solutes displaced OC. This unusual competition would have been more extensive if significant irreversible adsorption had not occurred. The time-concentration profiles in Tables 23 through 24 imply that adsorption thermodynamics favor the adsorption of OAP over OC. This could also be viewed as functional group preference for OAP over OC due to the chemisorption mechanism. The actual chemisorption mechanisms for all four solutes are unknown but probably involved the π -electron system of the benzene ring and

specific functional group interactions discussed in the literature review. Such time-construction profiles typically display narrow minima when solvent composition and concentration change. In order to develop dynamic models that accurately predict such observed behavior, equilibrium models must be improved to include the effects of the type of solvent competition observed here.

Application of the simplified IAS model to the univariant and four-solute experiments show similar effects of solvent competition. The predicted values of equilibrium solid phase concentrations for DAP are significantly underestimates the observed solid phase loadings. The model overpredicts the EC and ALP equilibrium solid phase loadings. A comparison of observed and predicted values is shown in Table 5-11. Some of the deviation can be attributed to the model development itself. The simplified IAS model was developed as a thermodynamic calculation, and, consequently, some accuracy was sacrificed. However, the consistent trends in over- and underpredicting equilibrium values illustrates the problems inherent in the assumption of equal competition and irreversibile adsorption when both the original IAS and simplified IAS models have made.

The application of the improved, simplified IAS model discussed for multi-solute studies cannot be accomplished until a satisfactory procedure can be developed to estimate competition factors for all solutes in the matrix. Several

different approaches in this study to use the binomial distribution to arrive at competition factors in the three-solute system were unsuccessful. The results of this research indicate that a competition factor for each solute could be significant. The work in which the improved model was developed found that only the competition factor of the solute with the lower Freundlich K value was significant (188). Since only these two solutes have attempted to use the improved model, much more work is needed to determine the validity and applicability of the competition factor approach. Extension of the improved model beyond binomial systems is warranted if the model is to be of value in multi-solute dynamic solute modeling approaches.

3.4 Sequential Solute Addition

Sequential solute addition studies can yield information concerning irreversible adsorption in binomial systems. If irreversible adsorption is a significant event, then current multi-solute equilibrium models will not be able to adequately describe such data. Single-solute irreversible adsorption has already been discussed. A series of sequential solute addition experiments were performed to determine whether or not irreversible adsorption was a significant mechanism in explaining deviations from expected behavior. Current multi-solute equilibrium models assume complete reversibility.

The results of the sequential addition experiments are provided in Table 3-13. The data are arranged by solute pairs and relative concentration ratios. The calculated amount of irreversible adsorption is tabulated for the fixed solute of the pair fed to the reactor. The amount of irreversible adsorption can be calculated by

$$A/R_{ir} = A/R_{seq} - A/R_{sim} \quad (3-10)$$

where A/R is in mg/g and the subscripts refer to irreversibly adsorbed (ir), adsorbed during sequential addition (seq), and adsorbed during simultaneous addition (sim) (14). Adsorption during simultaneous addition includes all effects of competition. The effect of irreversible adsorption is minimized when both solutes compete simultaneously for available sites. However, in sequential addition the sites on which both solutes can adsorb are already occupied by the primary solute. The desorption/adsorption isotherms have a wide range, and a series of displacement, or desorption/adsorption, reactions can occur. To compare simultaneous and sequential addition, all experiments must be done at the same concentration ratios.

The reversible adsorption described in Table 3-11 generally is less at lower concentrations. When the carbon is equilibrated first with a single solute, the solute begins to adsorb on the most thermodynamically favored

TABLE 3-13: Irreversible adsorption for bicyclic esters at differing equilibrium concentration ratios (mg/kg/μg). All values in mg/g.

Solute	Concentrations (mg/kg/μg) selected (mg/g)			
	10:100	10:1000	100:10	100:100
<u>SC/DBP</u>				
SC/ADP	85.8	77.4	84.8	180.0
SC/DBP	134.5	130.5	11.7	53.8
<u>ADP/DBP</u>				
ADP/SC	83.8	113.8	84.4	84.8
ADP/DBP	53.8	85.8	81.3	83.8
<u>DBP</u>				
DBP/ADP	-13.8	8.4	-13.8	-0.1
DBP/SC	18.4	4.5	-18.4	18.3

sites. Consequently, the chemisorption bonding energies are greatest at these sites. When these sites become occupied, the solute adsorbs on less energetically favored sites, and so on, until physical adsorption is the final mechanism. At lower solute concentrations a larger solute mass fraction is adsorbed at high energy sites. As the solute concentration is increased, the adsorption occurs primarily at lower energy sites. These are the sites where desorption begins. The high energy sites are where irreversible adsorption occurs.

As the second solute is added, it, too, adsorbs by thermodynamic preference. However, the desorption energy of an already adsorbed solute must be provided. Obviously, where the primary solute is most tightly bound, where the energies are most favorable for a desorption-adsorption interaction. If the primary solute is at a low concentration, most molecules will be bound on the high energy sites, and the greatest irreversibility is expected. As the secondary solute concentration increases, the effect on solute-solute repulsive energies improves the thermodynamics of displacement, and more desorption of the primary solute from higher energy sites is expected. When the initial concentrations of the primary solute are higher (100 mg/L versus 10 mg/L), then a larger mass fraction is adsorbed on lower energy sites. The addition of a second solute will result in greater desorption, or lower irreversibility. The

results as Table 2-11 show, in general, higher reversibility of lower solute concentrations and less reversibility at the 18-500 mg/l ratio. The extent of irreversibility is affected by concentration ratios. The difference in irreversibilities supports the concept of a wide spectrum of chemical and physical bonding energies. If most of the primary solute is bound on high energy sites, then the percent reversible adsorption will be less. If the primary solute is bound to a significant number of low energy sites, then the percent reversibility will be greater.

The lower amount of reversibility was demonstrated by 05, followed by 44B. The two solutes exhibited very little irreversibility with either 05 or 44B at any concentration ratio. Such results indicate a rather strong chemisorption bonding energy at a large number of sites for 05. The bonding energies for 44B were weaker. In the single-solute irreversibility studies 44B exhibited the lowest percent of irreversible adsorption of the three solutes used in this phase of study. However, in the simultaneous adsorption studies, 44B competed unexpectedly well in binary mixtures. This seems to indicate that competition was had a greater influence on final equilibrium conditions than irreversibility. The heterogeneity of the carbon surface and its functional group chemistry results in a system of adsorption phenomena spanning adsorption energies from the weak, physical adsorption to the strongest of the

chemisorption bands. The nature of the solute also plays a role in competition and irreversibility.

No current multi-solute equilibrium model attempts to include the effects of irreversible adsorption. The improved version of the Simplified IAS model was also modified to attempt to separately sites the equation by inclusion of statistically determined irreversibility parameters (184). Some improvement in model description of adsorption data was observed. Attempts to correlate the parameter with solute properties, like the previously discussed solubility term, showed some trends but lacked sufficient data to draw any conclusions. Little data are available in the literature to be used to validate the model. A successful competition parameter inclusion is a prerequisite for model modifications for irreversibility as well.

CHAPTER 4 SUMMARY AND CONCLUSIONS

The described work was undertaken to examine the effects of activated carbon heterogeneity on the competition and irreversible adsorption of four organic solutes in multi-component systems. Single-solute studies to develop isotherms and to determine the extent of irreversible adsorption were followed by kinetic simultaneous and sequential sorption studies. Several kinetic equilibrium models were compared and a recent improvement in the Simplified ISM model tested. Derived conclusions are drawn from this work:

1. Carbon particle size was significantly after isotherm equation parameters and must be considered in experimental design.
2. Good single-solute isotherm data and accurate mathematical descriptions of the data are critical for the success of equilibrium and dynamic predictive model development for the carbon adsorption process.
3. The solutes studied in this research showed significant irreversibility in single-solute systems, confirming the importance of

chemisorption, it specified active adsorption mechanisms in carbon adsorption.

4. Local competition for adsorption sites was a significant factor in the adsorption of the mixtures used in this research. Current multi-site equilibrium models did not successfully describe the experimental data.
5. Irreversibility in the biosolids experiments was significant and is not included in existing desorption or predictive equilibrium models.
6. An improved version of the Simplified SAS model was tested for description and prediction of local competition in adsorption. The improved version was superior to three other models in describing the experimental data. A correlation between competition factors and relative adsorbility terms indicated a predictive capability for the biosolids version of the model.

CHAPTER 7 ENGINEERING SIGNIFICANCE

As the understanding of the adsorption process improves, mathematical descriptions of the process find more application in design strategies. Several researchers are developing and applying dynamic adsorption models in an effort to reduce the time and costs associated with laboratory preliminary and pilot scale studies. Currently, design methods are based on empirical rules of thumb or single-solute adsorption parameters. Incorporating all solutes into total organic carbon or chemical oxygen demand parameters is an improper adaptation, given the concern for, and presence of, small concentrations of toxic or hazardous organic solutes in the nation's water resources. Design strategies must change to be able to optimally separate such solutes from aqueous systems, be they industrial waste systems or contaminated rivers and aquifers.

The development of predictive, dynamic, multi-solute models attempts to optimize the design process at minimum cost. Essential to the success of such dynamic models is the equilibrium portion of that model. Current multi-solute equilibrium models fail to adequately describe adsorption equilibria data where significant mutual competition and

Identifiable recognition error. These models are based on the assumptions of equal competition and complete reversibility. Improved understanding of these phenomena can lead to improvements in the multi-agent equilibrium model and eventually in the design process.

The improved, simplified IAB model has the potential to significantly upgrade existing dynamic models. The use of velocity data, single-agent motion parameters, and knowledge of the constituents of a water stream make the application of the model practical. However, the model must be validated for application to multi-agent systems beyond two-component systems before its application in design or process evaluation can occur.

APPENDIX A
SINGLE SCOUTS DESCRIPTION, ASSIGNMENT,
AND RELIABILITY DATA

TABLE 3-4. Single solute batch desorption data (all values in milligrams)

X_0	R_0	Allyl alcohol		2,4-dihydroxy- benzophenone		n-butylalcohol	
		X_d	R_d	X_d	R_d	X_d	R_d
275.5	15.4	294.8	25.4	298.5	43.5	293.4	34.9
278.2	8.5	261.6	12.4	260.2	18.7	248.5	12.9
282.4	2.4	285.8	8.6	288.5	12.7	276.6	16.6
294.8	1.8	286.5	3.7	275.8	9.5	218.8	12.8
283.1	1.2	291.5	2.7	240.2	8.4	262.2	5.2
266.8	0.8	288.8	2.6	298.8	5.4	198.8	—
285.8	8.8	298.8	2.7	278.5	8.4	—	—
254.5	4	280.1	—	268.8	2.7	—	—
—	—	—	—	292.4	—	—	—

R_0 : Solid phase solute mass at start of extraction.

R_d : Solute mass desorbed during extraction.

n : Batch limit of desorption.

—: Repetition furnished values reaching low-resolution limits.

Table A-2. Northern Gulf of Mexico oil & gas seeps.

C_m	Carbon mass	Carbon loading	C_p	α/η
(mg/L)	(g)	(mg/mg)	(mg/L)	(mg/g)
51.4	0.8323	0.20	3.4	222
51.4	0.8348	0.20	4.3	228
51.4	0.8389	0.20	3.8	225
51.4	0.8388	0.20	4.3	228
51.4	0.8380	0.20	3.3	222
51.4	0.8181	0.20	4.3	228
51.4	0.8183	0.20	8.1	234
51.4	0.8175	0.20	25.4	242
51.4	0.8187	0.20	28.4	244
51.4	0.8187	0.20	29.3	246
51.4	0.8187	0.20	28.8	247
289.8	0.4033	0.25	22.1	282
289.8	0.4033	0.24	48.2	277
289.8	0.4039	0.24	28.3	278
289.8	0.4033	0.24	27.1	282
289.8	0.4049	0.40	88.2	291
289.8	0.4043	0.30	88.7	292
289.8	0.4030	0.48	127.4	294
289.8	0.4030	2.80	188.8	299
289.8	0.4030	2.80	183.8	297
289.8	0.4030	2.40	145.4	293
140.8	0.4030	0.41	34.0	274
482	2.400	0.48	189	299

TABLE A-4. Isotherm data for α -crossed, α -H with carbon.

T_{eq} (deg/K)	Carbon mass (g)	Carbon loading (mg/g)	C_{eq} (mg/L)	k_1/k_2 (deg/g)
293.0	0.0002	0.24	1.1	242
293.0	0.0002	0.26	1.0	244
293.0	0.0050	0.29	1.0	270
293.0	0.0050	0.30	1.0	271
293.0	0.0050	0.30	1.4	271
293.0	0.0050	0.30	0.0	297
293.0	0.0052	0.32	10.0	322
293.0	0.0052	0.34	17.1	325
293.0	0.0055	0.37	20.0	327
293.0	0.0040	0.42	24.1	340
293.0	0.0050	0.46	47.0	354
293.0	0.0050	0.46	49.0	363
293.0	0.0050	0.46	47.0	366
293.0	0.0050	0.52	60.0	365
293.0	0.0040	0.55	77.2	372
293.0	0.0050	0.55	82.4	382
293.0	0.0062	0.63	100.4	389
293.0	0.0060	1.00	127.0	399
293.0	0.0122	1.20	128.4	396
293.0	0.0200	1.40	129.0	395
293.0	0.0100	2.07	197.2	397
<hr/>				
105.0	0.0000	0.21	0.0	295
105.0	0.0000	0.21	0.4	296
105.0	0.0001	0.26	1.0	295
105.0	0.0000	0.29	0.2	277
105.0	0.0000	0.34	13.0	300
105.0	0.0000	0.61	20.0	317
105.0	0.0000	0.52	16.0	312
105.0	0.0000	0.62	17.4	316
105.0	0.0001	0.61	16.0	316
105.0	0.0100	0.65	16.1	318
105.0	0.0101	1.02	46.0	347
<hr/>				
51.0	0.0000	1.04	51.0	410
51.0	0.0000	1.04	20.0	420
51.0	0.0000	1.04	10.0	414
51.0	0.0000	1.15	10.0	422
51.0	0.0001	1.20	10.0	446

TABLE A-1 Surface data for alloy 6060 (8) at 1% test carbon.

C_0 (mg/L)	Carbon conc. (g)	Carbon loading (mg/mg)	C_0 (mg/L)	X_0 (mg/g)
205.0	0.0000	0.34	18.3	293
205.0	0.0000	0.81	58.4	300
205.0	0.0000	0.97	48.4	295
205.0	0.0000	0.97	42.8	290
205.0	0.0000	0.97	40.5	287
205.0	0.0000	0.51	73.3	318
205.0	0.0000	1.03	136.8	331
205.0	0.0000	1.03	148.1	335
205.0	0.0000	1.03	138.8	333
183.0	0.0000	0.47	37.8	287
183.0	0.0000	0.50	42.0	288
183.0	0.0000	0.80	40.3	300
183.0	0.0000	0.50	40.7	302
183.0	0.0000	0.50	40.4	304
183.0	0.0000	0.80	48.5	309
183.0	0.0000	0.57	46.4	310
183.0	0.0000	0.80	48.8	315
183.0	0.0000	0.40	52.6	306
183.0	0.0000	0.44	50.0	304
183.0	0.0000	0.44	52.6	308
183.0	0.0000	0.44	52.6	309
183.0	0.0000	0.44	52.6	310
183.0	0.0000	0.40	7.0	334
183.0	0.0000	0.31	11.0	331
183.0	0.0000	0.31	13.0	340
183.0	0.0000	0.31	18.4	348
183.0	0.0000	0.34	21.8	353
183.0	0.0000	0.40	55.4	367
183.0	0.0000	0.51	68.1	387
183.0	0.0000	0.80	84.2	398
183.0	0.0000	1.00	78.2	312
183.0	0.0000	1.00	71.3	303
183.0	0.0000	1.00	71.8	318
183.0	0.0000	1.00	83.3	314
500	1.000	0.50	574	338

TABLE A-2. Continued.

C_D (mg/L)	Carbon mass (g)	Carbon loading (mg/kg)	C_M (mg/L)	$X(t)$ (mg/g)
55.5	0.0018	0.35	1.3	230
55.5	0.0053	0.35	1.4	242
55.5	0.0099	0.35	1.5	252
55.5	0.0093	0.35	1.6	261
55.5	0.0198	0.37	1.7	268
55.5	0.0145	0.38	1.8	273
55.5	0.0178	0.39	1.9	278
55.5	0.0171	0.39	2.0	285
55.5	0.0145	0.41	2.1	288
55.5	0.0180	0.43	2.2	293
55.5	0.0180	0.43	2.3	295
55.5	0.0180	0.43	2.5	298

TABLE 8-5. Feather data for wild geese, < 200 week
carbon.

δ_{13}^C (mg/L)	Carbon conc (g/g)	Carbon loading (mg/mg)	C_m (mg/L)	g/g
143.4	0.0401	0.34	0.3	237
143.4	0.0343	0.30	1.8	293
143.4	0.0282	0.38	4.1	303
143.4	0.0179	0.32	28.3	378
143.4	0.0208	0.32	38.3	376
143.4	0.0138	0.52	28.3	374
143.4	0.0148	1.83	40.7	407
147.5	0.0808	0.34	0.4	254
147.5	0.0798	0.29	0.3	270
147.5	0.0750	0.28	0.9	275
147.5	0.0730	0.38	0.8	273
147.5	0.0744	0.27	0.5	282
147.5	0.0431	0.22	1.8	313
147.5	0.0482	0.34	4.5	313
147.5	0.0880	0.38	12.7	313
147.5	0.0582	0.42	31.8	348
147.5	0.0432	0.44	24.8	374
147.5	0.0453	0.46	12.7	384
147.5	0.0431	0.48	33.3	385
147.5	0.0288	0.43	47.8	401
147.5	0.0349	0.38	43.3	405
147.5	0.0308	0.48	75.8	431
147.5	0.0289	0.45	35.4	431
147.5	0.0340	1.04	125.8	435
147.5	0.0270	0.44	124.8	435
147.5	0.0208	1.04	120.3	435
154	0.0561	1.05	177	473
154	0.0508	1.83	277	474
154	0.0479	1.83	277	475
154	0.0450	1.38	314	481
154	0.0387	1.47	340	489

TABLE A-1 Greenhouse data for 3,4-dichlorophenyl isothiocyanate, 200 x 140 mm carbon

C_{eq}	Carbon mass	Carbon loading	C_{eq}	q_{eq}
(mg/L)	(g)	(mg/g)	(mg/L)	(mg/g)
44.4	0.0242	0.38	5.9	273
44.4	0.0228	0.31	7.2	264
44.4	0.0218	0.27	8.4	248
44.4	0.0214	0.27	1.1	213
44.4	0.0208	0.23	1.2	211
44.4	0.0206	0.24	1.8	212
44.4	0.0175	0.23	4.7	224
44.4	0.0167	0.26	6.1	224
44.4	0.0163	0.26	6.6	223
44.4	0.0177	0.27	7.1	223
44.4	0.0177	0.27	7.2	223
44.4	0.0177	0.27	7.5	223
44.4	0.0152	0.28	8.6	232
44.4	0.0183	0.28	9.1	233
74.0	0.0413	0.23	8.8	232
74.0	0.0373	0.24	7.5	237
74.0	0.0314	0.21	14.1	216
74.0	0.0314	0.23	16.8	213
74.0	0.0314	0.23	16.8	213
74.0	0.0248	0.26	16.7	248
74.0	0.0223	0.43	16.8	274
74.0	0.0236	0.43	43.4	284
74.0	0.0243	0.47	36.2	282
74.0	0.0227	0.42	45.1	288
74.0	0.0270	1.17	75.2	288
74.0	0.0215	0.79	85.2	324
132.0	0.0542	0.38	37.4	282
132.0	0.0542	0.38	45.8	301
132.0	0.0492	0.42	66.7	270
132.0	0.0484	0.42	57.2	280
132.0	0.0426	0.45	64.2	288
132.0	0.0384	0.50	76.4	305
132.0	0.0344	0.66	68.4	301
132.0	0.0332	0.62	77.7	306
132.0	0.0272	0.71	140.0	307
132.0	0.0282	0.96	127.5	311
132.0	0.0282	0.96	128.0	318
132.0	0.0282	0.96	128.0	314
132.0	0.0121	1.40	155.0	278
132.0	0.0088	2.52	172.5	218

TABLE A-8
Isotopic data for α -hydrogenol, 100 x 100 mesh
carbon.

C_{10}	Carbon mass	Carbon loading	C_{10}	ΔC
(mg/L)	(g)	(mg/mg)	(mg/L)	(mg/g)
154.5	0.0000	0.33	10.7	334
154.5	0.0001	0.33	20.2	317
154.5	0.0002	0.33	31.4	314
154.5	0.0001	0.34	30.3	317
154.5	0.0002	0.33	31.3	333
154.5	0.0006	0.33	73.3	334
154.5	0.0002	0.33	71.8	333
154.5	0.0002	0.33	113.3	333
154.5	0.0002	0.43	113.3	343
154.5	0.0002	0.33	113.3	333
154.5	0.0002	0.37	113.3	373
45.5	0.0004	0.19	3.2	176
45.5	0.0004	0.20	3.4	180
45.5	0.0004	0.21	4.3	188
45.5	0.0004	0.21	5.8	193
45.5	0.0004	0.23	6.3	194
45.5	0.0004	0.23	6.9	202
45.5	0.0004	0.23	6.9	202
45.5	0.0004	0.23	7.3	213
45.5	0.0004	0.24	7.6	203
100.0	0.0009	0.26	5.5	186
100.0	0.0047	0.23	8.8	206
100.0	0.0047	0.23	9.3	203
100.0	0.0047	0.23	11.7	199
100.0	0.0079	0.27	13.6	216
100.0	0.0011	0.23	16.7	214
100.0	0.0008	0.36	18.6	218
100.0	0.0009	0.40	47.6	201
100.0	0.0003	0.33	48.6	213
100.0	0.0003	0.40	68.6	203
100.0	0.0003	0.33	68.3	203
RT7	1.000	0.40	133.3	184

TABLE A-8. Isotopic data for untopped, < 200 week samples.

C_{org} (mg/L)	Carbon conc. (g)	Carbon loading (mg/mg)	$\delta_{13}\text{C}$ (mg/L)	$\delta_{15}\text{N}$ (mg/g)
183.0	0.0383	0.20	1.3	200
183.0	0.0400	0.24	7.0	248
183.0	0.0398	0.24	3.8	249
183.0	0.0399	0.28	8.0	248
200.0	0.1080	0.23	1.3	200
200.0	0.0920	0.23	1.4	214
200.0	0.0920	0.23	2.2	219
200.0	0.0893	0.24	2.1	217
200.0	0.0798	0.28	8.3	243
200.0	0.0780	0.27	6.8	245
200.0	0.0754	0.27	8.0	248
200.0	0.0740	0.27	6.3	245
200.0	0.0703	0.28	9.2	248
200.0	0.0650	0.30	12.5	285
200.0	0.0600	0.38	18.2	300
200.0	0.0554	0.37	24.0	323
200.0	0.0500	0.41	41.5	327
200.0	0.0480	0.46	51.8	340
200.0	0.0450	0.46	51.4	341
200.0	0.0400	0.49	80.8	343
200.0	0.0400	0.51	65.0	357
200.0	0.0350	0.50	75.0	371
200.0	0.0300	0.88	87.0	345
200.0	0.0300	0.91	113.0	388
200.0	0.0200	0.91	120.0	378
200.0	0.0200	0.93	128.6	378
200.0	0.0200	1.61	169.4	374
200.0	0.0400	0.87	388.0	452
200.0	0.0300	1.08	398.3	423
200.0	0.0500	1.80	391.0	429
200.0	0.0300	1.88	399.4	440

Table A-18. A(1) phenol solubility data (25°C)

Sample	Concentration	Mean	Standard deviation
	(g/L)	(g/L)	(g/L)
A1	6.296 6.227 6.268	6.227	0.002
A2	6.227 6.248 6.245		
A3	6.274 6.298 6.227		
A11 a		6.244 6.266	6.400 6.640
B1	6.288 6.288 6.400	6.312	0.006
B3	6.400 6.242 6.242		
B5	6.288 6.288 6.227		
A11 b		6.278 6.278	2.813 2.818
C1	6.227	6.284	-
C2	6.227		
C3	6.288		
D4	6.227	6.227	-
D5	6.227		
D6	6.227		
E	6.227	6.227	0.002
F	6.227		
G	6.288		
All samples	6.227	6.227	0.002

Table A-11. Solubility data for o-cresol, p-cymenyl-
acetylenes and o-terpinolol (20°C).

Sample	Concentration (g/L)	Mean (g/L)	Standard deviation (g/L)
o-cresol			
A	21.6	21.6	0.25
B	22.0		
C	21.1		
D	21.7		
E	21.8		
2,4-DAP			
A	2.282	2.298	0.014
B	2.288		
C	2.287		
D	2.294		
E	2.294		
o-terpinolol			
A-1	2.268	2.264	0.001
	2.258		
	2.268		
A-2	2.262	2.265	0.008
	2.262		
	2.273		
A-3	2.423	2.428	0.004
	2.418		
	2.439		
All A		2.277	0.007
B	2.422	2.428	0.004
C	2.428		
D	2.431		
E	2.422		
All Samples		2.272	0.004

APPENDIX B

SEQUENTIA] AND SIMULATION SELETE NOCETON DATE
FOR THE D-CRUCIL/ALYL PRINEL ABOVE P4]B

TABLE 3-1. Sequential spike addition data, *o*-arsenal
followed by allyl phenyl.
Feed concentration: 10.0 mg/L (pre-spike)

Time (hr)	Effluent composite sample volume (L)	Concentration of <i>o</i> -arsenal (mg/L)	
		Composite sample	Grab sample
0.0	4.16	0.0	0.0
10.0	4.16	0.3	0.2
20.0	8.32	0.2	0.2
29.0	7.13	0.4	0.3
38.0	5.87	0.7	0.7
47.20	0.10	0.0	0.0
52.0	7.47	0.0	00.0

TABLE B-2. Sequential sucrose additions data, p-nitrophenol
 followed by allyl phenol.
 Feed concentrations: 50.0 mg/L [p-nitrophenol],
 10.0 mg/L [allyl phenol]

Time (hr)	Sample volume (L)	Concentration (mg/L)	
		p-nitrophenol	allyl phenol
0.00	0.000	10.0	1.0
0.10	0.000	11.1	1.0
0.18	0.000	11.4	1.0
0.25	0.000	11.6	1.0
0.37	0.000	11.8	1.0
0.50	0.000	11.7	1.0
0.68	0.000	11.6	1.0
0.80	0.000	12.0	1.0
0.90	0.000	12.0	1.0
0.95	0.000	12.0	1.0
1.00	0.000	12.0	1.0
1.05	0.000	12.0	1.0
1.10	0.000	12.0	1.0
1.15	0.000	12.0	1.0
1.20	0.000	12.0	1.0
1.25	0.000	12.0	1.0
1.30	0.000	12.0	1.0
1.35	0.000	12.0	1.0
1.40	0.000	12.0	1.0
1.45	0.000	12.0	1.0
1.50	0.000	12.0	1.0
1.55	0.000	12.0	1.0
1.60	0.000	12.0	1.0
1.65	0.000	12.0	1.0
1.70	0.000	12.0	1.0
1.75	0.000	12.0	1.0
1.80	0.000	12.0	1.0
1.85	0.000	12.0	1.0
1.90	0.000	12.0	1.0
1.95	0.000	12.0	1.0
2.00	0.000	12.0	1.0
2.05	0.000	12.0	1.0
2.10	0.000	12.0	1.0
2.15	0.000	12.0	1.0
2.20	0.000	12.0	1.0
2.25	0.000	12.0	1.0
2.30	0.000	12.0	1.0
2.35	0.000	12.0	1.0
2.40	0.000	12.0	1.0
2.45	0.000	12.0	1.0
2.50	0.000	12.0	1.0
2.55	0.000	12.0	1.0
2.60	0.000	12.0	1.0
2.65	0.000	12.0	1.0
2.70	0.000	12.0	1.0
2.75	0.000	12.0	1.0
2.80	0.000	12.0	1.0
2.85	0.000	12.0	1.0
2.90	0.000	12.0	1.0
2.95	0.000	12.0	1.0
3.00	0.000	12.0	1.0
3.05	0.000	12.0	1.0
3.10	0.000	12.0	1.0
3.15	0.000	12.0	1.0
3.20	0.000	12.0	1.0
3.25	0.000	12.0	1.0
3.30	0.000	12.0	1.0
3.35	0.000	12.0	1.0
3.40	0.000	12.0	1.0
3.45	0.000	12.0	1.0
3.50	0.000	12.0	1.0
3.55	0.000	12.0	1.0
3.60	0.000	12.0	1.0
3.65	0.000	12.0	1.0
3.70	0.000	12.0	1.0
3.75	0.000	12.0	1.0
3.80	0.000	12.0	1.0
3.85	0.000	12.0	1.0
3.90	0.000	12.0	1.0
3.95	0.000	12.0	1.0
4.00	0.000	12.0	1.0
4.05	0.000	12.0	1.0
4.10	0.000	12.0	1.0
4.15	0.000	12.0	1.0
4.20	0.000	12.0	1.0
4.25	0.000	12.0	1.0
4.30	0.000	12.0	1.0
4.35	0.000	12.0	1.0
4.40	0.000	12.0	1.0
4.45	0.000	12.0	1.0
4.50	0.000	12.0	1.0
4.55	0.000	12.0	1.0
4.60	0.000	12.0	1.0
4.65	0.000	12.0	1.0
4.70	0.000	12.0	1.0
4.75	0.000	12.0	1.0
4.80	0.000	12.0	1.0
4.85	0.000	12.0	1.0
4.90	0.000	12.0	1.0
4.95	0.000	12.0	1.0
5.00	0.000	12.0	1.0
5.05	0.000	12.0	1.0
5.10	0.000	12.0	1.0
5.15	0.000	12.0	1.0
5.20	0.000	12.0	1.0
5.25	0.000	12.0	1.0
5.30	0.000	12.0	1.0
5.35	0.000	12.0	1.0
5.40	0.000	12.0	1.0
5.45	0.000	12.0	1.0
5.50	0.000	12.0	1.0
5.55	0.000	12.0	1.0
5.60	0.000	12.0	1.0
5.65	0.000	12.0	1.0
5.70	0.000	12.0	1.0
5.75	0.000	12.0	1.0
5.80	0.000	12.0	1.0
5.85	0.000	12.0	1.0
5.90	0.000	12.0	1.0
5.95	0.000	12.0	1.0
6.00	0.000	12.0	1.0
6.05	0.000	12.0	1.0
6.10	0.000	12.0	1.0
6.15	0.000	12.0	1.0
6.20	0.000	12.0	1.0
6.25	0.000	12.0	1.0
6.30	0.000	12.0	1.0
6.35	0.000	12.0	1.0
6.40	0.000	12.0	1.0
6.45	0.000	12.0	1.0
6.50	0.000	12.0	1.0
6.55	0.000	12.0	1.0
6.60	0.000	12.0	1.0
6.65	0.000	12.0	1.0
6.70	0.000	12.0	1.0
6.75	0.000	12.0	1.0
6.80	0.000	12.0	1.0
6.85	0.000	12.0	1.0
6.90	0.000	12.0	1.0
6.95	0.000	12.0	1.0
7.00	0.000	12.0	1.0
7.05	0.000	12.0	1.0
7.10	0.000	12.0	1.0
7.15	0.000	12.0	1.0
7.20	0.000	12.0	1.0
7.25	0.000	12.0	1.0
7.30	0.000	12.0	1.0
7.35	0.000	12.0	1.0
7.40	0.000	12.0	1.0
7.45	0.000	12.0	1.0
7.50	0.000	12.0	1.0
7.55	0.000	12.0	1.0
7.60	0.000	12.0	1.0
7.65	0.000	12.0	1.0
7.70	0.000	12.0	1.0
7.75	0.000	12.0	1.0
7.80	0.000	12.0	1.0
7.85	0.000	12.0	1.0
7.90	0.000	12.0	1.0
7.95	0.000	12.0	1.0
8.00	0.000	12.0	1.0
8.05	0.000	12.0	1.0
8.10	0.000	12.0	1.0
8.15	0.000	12.0	1.0
8.20	0.000	12.0	1.0
8.25	0.000	12.0	1.0
8.30	0.000	12.0	1.0
8.35	0.000	12.0	1.0
8.40	0.000	12.0	1.0
8.45	0.000	12.0	1.0
8.50	0.000	12.0	1.0
8.55	0.000	12.0	1.0
8.60	0.000	12.0	1.0
8.65	0.000	12.0	1.0
8.70	0.000	12.0	1.0
8.75	0.000	12.0	1.0
8.80	0.000	12.0	1.0
8.85	0.000	12.0	1.0
8.90	0.000	12.0	1.0
8.95	0.000	12.0	1.0
9.00	0.000	12.0	1.0
9.05	0.000	12.0	1.0
9.10	0.000	12.0	1.0
9.15	0.000	12.0	1.0
9.20	0.000	12.0	1.0
9.25	0.000	12.0	1.0
9.30	0.000	12.0	1.0
9.35	0.000	12.0	1.0
9.40	0.000	12.0	1.0
9.45	0.000	12.0	1.0
9.50	0.000	12.0	1.0
9.55	0.000	12.0	1.0
9.60	0.000	12.0	1.0
9.65	0.000	12.0	1.0
9.70	0.000	12.0	1.0
9.75	0.000	12.0	1.0
9.80	0.000	12.0	1.0
9.85	0.000	12.0	1.0
9.90	0.000	12.0	1.0
9.95	0.000	12.0	1.0
10.00	0.000	12.0	1.0

TABLE 4-1. Sequential solute addition case, n=crust followed by shift phase.
Feed concentrations: 10.0 mg/l (n=crust),
50.0 mg/l (shift phase)

Time (hr)	Sample weight (g)	Concentration (mg/l)	
		n=crust	shift phase
0.07	0.010	11.0	51.0
0.23	0.010	11.3	51.5
0.39	0.010	11.9	54.0
0.54	0.010	12.0	71.0
0.70	0.010	12.7	74.4
0.86	0.010	13.4	75.0
0.99	0.010	13.3	79.0
0.99	0.002	13.3	84.0
0.91	0.004	11.0	84.3
0.94	0.000	10.0	84.0
0.80	0.000	10.0	87.5
0.67	0.000	10.7	87.0
0.73	0.000	10.0	87.0
0.70	0.000	10.0	89.5
0.83	0.000	10.4	87.0
0.89	0.000	10.4	88.0
0.94	0.000	10.4	88.0
0.89	0.000	10.4	89.0
1.30	0.100	10.4	89.0
2.01	0.100	10.2	87.8
1.33	0.100	10.1	89.0
1.02	0.100	10.0	89.0
1.53	0.100	10.1	88.0
1.01	0.100	10.1	90.0
1.74	0.100	10.1	90.0
1.00	0.100	10.1	89.0
1.00	0.100	10.0	89.0

TRACE 8-8 Sequential solvent release data. (continued)
 followed by allyl phenol.
 Peak concentration: 100.0 mg/L (continued)

Time (hr)	Sample value (%)	Concentration, (mg/L)
0.11	0.100	0
0.22	0.100	0.0
0.33	0.100	0.0
0.44	0.100	0.0
0.55	0.100	10.0
0.66	0.100	20.0
0.77	0.100	40.0
0.88	0.100	60.0
0.99	0.100	70.0
1.10	0.100	80.0
1.21	0.100	90.0
1.32	0.100	95.0
1.43	0.100	98.0
1.54	0.100	99.0
1.65	0.100	100.0
1.76	0.100	100.0
1.87	0.100	100.0
1.98	0.100	100.0
2.09	0.100	100.0
2.20	0.100	100.0
2.31	0.100	100.0
2.42	0.100	100.0
2.53	0.100	100.0
2.64	0.100	100.0
2.75	0.100	100.0
2.86	0.100	100.0
2.97	0.100	100.0
3.08	0.100	100.0
3.19	0.100	100.0
3.30	0.100	100.0
3.41	0.100	100.0
3.52	0.100	100.0
3.63	0.100	100.0
3.74	0.100	100.0
3.85	0.100	100.0
3.96	0.100	100.0
4.07	0.100	100.0
4.18	0.100	100.0
4.29	0.100	100.0
4.40	0.100	100.0
4.51	0.100	100.0
4.62	0.100	100.0
4.73	0.100	100.0
4.84	0.100	100.0
4.95	0.100	100.0
5.06	0.100	100.0
5.17	0.100	100.0
5.28	0.100	100.0
5.39	0.100	100.0
5.50	0.100	100.0
5.61	0.100	100.0
5.72	0.100	100.0
5.83	0.100	100.0
5.94	0.100	100.0
6.05	0.100	100.0
6.16	0.100	100.0
6.27	0.100	100.0
6.38	0.100	100.0
6.49	0.100	100.0
6.60	0.100	100.0
6.71	0.100	100.0
6.82	0.100	100.0
6.93	0.100	100.0
7.04	0.100	100.0
7.15	0.100	100.0
7.26	0.100	100.0
7.37	0.100	100.0
7.48	0.100	100.0
7.59	0.100	100.0
7.70	0.100	100.0
7.81	0.100	100.0
7.92	0.100	100.0
8.03	0.100	100.0
8.14	0.100	100.0
8.25	0.100	100.0
8.36	0.100	100.0
8.47	0.100	100.0
8.58	0.100	100.0
8.69	0.100	100.0
8.80	0.100	100.0
8.91	0.100	100.0
9.02	0.100	100.0
9.13	0.100	100.0
9.24	0.100	100.0
9.35	0.100	100.0
9.46	0.100	100.0
9.57	0.100	100.0
9.68	0.100	100.0
9.79	0.100	100.0
9.90	0.100	100.0
10.01	0.100	100.0
10.12	0.100	100.0
10.23	0.100	100.0
10.34	0.100	100.0
10.45	0.100	100.0
10.56	0.100	100.0
10.67	0.100	100.0
10.78	0.100	100.0
10.89	0.100	100.0
11.00	0.100	100.0
11.11	0.100	100.0
11.22	0.100	100.0
11.33	0.100	100.0
11.44	0.100	100.0
11.55	0.100	100.0
11.66	0.100	100.0
11.77	0.100	100.0
11.88	0.100	100.0
11.99	0.100	100.0
12.10	0.100	100.0
12.21	0.100	100.0
12.32	0.100	100.0
12.43	0.100	100.0
12.54	0.100	100.0
12.65	0.100	100.0
12.76	0.100	100.0
12.87	0.100	100.0
12.98	0.100	100.0
13.09	0.100	100.0
13.20	0.100	100.0
13.31	0.100	100.0
13.42	0.100	100.0
13.53	0.100	100.0
13.64	0.100	100.0
13.75	0.100	100.0
13.86	0.100	100.0
13.97	0.100	100.0
14.08	0.100	100.0
14.19	0.100	100.0
14.30	0.100	100.0
14.41	0.100	100.0
14.52	0.100	100.0
14.63	0.100	100.0
14.74	0.100	100.0
14.85	0.100	100.0
14.96	0.100	100.0
15.07	0.100	100.0
15.18	0.100	100.0
15.29	0.100	100.0
15.40	0.100	100.0
15.51	0.100	100.0
15.62	0.100	100.0
15.73	0.100	100.0
15.84	0.100	100.0
15.95	0.100	100.0
16.06	0.100	100.0
16.17	0.100	100.0
16.28	0.100	100.0
16.39	0.100	100.0
16.50	0.100	100.0
16.61	0.100	100.0
16.72	0.100	100.0
16.83	0.100	100.0
16.94	0.100	100.0
17.05	0.100	100.0
17.16	0.100	100.0
17.27	0.100	100.0
17.38	0.100	100.0
17.49	0.100	100.0
17.60	0.100	100.0
17.71	0.100	100.0
17.82	0.100	100.0
17.93	0.100	100.0
18.04	0.100	100.0
18.15	0.100	100.0
18.26	0.100	100.0
18.37	0.100	100.0
18.48	0.100	100.0
18.59	0.100	100.0
18.70	0.100	100.0
18.81	0.100	100.0
18.92	0.100	100.0
19.03	0.100	100.0
19.14	0.100	100.0
19.25	0.100	100.0
19.36	0.100	100.0
19.47	0.100	100.0
19.58	0.100	100.0
19.69	0.100	100.0
19.80	0.100	100.0
19.91	0.100	100.0
20.02	0.100	100.0
20.13	0.100	100.0
20.24	0.100	100.0
20.35	0.100	100.0
20.46	0.100	100.0
20.57	0.100	100.0
20.68	0.100	100.0
20.79	0.100	100.0
20.90	0.100	100.0
21.01	0.100	100.0
21.12	0.100	100.0
21.23	0.100	100.0
21.34	0.100	100.0
21.45	0.100	100.0
21.56	0.100	100.0
21.67	0.100	100.0
21.78	0.100	100.0
21.89	0.100	100.0
22.00	0.100	100.0
22.11	0.100	100.0
22.22	0.100	100.0
22.33	0.100	100.0
22.44	0.100	100.0
22.55	0.100	100.0
22.66	0.100	100.0
22.77	0.100	100.0
22.88	0.100	100.0
22.99	0.100	100.0
23.10	0.100	100.0
23.21	0.100	100.0
23.32	0.100	100.0
23.43	0.100	100.0
23.54	0.100	100.0
23.65	0.100	100.0
23.76	0.100	100.0
23.87	0.100	100.0
23.98	0.100	100.0
24.09	0.100	100.0
24.20	0.100	100.0
24.31	0.100	100.0
24.42	0.100	100.0
24.53	0.100	100.0
24.64	0.100	100.0
24.75	0.100	100.0
24.86	0.100	100.0
24.97	0.100	100.0
25.08	0.100	100.0
25.19	0.100	100.0
25.30	0.100	100.0
25.41	0.100	100.0
25.52	0.100	100.0
25.63	0.100	100.0
25.74	0.100	100.0
25.85	0.100	100.0
25.96	0.100	100.0
26.07	0.100	100.0
26.18	0.100	100.0
26.29	0.100	100.0
26.40	0.100	100.0
26.51	0.100	100.0
26.62	0.100	100.0
26.73	0.100	100.0
26.84	0.100	100.0
26.95	0.100	100.0
27.06	0.100	100.0
27.17	0.100	100.0
27.28	0.100	100.0
27.39	0.100	100.0
27.50	0.100	100.0
27.61	0.100	100.0
27.72	0.100	100.0
27.83	0.100	100.0
27.94	0.100	100.0
28.05	0.100	100.0
28.16	0.100	100.0
28.27	0.100	100.0
28.38	0.100	100.0
28.49	0.100	100.0
28.60	0.100	100.0
28.71	0.100	100.0
28.82	0.100	100.0
28.93	0.100	100.0
29.04	0.100	100.0
29.15	0.100	100.0
29.26	0.100	100.0
29.37	0.100	100.0
29.48	0.100	100.0
29.59	0.100	100.0
29.70	0.100	100.0
29.81	0.100	100.0
29.92	0.100	100.0
30.03	0.100	100.0
30.14	0.100	100.0
30.25	0.100	100.0
30.36	0.100	100.0
30.47	0.100	100.0
30.58	0.100	100.0
30.69	0.100	100.0
30.80	0.100	100.0
30.91	0.100	100.0
31.02	0.100	100.0
31.13	0.100	100.0
31.24	0.100	100.0
31.35	0.100	100.0
31.46	0.100	100.0
31.57	0.100	100.0
31.68	0.100	100.0
31.79	0.100	100.0
31.90	0.100	100.0
32.01	0.100	100.0
32.12	0.100	100.0
32.23	0.100	100.0
32.34	0.100	100.0
32.45	0.100	100.0
32.56	0.100	100.0
32.67	0.100	100.0
32.78	0.100	100.0
32.89	0.100	100.0
33.00	0.100	100.0
33.11	0.100	100.0
33.22	0.100	100.0
33.33	0.100	100.0
33.44	0.100	100.0
33.55	0.100	100.0
33.66	0.100	100.0
33.77	0.100	100.0
33.88	0.100	100.0
33.99	0.100	100.0
34.10	0.100	100.0
34.21	0.100	100.0
34.32	0.100	100.0
34.43	0.100	100.0
34.54	0.100	100.0
34.65	0.100	100.0
34.76	0.100	100.0
34.87	0.100	100.0
34.98	0.100	100.0
35.09	0.100	100.0
35.20	0.100	100.0
35.31	0.100	100.0
35.42	0.100	100.0
35.53	0.100	100.0
35.64	0.100	100.0
35.75	0.100	100.0
35.86	0.100	100.0
35.97	0.100	100.0
36.08	0.100	100.0
36.19	0.100	100.0
36.30	0.100	100.0
36.41	0.100	100.0
36.52	0.100	100.0
36.63	0.100	100.0
36.74	0.100	100.0
36.85	0.100	100.0
36.96	0.100	100.0
37.07	0.100	100.0
37.18	0.100	100.0
37.29	0.100	100.0
37.40	0.100	100.0
37.51	0.100	100.0
37.62	0.100	100.0
37.73	0.100	100.0
37.84	0.100	100.0
37.95	0.100	100.0
38.06	0.100	100.0
38.17	0.100	100.0
38.28	0.100	100.0
38.39	0.100	100.0
38.50	0.100	100.0
38.61	0.100	100.0
38.72	0.100	100.0</

TABLE 8-4. Sequential eluate addition data, o-cresol followed by allyl phenol.
Feed concentrations: 140.5 mg/L (o-cresol), 7.5 mg/L allyl phenol

Time (min)	Sample volume (L)	Concentration (mg/L)	
		o-cresol	allyl phenol
0.00	0.000	140.0	1.0
0.10	0.000	140.0	1.0
0.10	0.000	140.0	2.0
0.20	0.000	99.0	2.0
0.20	0.000	140.0	3.0
0.30	0.000	140.0	5.0
0.40	0.000	140.0	5.0
0.40	0.000	140.0	6.0
0.50	0.000	141.0	6.0
0.50	0.000	140.0	6.0
0.60	0.000	99.0	6.0
0.60	0.000	140.0	6.0
0.70	0.000	140.0	6.0
0.70	0.000	140.0	6.0
0.80	0.000	140.0	6.0
0.80	0.000	140.0	6.0
0.90	0.000	140.0	6.0
0.90	0.000	140.0	6.0
1.00	0.000	140.0	6.0
1.10	0.100	140.0	6.0
1.10	0.100	140.0	6.0
1.20	0.100	140.0	6.0
1.20	0.100	140.0	6.0
1.30	0.100	141.0	6.0
1.40	0.100	140.0	6.0
1.40	0.100	140.0	6.0
1.50	0.100	140.0	6.0
1.60	0.100	140.0	6.0
1.70	0.100	140.0	6.0
1.80	0.100	99.0	6.0
1.90	0.100	140.0	6.0
2.00	0.100	140.0	6.0
2.10	0.100	99.0	6.0
2.20	0.100	99.0	6.0
2.30	0.100	140.0	6.0
2.40	0.100	140.0	6.0
2.50	0.100	140.0	6.0
2.60	0.100	140.0	6.0
2.70	0.100	140.0	6.0
2.80	0.100	140.0	6.0
2.90	0.100	140.0	6.0
3.00	0.100	140.0	6.0
3.10	0.100	140.0	6.0
3.20	0.100	140.0	6.0
3.30	0.100	140.0	6.0
3.40	0.100	140.0	6.0
3.50	0.100	140.0	6.0
3.60	0.100	140.0	6.0
3.70	0.100	140.0	6.0
3.80	0.100	140.0	6.0
3.90	0.100	140.0	6.0
4.00	0.100	140.0	6.0
4.10	0.100	140.0	6.0
4.20	0.100	140.0	6.0
4.30	0.100	140.0	6.0
4.40	0.100	140.0	6.0
4.50	0.100	140.0	6.0
4.60	0.100	140.0	6.0
4.70	0.100	140.0	6.0
4.80	0.100	140.0	6.0
4.90	0.100	140.0	6.0
5.00	0.100	140.0	6.0
5.10	0.100	140.0	6.0
5.20	0.100	140.0	6.0
5.30	0.100	140.0	6.0
5.40	0.100	140.0	6.0
5.50	0.100	140.0	6.0
5.60	0.100	140.0	6.0
5.70	0.100	140.0	6.0
5.80	0.100	140.0	6.0
5.90	0.100	140.0	6.0
6.00	0.100	140.0	6.0
6.10	0.100	140.0	6.0
6.20	0.100	140.0	6.0
6.30	0.100	140.0	6.0
6.40	0.100	140.0	6.0
6.50	0.100	140.0	6.0
6.60	0.100	140.0	6.0
6.70	0.100	140.0	6.0
6.80	0.100	140.0	6.0
6.90	0.100	140.0	6.0
7.00	0.100	140.0	6.0
7.10	0.100	140.0	6.0
7.20	0.100	140.0	6.0
7.30	0.100	140.0	6.0
7.40	0.100	140.0	6.0
7.50	0.100	140.0	6.0
7.60	0.100	140.0	6.0
7.70	0.100	140.0	6.0
7.80	0.100	140.0	6.0
7.90	0.100	140.0	6.0
8.00	0.100	140.0	6.0
8.10	0.100	140.0	6.0
8.20	0.100	140.0	6.0
8.30	0.100	140.0	6.0
8.40	0.100	140.0	6.0
8.50	0.100	140.0	6.0
8.60	0.100	140.0	6.0
8.70	0.100	140.0	6.0
8.80	0.100	140.0	6.0
8.90	0.100	140.0	6.0
9.00	0.100	140.0	6.0
9.10	0.100	140.0	6.0
9.20	0.100	140.0	6.0
9.30	0.100	140.0	6.0
9.40	0.100	140.0	6.0
9.50	0.100	140.0	6.0
9.60	0.100	140.0	6.0
9.70	0.100	140.0	6.0
9.80	0.100	140.0	6.0
9.90	0.100	140.0	6.0
10.00	0.100	140.0	6.0

TABLE B-3. (Continued)

Time Out	Sample volume (L)	Concentrations, mg/L	
		o-cresol	o,t,p-phenol
6-24	1.025	221.0	0.1
7-24	1.439	222.0	0.2
8-24	1.080	222.3	0.4
11-13	4.380	222.0	0.2
12-13	0.070	222.0	0.4

TABLE 3-4. Sequential solvent addition test: o-cresol followed by allyl phenol. Feed concentrations, 121.6 mg/L (o-cresol), 94.8 mg/L (allyl phenol).

Time (hr)	Sample volume (L)	Concentrations (mg/L)	
		o-cresol	allyl phenol
0.00	0.000	121.6	94.8
0.05	0.003	120.0	94.0
0.10	0.006	108.0	71.0
0.20	0.012	107.0	77.0
0.25	0.015	106.0	80.5
0.30	0.018	107.0	81.0
0.35	0.021	107.0	84.0
0.40	0.024	107.0	85.5
0.45	0.027	107.0	87.0
0.50	0.030	107.0	87.5
0.55	0.033	106.0	88.5
0.60	0.036	106.0	88.5
0.70	0.042	104.0	87.5
0.75	0.045	104.0	88.5
0.80	0.048	104.0	89.0
0.85	0.051	104.0	90.0
0.90	0.054	104.0	90.5
1.00	0.060	104.0	90.5
1.10	0.066	103.0	91.0
1.20	0.072	103.0	91.0
1.30	0.078	103.0	91.0
1.40	0.084	102.0	91.0
1.50	0.090	102.0	91.0
1.60	0.096	102.0	91.0
1.70	0.102	102.0	91.0
1.80	0.108	101.0	91.0
1.90	0.114	101.0	91.0
2.00	0.120	101.0	91.0
2.10	0.126	101.0	91.0
2.20	0.132	101.0	91.0
2.30	0.138	101.0	91.0
2.40	0.144	101.0	91.0
2.50	0.150	101.0	91.0
2.60	0.156	101.0	91.0
2.70	0.162	101.0	91.0
2.80	0.168	101.0	91.0
2.90	0.174	101.0	91.0
3.00	0.180	101.0	91.0

TABLE 8-8 Sequential eluate additive data; allyl phenol followed by o-cresol. Feed concentrations: 8.8 mg/L allyl phenol, 10.2 mg/L (increased)

Time (hr)	Sample volume (L)	Concentration (mg/L)	
		allyl phenol	o-cresol
0.00	0.000	0.0	0.1
0.05	0.000	10.0	0.0
0.10	0.000	10.4	0.0
0.15	0.000	10.4	0.4
0.20	0.000	10.8	0.1
0.25	0.000	10.0	0.4
0.30	0.000	10.9	0.8
0.35	0.000	10.0	7.4
0.40	0.000	10.0	7.3
0.45	0.000	11.0	7.4
0.50	0.000	10.0	7.4
0.55	0.000	11.1	7.0
0.60	0.000	10.7	7.9
0.65	0.000	10.8	8.1
0.70	0.000	11.1	8.3
0.75	0.000	11.0	8.4
0.80	0.000	11.0	8.5
0.85	0.000	11.4	8.8
0.90	0.000	11.1	8.9
0.95	0.000	10.9	9.0
1.00	0.000	11.4	9.1
1.05	0.000	10.9	9.2
1.10	0.000	10.9	9.3
1.15	0.000	10.7	9.5
1.20	0.000	10.8	9.6
1.25	0.000	10.7	9.6
1.30	0.000	10.6	9.7
1.35	0.000	10.0	9.4
1.40	0.000	10.0	9.5
1.45	0.000	10.0	9.5
1.50	0.000	9.9	10.0
1.55	0.000	9.9	10.0
1.60	0.000	9.8	10.0

TABLE 8-9. Sequential eluate absorber test: allyl phenol followed by o-cresol.
Feed concentrations: 14.3 mg/L (allyl phenol),
17.8 mg/L (o-cresol).

Time Sec	Sample volume (L)	Concentrations (mg/L)	
		allyl phenol	o-cresol
0.00	0.000	11.4	18.0
0.12	0.000	14.3	16.7
0.18	0.000	14.4	11.0
0.23	0.000	13.3	16.5
0.28	0.000	13.6	16.0
0.30	0.000	13.4	17.5
0.40	0.000	13.6	16.0
0.48	0.000	13.3	11.0
0.53	0.000	14.0	16.0
0.55	0.000	16.7	16.0
0.60	0.000	14.4	11.5
0.66	0.000	14.6	14.5
0.70	0.000	13.8	14.5
0.80	0.000	16.7	17.5
0.91	0.000	13.4	15.0
1.02	0.000	14.0	15.5
1.10	0.000	14.7	16.0
1.20	0.000	14.1	15.5
1.25	0.000	13.7	16.0
1.40	0.000	13.4	16.0
1.67	0.100	13.0	16.0
1.68	0.100	13.2	16.5
1.80	0.100	13.8	17.0
1.81	0.100	12.4	16.0
2.00	0.250	13.0	14.0
2.00	0.250	11.0	17.0
2.20	0.250	11.0	16.5
2.33	0.250	11.1	16.0
4.20	1.000	14.0	17.0
8.00	1.000	10.0	17.0
11.00	2.400	10.1	17.0
11.00	0.010	10.0	12.5

TABLE 3-13 Sequential volume addition data, alkyl phenols followed by cresols, fixed concentration, 20.5 mg/L initial phenol

Time (hr)	Distilled water sample volume (L)	Concentration of alkyl phenol (mg/L)
0.05	0.010	0.1
0.11	0.020	1.1
0.17	0.030	1.2
0.23	0.050	1.6
0.29	0.070	1.9
0.35	0.090	2.0
0.41	0.110	2.1
0.47	0.130	2.3
0.53	0.150	2.5
0.59	0.170	2.6
0.65	0.190	2.7
0.71	0.210	2.8
0.77	0.230	2.9
0.83	0.250	3.0
0.89	0.270	3.1
0.95	0.290	3.2
1.01	0.310	3.3
1.07	0.330	3.4
1.13	0.350	3.5
1.19	0.370	3.6
1.25	0.390	3.7
1.31	0.410	3.8
1.37	0.430	3.9
1.43	0.450	4.0
1.49	0.470	4.1
1.55	0.490	4.2
1.61	0.510	4.3
1.67	0.530	4.4
1.73	0.550	4.5
1.79	0.570	4.6
1.85	0.590	4.7
1.91	0.610	4.8
1.97	0.630	4.9
2.03	0.650	5.0
2.09	0.670	5.1
2.15	0.690	5.2
2.21	0.710	5.3
2.27	0.730	5.4
2.33	0.750	5.5
2.39	0.770	5.6
2.45	0.790	5.7
2.51	0.810	5.8
2.57	0.830	5.9
2.63	0.850	6.0
2.69	0.870	6.1
2.75	0.890	6.2
2.81	0.910	6.3
2.87	0.930	6.4
2.93	0.950	6.5
2.99	0.970	6.6
3.05	0.990	6.7
3.11	1.010	6.8
3.17	1.030	6.9
3.23	1.050	7.0
3.29	1.070	7.1
3.35	1.090	7.2
3.41	1.110	7.3
3.47	1.130	7.4
3.53	1.150	7.5
3.59	1.170	7.6
3.65	1.190	7.7
3.71	1.210	7.8
3.77	1.230	7.9
3.83	1.250	8.0
3.89	1.270	8.1
3.95	1.290	8.2
4.01	1.310	8.3
4.07	1.330	8.4
4.13	1.350	8.5
4.19	1.370	8.6
4.25	1.390	8.7
4.31	1.410	8.8
4.37	1.430	8.9
4.43	1.450	9.0
4.49	1.470	9.1
4.55	1.490	9.2
4.61	1.510	9.3
4.67	1.530	9.4
4.73	1.550	9.5
4.79	1.570	9.6
4.85	1.590	9.7
4.91	1.610	9.8
4.97	1.630	9.9
5.03	1.650	10.0

TABLE 4-11. Sequential volume addition cases which proved followed by α -arrest.
 Feed concentrations: 97.5 mg/l allyl phenol,
 9.9 mg/l α -cresol

Time (hr)	Sample volume (l)	Concentrations (mg/l)	
		allyl phenol	α -cresol
0.00	0.000	94.1	9.8
0.10	0.010	94.5	9.5
0.18	0.018	97.5	9.8
0.20	0.020	96.0	7.4
0.25	0.025	96.8	6.9
0.30	0.030	97.5	6.5
0.35	0.035	96.0	6.7
0.40	0.040	97.0	6.9
0.45	0.045	96.0	6.9
0.50	0.100	97.5	6.5
0.70	0.100	97.5	7.5
0.80	0.100	97.0	6.8
0.91	0.100	97.0	6.7
0.92	0.100	97.0	6.4
1.30	0.250	96.0	6.0
1.64	0.250	96.0	6.4

TABLE B-12 Sequential sulfate addition data, γ -irradiation followed by α -growth
Feed concentrations: 10.0 mg/L (silyl phenol), 500.0 mg/L (α -growth)

Time Day	Sample volume (L)	Concentrations (mg/L)	
		silyl phenol	α -growth
0.05	0.050	100.0	45.0
0.10	0.050	110.0	50.0
0.15	0.050	118.0	51.0
0.21	0.051	120.0	50.0
0.26	0.050	120.0	49.0
0.33	0.050	101.0	51.0
0.37	0.050	100.0	50.0
0.43	0.050	100.0	50.0
0.47	0.050	99.0	50.0
0.50	0.100	99.0	50.0
0.53	0.100	97.0	50.0
0.79	0.100	96.0	50.0
0.90	0.100	96.0	50.0
1.00	0.100	95.0	50.0
1.20	0.100	95.0	50.0
1.34	0.100	95.0	50.0
1.41	0.100	94.0	50.0
1.57	0.100	93.0	100.0

TABLE 3-13. Simultaneous column elution of 1,4-dioxane and 2,4-dimethyl-5-nitrophenol (10, 1 mg/l; 100, 1 mg/l) in 100% methanol.
Peak concentrations: 1,4-dioxane, 100 mg/l; 2,4-dimethyl-5-nitrophenol, 10 mg/l (100:1000).

Time (hr)	Sample volume (l)	Concentration (mg/l)	
		1,4-dioxane	2,4-dimethyl-5-nitrophenol
0.40	0.000	0	0
0.48	0.000	0	0.3
0.56	0.000	0	0.3
0.64	0.000	0	0.3
0.72	0.000	0	0.3
0.80	0.000	0	0.3
0.88	0.000	0	0.3
0.96	0.100	0	0.3
1.04	0.100	0.1	0.3
1.12	0.100	0.1	0.3
1.20	0.100	0.1	0.3
1.28	0.100	0.1	0.3
1.36	0.100	0.1	0.3
1.44	0.100	0.1	0.3
1.52	0.100	0.1	0.3
1.60	0.100	0.1	0.3
1.68	0.100	0.1	0.3
1.76	0.100	0.1	0.3
1.84	0.100	0.1	0.3
1.92	0.100	0.1	0.3
2.00	0.100	0.1	0.3
2.08	0.100	0.1	0.3
2.16	0.100	0.1	0.3
2.24	0.100	0.1	0.3
2.32	0.100	0.1	0.3
2.40	0.100	0.1	0.3
2.48	0.100	0.1	0.3
2.56	0.100	0.1	0.3
2.64	0.100	0.1	0.3
2.72	0.100	0.1	0.3
2.80	0.100	0.1	0.3
2.88	0.100	0.1	0.3
2.96	0.100	0.1	0.3
3.04	0.100	0.1	0.3
3.12	0.100	0.1	0.3
3.20	0.100	0.1	0.3
3.28	0.100	0.1	0.3
3.36	0.100	0.1	0.3
3.44	0.100	0.1	0.3
3.52	0.100	0.1	0.3
3.60	0.100	0.1	0.3
3.68	0.100	0.1	0.3
3.76	0.100	0.1	0.3
3.84	0.100	0.1	0.3
3.92	0.100	0.1	0.3
4.00	0.100	0.1	0.3
4.08	0.100	0.1	0.3
4.16	0.100	0.1	0.3
4.24	0.100	0.1	0.3
4.32	0.100	0.1	0.3
4.40	0.100	0.1	0.3
4.48	0.100	0.1	0.3
4.56	0.100	0.1	0.3
4.64	0.100	0.1	0.3
4.72	0.100	0.1	0.3
4.80	0.100	0.1	0.3
4.88	0.100	0.1	0.3
4.96	0.100	0.1	0.3
5.04	0.100	0.1	0.3
5.12	0.100	0.1	0.3
5.20	0.100	0.1	0.3
5.28	0.100	0.1	0.3
5.36	0.100	0.1	0.3
5.44	0.100	0.1	0.3
5.52	0.100	0.1	0.3
5.60	0.100	0.1	0.3
5.68	0.100	0.1	0.3
5.76	0.100	0.1	0.3
5.84	0.100	0.1	0.3
5.92	0.100	0.1	0.3
6.00	0.100	0.1	0.3
6.08	0.100	0.1	0.3
6.16	0.100	0.1	0.3
6.24	0.100	0.1	0.3
6.32	0.100	0.1	0.3
6.40	0.100	0.1	0.3
6.48	0.100	0.1	0.3
6.56	0.100	0.1	0.3
6.64	0.100	0.1	0.3
6.72	0.100	0.1	0.3
6.80	0.100	0.1	0.3
6.88	0.100	0.1	0.3
6.96	0.100	0.1	0.3
7.04	0.100	0.1	0.3
7.12	0.100	0.1	0.3
7.20	0.100	0.1	0.3
7.28	0.100	0.1	0.3
7.36	0.100	0.1	0.3
7.44	0.100	0.1	0.3
7.52	0.100	0.1	0.3
7.60	0.100	0.1	0.3
7.68	0.100	0.1	0.3
7.76	0.100	0.1	0.3
7.84	0.100	0.1	0.3
7.92	0.100	0.1	0.3
8.00	0.100	0.1	0.3
8.08	0.100	0.1	0.3
8.16	0.100	0.1	0.3
8.24	0.100	0.1	0.3
8.32	0.100	0.1	0.3
8.40	0.100	0.1	0.3
8.48	0.100	0.1	0.3
8.56	0.100	0.1	0.3
8.64	0.100	0.1	0.3
8.72	0.100	0.1	0.3
8.80	0.100	0.1	0.3
8.88	0.100	0.1	0.3
8.96	0.100	0.1	0.3
9.04	0.100	0.1	0.3
9.12	0.100	0.1	0.3
9.20	0.100	0.1	0.3
9.28	0.100	0.1	0.3
9.36	0.100	0.1	0.3
9.44	0.100	0.1	0.3
9.52	0.100	0.1	0.3
9.60	0.100	0.1	0.3
9.68	0.100	0.1	0.3
9.76	0.100	0.1	0.3
9.84	0.100	0.1	0.3
9.92	0.100	0.1	0.3
10.00	0.100	0.1	0.3

*Below detection limit.

TABLE 4.14. *Emulsification index* (emulsion conc., allyl phenol and *p*-cresol).
Feed concentrations: 57.5 mg/L allyl phenol,
5.0 mg/L *p*-cresol

Time (hr)	Sample volume (L)	Concentration, mg/L	
		allyl phaseol	n-octanol
0.04	0.010	0.0	0.0
0.08	0.010	0.0	0.0
0.16	0.010	0.0	0.0
0.32	0.010	0.0	0.0
0.64	0.010	0.0	0.0
0.128	0.010	1.0	0.0
0.256	0.010	1.0	0.0
0.512	0.010	2.0	0.0
1.024	0.010	3.0	1.0
2.048	0.010	6.0	2.0
4.096	0.010	12.0	4.0
8.192	0.010	18.0	6.0
16.384	0.010	24.0	8.0
32.768	0.010	40.0	12.0
65.536	0.010	60.0	18.0
131.072	0.010	72.0	24.0
262.144	0.010	80.0	28.0
524.288	0.010	90.0	30.0
1048.576	0.010	96.0	30.0

TABLE B-18. Simultaneous sulfate addition data, allyl phenol and o-cresol
 Feed concentrations: 10.3 mg/L (allyl phenol),
 11.3 mg/L (o-cresol)

Time (hr)	Sample volume (L)	Concentrations (mg/L)	
		allyl phenol	o-cresol
0.00	0.000	0	0
0.15	0.050	0.1	0.4
0.31	0.050	0.4	1.0
0.39	0.050	1.1	3.0
0.52	0.050	3.0	13.4
0.57	0.050	4.0	24.5
0.63	0.050	7.0	27.0
0.68	0.050	10.1	40.1
0.74	0.050	14.1	49.1
0.80	0.100	28.1	55.5
0.80	0.100	40.3	110.0
0.91	0.100	62.5	170.3
1.02	0.100	66.5	117.5
1.10	0.150	73.0	110.0
1.34	0.200	84.5	104.3
1.60	0.250	89.0	100.0
2.00	1.000	93.0	90.0
2.00	0.010	95.0	90.0
4.00	1.000	95.0	90.0
4.00	0.010	95.0	90.0
5.10	1.010	96.0	90.0
5.10	0.010	97.0	90.0

APPENDIX C
EXPERIMENTAL AND CALCULATED ROADSIDE ADDITION DATA FOR
1,4-DIHYDROXYNAPHTHENE (OHF/LALYL) FROM
ROADSIDE TAIR

TABLE C-1. Sequential volume addition data, 3,4-dihydroxynicotinaphenone (DHP) followed by allyl phenol.
Feed concentration: 1.4 mg/L (DHP)

Time (hr)	Effluent composite sample volume (L)	Concentration of DHP (mg/L)	
		Composite sample	Grab sample*
1.00	-	-	0.2
2.10	1.000	0.2	0.0
4.10	1.000	0.0	1.1
5.30	1.000	1.0	0.0
6.40	1.000	2.0	0.2
7.50	1.000	3.0	0.0
8.50	1.000	0.2	0.0
9.70	1.000	0.0	0.0
10.80	1.010	1.4	0.0
11.90	1.000	0.2	0.0
13.00	1.000	0.0	0.0
14.10	1.000	0.0	0.0
15.20	1.000	0.2	0.0
24.00	0.400	0.0	0.0

*Grab sample volume was 0.050 L.

TABLE 4-16. Sequential 100- μ L GPC-MS data. 250- μ L dihydroxyacetophenone (DAP) followed by allyl phenol.
 Feed concentrations: 5.5 mg/L DAP, 5.5 mg/L allyl phenol

Time [hr]	Sample volume [L]	Concentration of DAP [mg/L]	
		DAP	allyl phenol
0.00	0.000	5.5	0.0
0.10	0.005	10.4	3.1
0.20	0.010	11.1	3.8
0.30	0.015	11.5	3.4
0.50	0.025	12.1	3.0
0.60	0.030	12.3	3.5
0.81	0.050	13.0	4.3
1.00	0.060	13.0	5.0
1.40	0.090	13.0	6.0
2.00	1.000	12.0	6.0
2.40	0.000	12.2	2.0
3.00	1.000	10.0	3.0
3.60	0.000	10.4	3.0
4.00	1.000	10.4	6.0
4.80	0.000	10.0	6.3
6.00	1.000	10.0	6.4
6.60	0.000	10.7	6.0
7.00	0.000	10.4	6.2
7.20	0.000	10.0	6.2
8.00	1.000	10.5	6.0
8.60	0.000	10.3	6.0
9.00	1.000	10.0	6.0
9.60	0.000	10.0	6.0
10.00	1.000	10.0	6.0
10.40	0.000	10.0	6.0
11.00	1.000	10.0	6.0
11.60	0.000	10.0	6.0
12.00	1.000	10.0	6.0

TABLE C-3. Sequential sample addition data, E. coli diphenylacetate-sulfonate (DAP) followed by allyl phenol.
 Feed concentrations: 18.6 mg/L (DAP), 55.5 mg/L (allyl phenol).

Time (hr)	Sample volume (L)	Concentration of DAP (mg/L)	
		DAP	allyl phenol
0.00	0.000	18.6	55.5
0.10	0.050	18.1	55.0
0.13	0.060	17.1	57.0
0.16	0.080	16.8	62.3
0.18	0.090	16.1	66.5
0.21	0.100	16.6	71.5
0.18	0.080	16.7	70.3
0.41	0.050	17.9	71.0
0.47	0.050	17.1	74.0
0.52	0.050	17.5	76.6
0.63	0.050	17.1	76.5
0.73	0.050	17.0	80.5
0.88	0.050	16.7	83.8
0.94	0.050	17.0	83.0
1.08	0.050	16.0	84.8
1.16	0.050	16.0	86.0
1.26	0.050	16.1	86.5
1.36	0.050	16.6	87.3
1.47	0.050	16.7	89.0
1.73	0.050	15.0	91.0
2.00	0.050	16.7	91.8
2.28	0.050	16.0	91.5
2.58	0.050	15.0	93.0
2.88	0.050	12.9	93.0
3.08	0.050	13.0	94.5
3.48	0.050	13.0	96.5
3.88	0.050	11.7	97.0
4.28	0.050	11.0	97.5
4.68	0.050	10.9	97.3
5.08	0.050	10.7	98.8
5.48	0.050	10.0	99.5
5.88	0.050	10.4	99.3
6.27	0.050	10.0	99.8
6.68	0.050	10.0	99.5

TABLE C-4 Sequential elution addition data, 2,6-dihydroxyacetophenone (DAP) followed by 813g1 phenol.
Feed concentration: 55.3 mg/g (DAP)

Time hr:min	Sample volume (L)	Concentration of DAP (mg/g)
0:00	0.000	0.0
0:10	0.000	0.0
0:16	0.000	0.0
0:27	0.100	0.5
0:30	0.100	1.0
0:40	0.100	2.0
0:50	0.100	4.0
0:45	0.100	6.0
0:55	0.100	14.0
0:52	0.100	24.0
1:04	0.100	31.0
1:10	0.100	44.7
1:20	0.100	52.0
1:26	0.100	60.0
1:47	0.100	66.0
1:57	0.100	71.0
2:00	0.100	76.4
2:00	0-21.7	80.0
2:00	0.100	84.0
2:00	0.100	86.0
2:30	0.050	87.5
2:55	0.100	
2:55	0.243	92.0
3:30	0.050	93.5
4:20	0.050	94.0
4:20	0.050	95.5
4:35	1.000	99.0
5:35	0.050	99.0
6:00	1.000	99.5
6:00	0.050	99.0
7:50	1.000	99.0
7:50	0.050	99.5

TABLE C-3. Sequential solute addition data: 2,4-dichlorophenanthroline (DAP) followed by allyl phenol.
Feed concentrations: 97.0 mg/L (DAP), 9.9 mg/L (allyl phenol)

Time (hr)	Sample volume (L)	Concentrations of DAP (mg/L)	
		DAP	allyl phenol
0.05	0.050	100.0	0.0
0.10	0.050	100.0	0.1
0.20	0.050	100.0	0.5
0.30	0.050	100.0	1.5
0.40	0.050	100.0	2.5
0.50	0.050	100.0	3.5
0.60	0.050	100.0	4.5
0.70	0.050	100.0	5.5
0.80	0.050	100.0	6.5
0.90	0.050	100.0	7.5
0.95	0.050	100.0	7.8
0.98	0.050	99.0	7.8
0.99	0.050	98.0	7.8
1.00	0.100	98.0	8.0
0.90	0.100	98.0	8.3
0.90	0.100	98.0	8.6
1.00	0.113	98.0	8.8
1.00	0.200	98.0	9.0
1.00	0.200	98.0	9.3
2.00	0.400	98.0	9.4
3.00	1.000	98.0	9.4
3.00	2.000	90.0	9.4
4.00	3.000	90.0	10.0
4.00	0.000	---	10.0
5.00	0.000	---	9.8
6.00	0.000	---	9.8

TABLE C-4. Sequential elution addition data, 2,6-dithiodiphenylphosphone (DAP) followed by allyl phenol.
Feed concentrations: 32.5 mg/L (DAP), 14.3 mg/L (allyl phenol)

Time (hr)	Sample volume (L)	Concentration of DAP (mg/L)	
		DAP	allyl phenol
0.00	0.000	104.0	41.5
0.10	0.010	114.0	58.5
0.15	0.015	112.0	45.5
0.20	0.020	112.0	50.5
0.25	0.025	108.0	70.5
0.30	0.030	108.0	75.5
0.37	0.038	103.0	72.5
0.40	0.040	103.0	75.5
0.47	0.048	100.0	81.5
0.50	0.100	100.0	82.5
0.60	0.100	103.0	84.5
0.70	0.100	105.0	85.0
0.80	0.100	103.0	87.5
0.90	0.100	102.0	89.5
1.01	0.100	100.0	89.5
1.30	1.000	97.0	92.0
1.60	0.000	85.0	91.0
1.70	0.000	94.0	93.0
1.74	0.000	92.0	92.0
1.80	0.000	95.0	93.0
1.90	0.000	97.0	94.0

TABLE 4-3. Sequential eluate addition data, elute period followed by 2,4-dihydroxyacetophenone.
Feed concentration 14.6 mg/l (elute period)

Time	Effluent composite	Concentration of elute (mg/L)	
(hr)	Sample volume (l)	Composite sample	Grab sample*
2.13	1.000	0.1	0.2
3.31	1.000	0.2	0.4
4.30	1.000	0.4	0.8
5.40	1.000	1.0	2.0
6.40	1.000	1.4	4.4
8.00	2.000	4.0	7.1
10.01	2.000	3.8	8.4
12.40	4.000	9.0	9.4
14.40	8.000	2.4	8.7

*Grab sample volume was 0.400L.

TABLE 11. Sequential dilution addition data, allyl phenyl
followed by 2,4-dichlorophenoxystyrene (DAP)
Feed concentrations: 18.1 mg/L allyl phenyl,
7.1 mg/L DAP

conc	sample volume	Concentrations, mg/L	
		allyl phenyl	DAP
0.00	0.000	10.1	0.1
0.10	0.100	10.0	0.1
0.20	0.100	11.0	0.1
0.30	0.100	11.4	0.1
0.40	0.100	10.0	0.1
0.50	0.100	12.0	0.1
0.60	0.100	13.4	0.1
0.70	0.100	11.0	0.1
1.00	0.100	10.4	0.1
1.40	0.100	10.0	0.1
1.70	0.100	10.0	0.1
2.00	1.000	10.0	0.1
2.00	0.000	10.0	0.1
3.00	1.000	10.0	0.1
3.00	0.000	10.0	0.1
4.00	1.000	10.0	0.1
4.00	0.000	10.0	0.1
5.00	1.000	10.0	0.1
5.00	0.000	10.0	0.1
10.00	0.000	10.0	0.1
10.00	0.000	10.0	0.1
10.00	0.000	10.0	0.1
10.00	0.000	10.0	0.1

TABLE 2-3. Sequential solute addition data, allyl phenol followed by 3,4-dihydroxyacetophenone (DAP). Feed concentrations: 8.5 mg/L (allyl phenol), 10.8 mg/L (DAP).

Time (hr)	Sample volume (L)	Concentrations (mg/L)	
		allyl phenol	DAP
0-04	0.050	14.5	15.8
0-10	0.050	16.4	18.3
0-13	0.050	17.4	20.1
0-18	0.050	17.4	22.3
0-24	0.050	17.3	24.5
0-30	0.050	16.4	21.5
0-38	0.050	16.3	27.0
0-44	0.100	16.7	29.0
0-50	0.100	14.5	32.0
0-57	0.100	14.3	35.5
0-78	0.200	13.7	37.0
0-88	0.200	13.0	38.5
0-98	0.200	13.7	39.0
1-05	0.300	13.8	41.0
1-09	0.300	13.3	43.0
1-13	0.300	13.3	43.8
1-15	0.300	13.8	43.0
1-24	1.000	13.0	43.8
1-33	0.350	12.3	43.8
4-34	1.000	-	43.0
6-38	0.750	-	43.0

TABLE C-18. Sequential solvent addition data, allyl phenol followed by 2,6-dihydroxyacetophenone (DAF), Feed concentration: 54.9 wt% allyl phenol

Time (hr)	Effluent composite sample volume (L)	Concentration of allyl phenol (mg/L)
0.37	0.250	3.4
0.39	0.250	17.8
0.40	0.250	24.0
0.49	0.250	28.2
0.50	0.250	33.7
0.80	0.250	37.3
0.81	0.250	44.8
1.00	0.250	48.2
1.13	0.250	53.2
1.20	0.250	57.4
1.30	0.250	62.6
1.40	0.250	66.8
1.54	0.250	70.8
1.64	0.250	73.5
1.70	0.250	76.2
1.80	0.250	78.8
1.99	0.250	81.8
2.14	0.250	86.2
2.34	0.250	88.8
2.40	1.000	88.2
2.40	0.250	87.2
4.78	1.000	88.8
4.78	0.250	87.0
8.88	2.000	88.0
8.88	0.250	86.0

TABLE C-11 Sequential culture addition data, algal phase followed by *L. longipharyngoscyphus* (CSP). Feed concentrations: 17.5 mg/L (algal phase), 5.0 mg/L (CSP).

[illegible]

TABLE C-11: Sequential sodium addition data, adipic phenol followed by 2,4-dihydroxyacetophenone (DAP). Feed concentrations: 39.8 mg/L (adipic phenol), 140.0 mg/L (DAP)

Time (hr)	Effluent composite sample values (C)	Concentration (mg/L)	
		adipic phenol	DAP
0.05	0.050	394.0	34.3
0.11	0.050	313.0	40.7
0.17	0.050	314.4	40.4
0.23	0.050	313.5	37.3
0.27	0.050	313.0	42.3
0.33	0.050	313.0	39.8
0.39	0.050	313.5	39.8
0.44	0.050	313.0	39.3
0.49	0.050	307.5	39.8
0.55	0.050	304.0	38.0
0.71	0.050	304.5	34.3
0.82	0.050	303.0	38.0
0.93	0.050	303.0	38.0
1.03	0.050	303.5	39.0
1.18	0.050	303.5	39.3
1.34	0.050	30.0	39.0
1.49	1.000	300.0	38.0
1.78	0.050	39.5	39.5
2.53	0.040	100.0	38.3
3.32	0.030	39.0	100.0

TABLE 6-11. Simultaneous solvent addition data, allyl phenyl and 2,4-dichlorophenylisothiocyanate (DSC).

Time	Sample volume	Concentration (mg/L)	OD
(hr)	(L)	adipic phenol	
2.12	0.000	0.1	0.1
2.12	0.050	0.1	0.1
2.12	0.100	0.1	0.1
2.12	0.000	0.0	0.1
2.48	0.000	2.4	0.8
2.48	0.050	2.6	0.7
4.00	0.100	3.7	0.8
4.00	0.050	4.0	1.0
4.00	0.100	4.2	1.7
4.00	0.000	7.4	2.3
7.12	0.100	8.5	3.7
7.12	0.000	9.3	3.3
8.48	0.000	10.1	4.3
8.48	0.050	11.4	3.8
7.00	0.100	11.0	3.4
7.00	0.000	11.3	4.1
7.42	0.100	11.1	4.5
7.00	0.000	12.0	4.8
8.12	0.100	12.3	7.1
8.12	0.000	11.1	7.3
8.12	0.000	10.0	7.7
8.12	0.050	10.9	4.2
11.12	0.000	10.4	8.3
11.12	0.000	10.4	8.3
11.78	0.000	10.5	9.5
11.78	0.000	10.1	8.7
14.00	0.000	10.3	9.7
14.31	0.050	10.0	9.9

TABLE C-14
 Equilibrium solute addition data, allyl phenol
 and 2,4-dihydroxyacetophenone (DAP)
 Feed concentrations: 15.1 mg/L (allyl phenol),
 94.5 mg/L (DAP)

Time (hr)	Sample volume (L)	Concentration (mg/L)	
		allyl phenol	DAP
0.04	0.008	0.1	0.3
0.12	0.008	0.3	1.3
0.14	0.008	0.3	1.3
0.24	0.008	0.3	2.3
0.29	0.008	0.7	3.3
0.33	0.008	0.9	4.3
0.41	0.008	1.1	6.3
0.48	0.008	1.3	7.3
0.62	0.008	1.7	9.3
0.65	0.100	2.1	13.3
0.74	0.100	3.0	18.3
0.85	0.100	3.3	23.3
0.94	0.100	4.3	28.3
1.00	0.100	4.4	34.3
1.04	0.250	9.4	49.3
1.05	0.250	10.3	49.3
1.01	0.200	11.1	74.3
2.00	0.250	11.1	81.3
0.00	0.000	10.7	87.3
2.00	0.000	10.3	87.3
0.00	0.000	10.4	88.3
2.00	0.000	10.3	89.3
0.00	1.000	10.3	91.3
0.00	0.000	10.3	91.3
0.00	1.000	10.1	92.3
0.07	1.000	10.1	94.3
0.07	0.000	10.1	95.3
0.01	1.000	10.1	94.3
0.01	0.000	10.1	94.3

TABLE C-28. Benzofuran solute addition data, allyl phenyl and 2,4-dichlorobenzophenone (DBP). Feed concentrations: 91.8 mg/L (allyl phenyl), 9.1 mg/L (DBP).

Time (hr)	Sample volume (L)	Concentrations, mg/L	
		allyl phenyl	DBP
0.00	0.050	0.1	0.1
0.10	0.050	0.4	0.1
0.18	0.050	1.0	0.1
0.20	0.050	1.3	0.1
0.28	0.050	1.2	0.1
0.30	0.050	1.8	0.1
0.35	0.050	4.4	0.1
0.40	0.050	4.5	0.1
0.45	0.050	9.0	0.1
0.50	0.100	14.3	0.3
0.60	0.100	24.1	0.7
0.75	0.100	20.4	1.0
0.80	0.100	18.9	1.4
1.00	0.100	20.5	1.8
1.20	0.200	40.0	2.3
1.50	0.200	70.0	2.6
1.80	0.200	44.0	3.3
2.00	0.200	40.0	4.0
2.50	0.300	50.5	4.8
2.80	0.300	70.0	5.6
3.00	0.300	60.0	6.1
3.20	0.300	70.0	6.6
3.30	1.000	10.0	7.0
3.31	0.300	64.0	7.5
3.60	1.000	70.0	8.1
3.65	0.400	-	8.6
3.70	1.000	91.5	9.5
3.80	0.600	90.0	9.8
3.85	1.000	90.5	10.4
3.90	0.500	88.0	10.7
3.95	1.000	91.0	11.1
4.00	0.500	91.0	11.9

TABLE C-14. Dissolution* versus addition data, allyl phenol and 2,2-dichloroacrylonitrilbenzene (DAF).
Feed concentrations: 100.0 mg/L (allyl phenol),
20.0 mg/L (DAF)

Time (hr)	Sample volume (L)	Concentration (mg/L)	
		allyl phenol	DAF
0.10	0.114	0.0	0.1
0.20	0.100	1.0	0.0
0.30	0.100	0.0	0.0
0.40	0.100	10.0	12.1
0.50	0.100	42.0	24.4
0.60	0.100	70.0	40.0
0.70	0.100	88.0	54.0
0.80	0.100	94.0	64.0
0.90	0.100	95.0	69.0
1.00	0.100	100.0	70.0
1.10	0.100	100.0	80.0
1.20	0.100	100.0	81.0
1.30	0.100	100.0	80.0
1.40	0.100	100.0	84.0
1.50	0.100	100.0	86.0
1.60	0.100	100.0	88.0
1.70	0.100	100.0	89.0
1.80	0.100	100.0	90.0
1.90	0.100	100.0	91.0
2.00	0.100	100.0	91.0
2.10	0.100	100.0	91.0
2.20	0.100	100.0	91.0
2.30	0.100	100.0	91.0
2.40	0.100	100.0	91.0
2.50	0.100	100.0	91.0
2.60	0.100	100.0	91.0
2.70	0.100	100.0	91.0
2.80	0.100	100.0	91.0
2.90	0.100	100.0	91.0
3.00	0.100	100.0	91.0
3.10	0.100	100.0	91.0
3.20	0.100	100.0	91.0
3.30	0.100	100.0	91.0
3.40	0.100	100.0	91.0
3.50	0.100	100.0	91.0
3.60	0.100	100.0	91.0
3.70	0.100	100.0	91.0
3.80	0.100	100.0	91.0
3.90	0.100	100.0	91.0
4.00	0.100	100.0	91.0
4.10	0.100	100.0	91.0
4.20	0.100	100.0	91.0
4.30	0.100	100.0	91.0
4.40	0.100	100.0	91.0
4.50	0.100	100.0	91.0
4.60	0.100	100.0	91.0
4.70	0.100	100.0	91.0
4.80	0.100	100.0	91.0
4.90	0.100	100.0	91.0
5.00	0.100	100.0	91.0
5.10	0.100	100.0	91.0
5.20	0.100	100.0	91.0
5.30	0.100	100.0	91.0
5.40	0.100	100.0	91.0
5.50	0.100	100.0	91.0
5.60	0.100	100.0	91.0
5.70	0.100	100.0	91.0
5.80	0.100	100.0	91.0
5.90	0.100	100.0	91.0
6.00	0.100	100.0	91.0
6.10	0.100	100.0	91.0
6.20	0.100	100.0	91.0
6.30	0.100	100.0	91.0
6.40	0.100	100.0	91.0
6.50	0.100	100.0	91.0
6.60	0.100	100.0	91.0
6.70	0.100	100.0	91.0
6.80	0.100	100.0	91.0
6.90	0.100	100.0	91.0
7.00	0.100	100.0	91.0
7.10	0.100	100.0	91.0
7.20	0.100	100.0	91.0
7.30	0.100	100.0	91.0
7.40	0.100	100.0	91.0
7.50	0.100	100.0	91.0
7.60	0.100	100.0	91.0
7.70	0.100	100.0	91.0
7.80	0.100	100.0	91.0
7.90	0.100	100.0	91.0
8.00	0.100	100.0	91.0
8.10	0.100	100.0	91.0
8.20	0.100	100.0	91.0
8.30	0.100	100.0	91.0
8.40	0.100	100.0	91.0
8.50	0.100	100.0	91.0
8.60	0.100	100.0	91.0
8.70	0.100	100.0	91.0
8.80	0.100	100.0	91.0
8.90	0.100	100.0	91.0
9.00	0.100	100.0	91.0
9.10	0.100	100.0	91.0
9.20	0.100	100.0	91.0
9.30	0.100	100.0	91.0
9.40	0.100	100.0	91.0
9.50	0.100	100.0	91.0
9.60	0.100	100.0	91.0
9.70	0.100	100.0	91.0
9.80	0.100	100.0	91.0
9.90	0.100	100.0	91.0
10.00	0.100	100.0	91.0

APPENDIX B
EXPERIMENTAL AND SIMULTANEOUS SOLUTE ADSORPTION DATA
FOR 6-CARBON-2,4-DINITROPHENOL (CDNF) (SOLUTE PAIR)
SOLUTE PAIR

TABLE 8-6. Sequential eluate addition data, *n*-cresol followed by 2,4-dichlorophenoxyphenol (DAP). Feed concentration: 10.2 mg/L (*n*-cresol).

Time (hr)	Sample volume (L)	Concentration of <i>n</i> -cresol (mg/L)
3.10	3.000	0.3
3.35	6.000	0.4
4.10	3.000	1.3
4.35	6.000	5.7
5.10	3.000	6.8
5.35	6.000	6.3
6.10	3.000	7.1
6.40	6.000	7.8
7.10	3.000	8.1
7.35	6.000	8.9
8.10	3.000	8.7
8.35	6.000	9.9
14.10	4.000	9.1
14.35	8.000	9.5
16.17	10.150	9.7
16.37	8.050	9.7
16.59	10.450	9.7
19.39	8.850	10.1
41.10	10.300	10.5
41.31	8.850	10.8

TABLE 10. Sequential assays: oxidized state, unreacted, followed by 2,2-dihydroxyacetophenone (DAF). Feed concentrations: 10.2 mg/L 10-oxo-11, 5.7 mg/L (DAF)

Time	Sample volume	Concentration (mg/L)	
		unreacted	DAF
0.20	0.200	11.0	3.8
0.34	0.200	11.5	4.1
0.63	0.200	11.7	4.5
1.00	0.200	12.7	4.6
1.34	0.200	12.7	4.8
1.63	0.200	12.7	5.2
1.88	0.200	12.7	5.4
2.14	0.200	12.8	5.2
2.40	0.200	12.9	5.6
2.67	0.200	12.9	5.8
2.93	0.200	12.4	6.2
3.20	0.200	12.4	6.3
4.36	0.400	12.2	6.2
4.66	0.400	12.2	6.6
5.47	0.400	12.2	7.0
5.47	0.800	12.8	7.4
7.00	2.000	12.8	7.2
7.48	0.400	12.8	8.0
11.40	0.800	12.8	8.4
11.87	0.800	12.8	8.2
14.50	0.400	12.4	8.8
14.50	0.800	12.2	8.8
23.80	2.000	12.2	8.5
23.80	0.800	12.2	8.2

TABLE 2. Sequential volume elution data, reversed, followed by 2,4-dihydroxyacetophenone (DAP) feed concentrations: 1.5 mg/L is-arsenol, 54.5 mg/L (DAP)

Time (hr)	Sample volume (L)	Concentration (mg/L)	
		is-arsenol	DAP
0.001	0.005	0	0
0.005	0.005	11.1	82.0
0.001	0.005	11.1	87.5
0.05	0.005	11.1	92.0
0.11	0.005	11.0	96.0
0.26	0.005	11.0	96.0
0.31	0.005	11.0	96.0
0.36	0.005	11.0	92.0
0.47	0.100	11.0	92.0
0.57	0.100	18.7	85.0
0.67	0.113	18.7	85.0
0.79	0.100	18.7	82.0
0.87	0.100	18.7	87.5
1.00	0.100	18.6	87.0
1.07	0.500	18.6	89.0
1.57	0.500	18.0	87.5
2.13	0.500	18.1	88.5
2.13	0.050	18.3	91.0
2.25	1.000	18.3	92.0
2.35	0.070	18.3	92.0
4.53	1.000	18.3	92.0
4.53	0.050	18.3	92.0
5.09	1.010	18.0	92.0
5.09	0.050	18.0	92.0
6.34	1.000	18.2	94.0
6.34	0.050	0.0	95.0
7.43	1.000	0.0	95.0
7.43	0.020	0.0	95.0
8.72	1.000	0.0	95.0
8.72	0.050	0.0	95.0
9.85	1.000	0.0	94.0
9.85	0.050	0.0	95.0

*Sample loss.

TABLE 2-4. Sequential volume addition data, *m*-arsenol followed by 2,4-dihydroxyacetophenone (DHAP). Feed concentration: 100.0 mg/L (*m*-arsenol).

Time (hr)	Sample volume (L)	Concentration of <i>m</i> -arsenol (mg/L)
0.15	0.100	0.3
0.30	0.100	3.9
0.45	0.100	8.3
0.60	0.100	15.4
0.75	0.100	27.8
0.90	0.100	42.4
0.75	0.100	54.0
0.90	0.100	63.0
0.90	0.100	68.3
1.05	0.100	73.0
1.15	0.100	83.0
1.20	0.100	87.0
1.30	0.100	90.3
1.40	0.100	93.0
1.50	0.100	94.0
1.60	1.000	98.0
1.60	0.030	99.3
4.00	1.000	100.0
4.00	0.030	100.0
4.00	1.000	100.0
4.00	0.030	100.0

TABLE P-5. Sequential eluate addition data, o-cresol followed by 2,4-dinitrophenylhydrazones (DNP). Feed concentrations: 104.5 mg/L (o-cresol), 9.7 mg/L (DNP)

Time (hr)	Sample values (L)	Concentrations (mg/L)	
		o-cresol	DNP
0.05	0.050	100.0	0.1
0.11	0.010	101.0	0.1
0.22	0.010	102.0	0.2
0.41	0.010	103.0	0.3
0.77	0.010	103.0	0.5
0.93	0.010	103.5	0.6
0.92	0.100	104.0	0.8
0.93	0.100	103.5	0.6
0.79	0.250	103.0	0.7
1.05	0.010	103.0	1.0
1.21	0.200	103.0	1.0
1.97	0.250	103.5	1.0
1.99	0.050	103.0	1.2
2.00	0.250	103.0	0.7
2.45	0.500	104.0	1.4
3.45	0.010	104.0	1.7
3.53	0.000	104.0	4.0
3.53	0.000	104.0	4.0
4.09	1.000	103.0	6.7
4.28	0.000	103.0	6.3
4.79	0.000	103.0	7.0
4.79	0.000	103.0	6.6
5.00	2.000	100.0	9.1
5.04	0.000	100.0	9.4
24.22	0.000	100.0	9.4
24.23	0.000	100.0	9.4

Table 1. Sequential elute addition data, α -crystal
 obtained by 2,4-dichlorophenylhydrazine (DCH).
 Feed concentrations: 140.5 mg/L α -crystal,
 14.0 mg/L (DCH)

Time (hr)	Eluate volume (L)	Concentration (mg/L)	
		α -crystal	DCH
0.015	0.015	101.5	10.7
0.020	0.020	115.0	10.0
0.10	0.020	118.0	10.0
0.15	0.030	117.0	10.0
0.20	0.030	114.0	10.0
0.25	0.030	112.0	10.0
0.30	0.030	109.0	7.5
0.35	0.030	108.0	75.0
0.40	0.100	106.0	70.0
0.50	0.100	106.0	64.0
0.60	0.140	103.0	60.0
1.00	1.000	100.0	61.0
2.00	0.000	100.0	55.0
3.00	1.000	100.0	56.0
4.00	0.000	100.0	56.0

TABLE D-7. Sequential volume addition data, 2,4-dihydroxy-
acetophenone followed by o-cresol
Feed concentration = 0.7 mg/L (DAP)

Time (hr)	Sample volume (L)	Concentration of bar (mg/L)
2.11	2.000	0
3.11	0.000	0
4.23	2.000	0.2
4.23	0.000	0.1
5.31	2.000	0.4
5.31	0.000	1.2
6.40	2.000	1.8
6.40	0.000	2.4
7.48	2.000	3.2
7.48	0.000	4.2
8.58	2.000	4.7
8.58	0.000	5.4
9.45	2.000	6.8
9.45	0.000	6.2
10.55	2.000	6.8
10.55	0.000	7.1
12.49	2.000	7.6
12.49	0.000	8.2
13.00	2.000	8.8
13.00	0.000	8.7
24.55	4.300	8.2
24.55	0.000	9.7

*Barium detection limit.

TABLE D-1. Deposition, surface addition data, 2,4-dihydroxy-
acetophenone followed by α -arsenal.
Feed concentrations: 8.8 mg/L (DAP), 10.1 mg/L
(α -arsenal)

Time (hr)	Sample volume (L)	Concentration (mg/L)	
		DAP	α -arsenal
0.00	0.000	18.8	8.8
0.25	0.100	18.4	8.8
0.50	0.100	18.7	8.8
0.75	0.100	18.8	8.8
0.99	0.100	18.3	7.3
2.00	0.100	18.3	7.8
2.07	0.100	18.3	8.0
4.77	0.200	18.3	8.8
1.00	0.200	18.3	8.8
1.79	0.200	18.3	8.8
1.55	0.200	18.8	8.8
1.81	0.200	18.7	8.5
2.88	0.400	18.3	8.7
2.89	0.400	18.3	8.8
2.97	0.400	18.2	7.8
2.97	0.400	8.8	8.8
4.00	0.600	18.3	10.1
4.00	0.600	18.8	10.1
4.73	0.600	8.8	10.1
4.73	0.600	8.7	10.1

TABLE 6-3. Sequential volume addition data, 2,6-diisopropyl-antipyrene followed by α -crystal.
Feed concentrations: 9.5 mg/L 18AP, 122.5 mg/L α -crystal.

Time (hr)	Sample volume (L)	Concentration (mg/L)	
		18AP	α -crystal
0.00	0.000	13.8	46.8
0.10	0.010	14.0	46.8
0.15	0.015	14.3	46.8
0.20	0.020	14.6	47.5
0.25	0.025	17.3	48.5
0.31	0.030	17.7	48.8
0.41	0.100	17.7	49.5
0.51	0.100	17.7	51.8
0.60	0.100	17.8	54.8
0.70	0.100	17.9	55.8
0.80	0.100	17.9	56.8
1.10	0.200	14.8	57.5
1.30	0.300	15.0	58.5
1.40	1.000	13.8	59.5
1.45	0.000	13.8	100.0
1.50	1.000	13.3	100.0
1.55	0.000	13.8	101.0
1.60	1.000	13.6	101.5
1.70	0.000	18.0	102.0
1.80	1.000	18.3	102.0
1.85	0.000	18.0	102.0
1.90	1.000	18.0	102.0
1.95	0.000	17.8	102.0

TABLE G-10 Sequential sulfate addition data, 3,4-diaminobenzoic acidophenone followed by 6-aminol. Feed concentration, 75.5 mg/L OAP^a

Time hr ^b	Sample volume L ^c	Concentration of OAP mg/L ^d
0.04	0.010	0
0.10	0.010	8.3
0.18	0.010	8.3
0.33	0.100	8.7
0.37	0.100	1.4
0.47	0.100	3.8
0.80	0.100	7.7
0.88	0.180	13.0
0.98	0.180	25.0
0.98	0.180	30.3
0.98	0.180	43.1
1.08	0.180	50.0
1.30	0.180	58.6
1.30	0.180	64.0
1.40	0.180	68.5
1.50	0.180	70.0
1.68	0.137	70.0
1.78	0.180	70.0
1.88	0.150	81.0
1.98	0.180	83.5
2.00	1.000	87.0
2.00	0.000	90.0
2.25	1.000	90.0
2.25	0.000	90.0
2.25	1.000	90.0
2.25	0.000	90.0
2.30	1.000	90.0
2.30	0.000	90.0

^aInitial substrate time.

Figure 10.11. Approximate elution volume data, 3,4-dichlorobenzoyl succinate followed by 8-oxadecol.
Peak concentrations: 99.8 mg/L (DAP), 9.7 mg/L (8-oxadecol)

Time	Sample volume	Concentration (mg/L)	
		DAP	8-oxadecol
0.010	0.000	100.0	0.0
0.04	0.000	100.0	0.0
0.07	0.000	100.0	0.0
0.10	0.000	100.0	0.0
0.24	0.000	101.0	0.0
0.37	0.000	100.0	0.0
0.49	0.100	100.0	0.0
0.51	0.100	100.0	0.0
0.77	0.200	100.0	0.0
1.04	0.300	99.0	0.0
2.07	1.000	99.0	0.0
4.05	0.000	99.0	0.0
5.34	1.000	99.0	0.0
7.05	0.000	99.0	0.0
8.34	1.000	99.0	0.0
9.34	0.000	99.0	0.0

TABLE 6(12). Sequential eluate addition data, 2,4-dichloro-
 anisophenolate followed by pyreneol.
 Feed concentrations: 50 mg/L DAP1, 101.0 mg/L
 2,4-dichloro.

Time	Sample Volume	Concentration (mg/L)	
		CBP	2,4-dichloro
0.000	0.000	100.0	40.0
0.010	0.001	107.0	70.0
0.10	0.000	100.0	82.0
0.15	0.000	100.0	87.0
0.20	0.000	100.0	90.0
0.25	0.000	100.0	92.0
0.30	0.000	100.0	94.0
0.35	0.000	100.0	96.0
0.40	0.000	100.0	97.0
0.50	0.000	100.0	97.0
0.60	0.000	100.0	98.0
0.70	0.000	100.0	98.0
1.00	0.000	98.0	100.0
1.10	0.000	97.0	100.0
1.20	0.000	97.0	100.0
1.30	0.000	96.0	100.0

TABLE 2-11. Simultaneous sulfate addition data, increased and 2,4-dichlorophenylsulfonate. Feed concentrations: 10.3 mg/L (p-sulfate), 5.8 mg/L (2,4-DCP).

Yeast (mg/L): 4-methylumbelliferyl addition salts, (arabitol) and 2,4-dihydroxy-2-methylpentane.
 Feed concentrations: 100.0 mg/L (arabitol), 10.0 mg/L (BAP)

Time	Sample volume	Concentration (mg/L)	
		arabitol	BAP
0.00	0.100	0	0
0.01	0.100	0.0	0
0.01	0.100	1.0	0
0.02	0.100	2.0	0
0.02	0.100	12.0	0
0.03	0.100	20.0	0
0.03	0.100	50.0	0
0.04	0.100	70.0	0
0.05	0.100	80.0	0.1
0.05	0.100	90.0	0.1
0.06	0.200	100.0	0.1
0.08	0.200	104.0	0.3
0.09	0.200	104.0	0.3
0.10	0.200	104.0	0.5
0.2	0.200	104.0	0.7
0.3	0.200	104.0	1.0
0.3	0.200	104.0	1.0
0.3	0.200	104.0	1.0
0.40	0.200	100.0	1.0
0.40	0.200	100.0	1.0
0.60	0.200	100.0	1.7
0.60	0.200	100.0	1.7
0.70	0.200	100.0	1.7
0.70	0.200	100.0	1.7

*Glow detection limit.

TABLE B-1a. Single-point water sampling data: 6-1994
 (all data are uncorrected for recovery,
 post correction, see 185.0 mg/L in example
 B4.0 (see 185.0))

Time	Sample volume	Concentration (mg/L)	
		6-arsenic	52P
0.11	0.100	0	0
0.22	0.100	2.0	0.0
0.33	0.100	11.4	1.0
0.44	0.100	41.0	4.0
0.55	0.100	70.5	11.2
0.66	0.100	101.8	18.0
0.74	0.100	115.5	20.0
0.85	0.100	121.0	20.0
0.95	0.100	120.5	43.5
1.00	0.210	121.0	20.0
1.07	0.210	110.0	18.5
1.73	0.210	111.0	18.5
1.87	0.210	111.0	20.0
2.04	0.300	100.0	20.5
2.34	0.315	100.0	20.0
2.12	0.345	100.0	20.0
2.13	0.315	100.0	20.0
2.28	2.015	100.0	20.5

*Below detection limit.

APPENDIX B
MULTI-ROUTE SIMULTANEOUS ADDITION DATA

TABLE 8-1. Incubation and spike addition data, 1,4-dihydroxybenzophenone, o-cresol, and allyl phenol.
 Feed concentrations: 8.4 mg/L OMP, 10.1 mg/L o-cresol, 94.2 mg/L allyl phenol

Time (hrs)	Sample volume (L)	Concentration (mg/L)		
		OMP	o-cresol	allyl phenol
0.01	0.100	*	0.1	*
0.01	0.100	*	0.3	0.4
0.03	0.100	*	0.6	1.5
0.05	0.100	0.2	1.3	4.3
0.04	0.100	0.3	3.3	9.0
0.09	0.100	0.5	5.1	13.7
0.10	0.100	0.7	6.8	23.7
0.07	0.100	0.9	8.8	34.9
0.07	0.100	0.7	9.8	38.1
1.00	0.100	1.0	11.0	48.3
1.30	0.100	1.8	15.5	59.5
1.03	0.100	2.3	19.5	73.0
1.09	0.100	1.9	22.3	84.0
2.10	0.100	1.4	21.7	89.0
3.10	1.000	4.9	10.6	90.3
3.10	0.020	8.0	10.3	90.0
3.40	2.000	7.4	10.3	90.3
3.40	0.020	6.4	10.1	91.0
7.10	2.000	8.0	10.1	90.0
7.10	0.020	8.3	10.1	90.3
8.00	2.000	9.4	10.1	90.0
8.00	0.020	8.0	10.1	90.0

*Below detection limit.

TABLE B-2... Simultaneous solvent addition data, 2,4-dihydroxyacetophenone, o-cresol, and allyl phenyl.
Feed concentrations, 5.3 mg/L (over), 100.8 mg/L (o-cresol), 5.9 mg/L (allyl phenyl)

Time	Sample volume	Concentration (mg/L)		
		2AP	o-cresol	allyl phenyl
0.10	0.100	"	"	"
0.12	0.100	"	"	"
0.20	0.100	"	0.7	"
0.40	0.100	"	4.5	"
0.50	0.100	0.2	15.5	0.1
0.60	0.100	0.2	20.0	0.2
0.70	0.100	0.2	27.0	0.4
0.80	0.100	0.2	30.0	0.8
0.90	0.100	0.2	100.0	0.8
1.00	0.100	0.2	100.5	1.0
1.10	0.200	0.4	100.5	1.0
1.20	0.200	0.4	100.5	1.0
1.30	0.200	0.4	100.5	1.0
1.40	0.200	0.4	100.5	1.0
1.50	0.200	0.4	100.5	1.0
1.60	0.200	0.4	100.5	1.0
1.70	0.200	0.4	100.5	1.0
1.80	0.200	0.4	100.5	1.0
1.90	0.200	0.4	100.5	1.0
2.00	0.200	0.4	100.5	1.0
2.10	0.200	0.4	100.5	1.0
2.20	0.200	0.4	100.5	1.0
2.30	0.200	0.4	100.5	1.0
2.40	0.200	0.4	100.5	1.0
2.50	0.200	0.4	100.5	1.0
2.60	0.200	0.4	100.5	1.0
2.70	0.200	0.4	100.5	1.0
2.80	0.200	0.4	100.5	1.0
2.90	0.200	0.4	100.5	1.0
3.00	0.200	0.4	100.5	1.0
3.10	0.200	0.4	100.5	1.0
3.20	0.200	0.4	100.5	1.0
3.30	0.200	0.4	100.5	1.0
3.40	0.200	0.4	100.5	1.0
3.50	0.200	0.4	100.5	1.0
3.60	0.200	0.4	100.5	1.0
3.70	0.200	0.4	100.5	1.0
3.80	0.200	0.4	100.5	1.0
3.90	0.200	0.4	100.5	1.0
4.00	0.200	0.4	100.5	1.0
4.10	0.200	0.4	100.5	1.0
4.20	0.200	0.4	100.5	1.0
4.30	0.200	0.4	100.5	1.0
4.40	0.200	0.4	100.5	1.0
4.50	0.200	0.4	100.5	1.0
4.60	0.200	0.4	100.5	1.0
4.70	0.200	0.4	100.5	1.0
4.80	0.200	0.4	100.5	1.0
4.90	0.200	0.4	100.5	1.0
5.00	0.200	0.4	100.5	1.0
5.10	0.200	0.4	100.5	1.0
5.20	0.200	0.4	100.5	1.0
5.30	0.200	0.4	100.5	1.0
5.40	0.200	0.4	100.5	1.0
5.50	0.200	0.4	100.5	1.0
5.60	0.200	0.4	100.5	1.0
5.70	0.200	0.4	100.5	1.0
5.80	0.200	0.4	100.5	1.0
5.90	0.200	0.4	100.5	1.0
6.00	0.200	0.4	100.5	1.0
6.10	0.200	0.4	100.5	1.0
6.20	0.200	0.4	100.5	1.0
6.30	0.200	0.4	100.5	1.0
6.40	0.200	0.4	100.5	1.0
6.50	0.200	0.4	100.5	1.0
6.60	0.200	0.4	100.5	1.0
6.70	0.200	0.4	100.5	1.0
6.80	0.200	0.4	100.5	1.0
6.90	0.200	0.4	100.5	1.0
7.00	0.200	0.4	100.5	1.0
7.10	0.200	0.4	100.5	1.0
7.20	0.200	0.4	100.5	1.0
7.30	0.200	0.4	100.5	1.0
7.40	0.200	0.4	100.5	1.0
7.50	0.200	0.4	100.5	1.0
7.60	0.200	0.4	100.5	1.0
7.70	0.200	0.4	100.5	1.0
7.80	0.200	0.4	100.5	1.0
7.90	0.200	0.4	100.5	1.0
8.00	0.200	0.4	100.5	1.0
8.10	0.200	0.4	100.5	1.0
8.20	0.200	0.4	100.5	1.0
8.30	0.200	0.4	100.5	1.0
8.40	0.200	0.4	100.5	1.0
8.50	0.200	0.4	100.5	1.0
8.60	0.200	0.4	100.5	1.0
8.70	0.200	0.4	100.5	1.0
8.80	0.200	0.4	100.5	1.0
8.90	0.200	0.4	100.5	1.0
9.00	0.200	0.4	100.5	1.0
9.10	0.200	0.4	100.5	1.0
9.20	0.200	0.4	100.5	1.0
9.30	0.200	0.4	100.5	1.0
9.40	0.200	0.4	100.5	1.0
9.50	0.200	0.4	100.5	1.0
9.60	0.200	0.4	100.5	1.0
9.70	0.200	0.4	100.5	1.0
9.80	0.200	0.4	100.5	1.0
9.90	0.200	0.4	100.5	1.0
10.00	0.200	0.4	100.5	1.0

"Below detection limit.

TABLE E-3 Benzenehexene solute addition data, 2,4-dihydroxyacetophenone, *p*-cresol, and allyl phenol
 Feed concentrations: 91.8 mg/L (BAP), 9.9 mg/L (*p*-cresol), 14.8 mg/L (allyl phenol)

Time (hr)	Sample Volume (L)	Concentrations (mg/L)		
		BAP	<i>p</i> -cresol	allyl phenol
0.10	0.100	*	*	*
0.20	0.100	*	0.1	*
0.30	0.100	0.0	0.0	0.2
0.40	0.100	0.0	1.0	0.0
0.50	0.100	0.0	1.0	1.0
0.60	0.100	10.0	0.1	0.2
0.70	0.100	21.0	7.1	0.0
0.80	0.104	29.0	0.4	0.0
0.90	0.100	40.0	0.0	0.0
1.00	0.100	47.0	10.0	0.0
1.10	0.104	50.0	11.0	0.0
1.20	0.100	70.0	11.0	10.0
1.30	0.104	80.0	11.0	11.0
1.40	0.140	83.0	11.7	11.1
1.50	1.000	85.0	10.0	10.0
1.60	0.870	86.0	10.1	10.0
1.80	0.800	88.0	10.0	10.0
2.00	0.820	87.0	9.9	10.0

*Below detection limit.

TABLE 3.- Simultaneous anion addition data. 2,4-dichlorophenylphosphonic acid, *m*-arsenol, and allyl phenol
Feed concentrations: 10.3 mg/L (DBP), 10.8 mg/L (*m*-arsenol), 9.8 mg/L (allyl phenol)

Time (hr)	Sample volume (L)	Concentration (mg/L)		
		DBP	<i>m</i> -arsenol	allyl phenol
0.20	0.250	*	*	*
0.30	0.250	*	0.3	*
0.35	0.250	*	0.3	*
1.00	0.250	*	1.1	0.1
1.35	0.250	*	0.0	0.0
1.40	0.250	0.3	0.0	0.0
1.50	0.250	0.4	5.7	1.0
1.55	0.250	0.0	0.0	1.0
2.20	0.250	0.0	10.3	3.0
2.55	0.250	0.1	11.0	3.0
3.00	0.250	0.0	10.1	4.0
3.15	0.250	0.0	10.3	0.0
3.20	0.250	0.0	10.3	4.0
3.25	0.250	2.0	10.3	7.0
4.20	0.500	3.0	10.3	0.0
4.25	0.500	3.0	10.3	0.0
4.30	0.500	3.0	10.3	0.0
4.35	0.500	4.4	11.0	0.0
4.39	0.500	4.0	11.3	0.0
5.10	0.500	0.0	11.3	0.0
5.15	0.500	0.0	11.4	0.0
5.20	0.500	0.0	11.0	0.0
5.25	0.500	0.0	11.3	0.0
5.30	0.500	0.0	11.3	0.0
5.35	0.500	0.0	11.3	0.0
5.39	0.500	0.0	11.3	0.0
5.40	0.500	0.0	11.0	0.0
5.45	0.500	0.0	10.0	0.0
7.40	1.000	7.0	10.0	0.0
7.45	0.500	7.0	10.0	0.0
8.20	1.000	0.0	10.0	0.0
8.25	0.500	0.0	10.0	0.0
10.00	2.000	0.0	10.0	0.0
10.05	0.500	0.0	10.4	0.0
12.00	2.000	0.0	10.4	0.0
12.05	0.500	0.0	10.3	0.0
14.00	2.000	10.0	10.0	0.0
14.05	0.500	10.0	10.4	0.0
24.00	2.000	10.0	10.4	0.0
24.05	0.500	10.0	10.4	0.0

*Below detection limit.

Table 1-3: Simultaneous solute addition data. 3,4-dihydroxybenzophenone, *o*-cresol, allyl phenyl, and *n*-terpinolol. Feed concentrations: 8.8 mg/L (BAP), 10.8 mg/L (*o*-cresol), 18.8 mg/L (allyl phenyl), 18.8 mg/L (*n*-terpinolol).

Time	Sample values	Concentration (mg/L)	
		BAP	<i>o</i> -cresol
0.30	0.000	0	0
0.50	0.000	0	0.3
0.80	0.000	0	0.3
1.00	0.000	0	0.8
1.30	0.000	0.1	1.8
1.60	0.000	0.3	3.3
1.90	0.000	0.5	5.8
2.20	0.000	0.8	8.4
2.40	0.000	0.1	10.3
2.60	0.000	1.7	11.3
2.80	0.000	2.8	12.3
3.00	0.000	3.8	12.8
3.30	0.000	4.7	12.8
3.60	0.000	4.4	12.8
4.00	0.000	5.0	12.3
4.30	0.000	5.4	12.3
4.60	0.000	5.8	11.8
4.90	0.000	6.4	11.3
5.30	1.000	7.0	11.4
5.60	0.000	7.0	11.8
7.00	1.000	8.0	10.3
7.30	0.000	8.4	10.3
8.20	0.000	8.8	10.3
9.20	0.000	9.3	10.3
14.01	0.000	9.5	10.8
14.01	0.000	9.7	10.2

*Before benzophenone launch.

Reagents: Spectroscopic grade addition salts, 2,4-dihydroxyacetophenone, *o*-cresol, allyl phenol, and *n*-deciphenol.
Feed concentrations: 20.0 mg/L (BAP), 181.0 mg/L (*o*-cresol), 18.0 mg/L (allyl phenol), 10.0 mg/L (*n*-deciphenol)

Time (hr)	Sample volume (L)	Concentration (mg/L)	
		BAP	<i>o</i> -cresol
0.25	0.100	0	0.4
0.25	0.100	0	4.3
0.40	0.100	0-1	14.4
0.50	0.100	0-1	18.3
0.67	0.100	0-2	44.5
0.70	0.100	0-2	90.3
0.80	0.100	0-3	102.5
0.80	0.100	0-3	114.0
1.00	0.100	0-4	110.0
1.10	0.100	0-5	113.0
1.40	0.100	0-7	110.3
1.70	0.100	1-1	119.0
1.80	0.100	1-7	115.0
2.10	0.100	2-0	111.0
2.20	1.000	4-0	110.0
2.30	0.100	4-0	111.0
0.10	1.000	0-1	102.0
0.10	0.100	0-4	101.0
1.40	1.000	0-0	100.0
1.40	0.100	10-0	100.0
0.40	1.000	10-0	101.0
0.40	0.100	10-0	100.0

*NoColor detection limit.

REFERENCES

1. Salganov, S. I. 1943. Surface Chemistry. Robert E. Krieger Publishing Company, Huntington, New York.
2. Clark, A. 1979. The Theory of Adsorption and Catalysis. Academic Press, New York.
3. Rosen, M. J. 1979. Surfactants and Interfacial Phenomena. Wiley-Interscience, New York.
4. Adamson, A. W. 1942. Physical Chemistry of Surfaces. Wiley-Interscience, New York.
5. Parrillo, G. D., and Rochester, C. B., eds. 1973. Absorption from Solutions at the Solid-Liquid Interface. Academic Press, London.
6. Grice, J., B. R., Rochester, C. B., and Smith, R. L. Eds. 1974. Absorption from Solutions. Academic Press, London.
7. Matheson, D. W. 1968. Principles of Adsorption and Desorption. Wiley-Interscience, New York.
8. Smith, R., and Corp, B. 1979. Active Carbon: Manufacture, Properties and Applications. Elsevier Publishing Company, Amsterdam.
9. Weber, M. J., Jr. 1972. Physicochemical Principles for water quality control. Wiley-Interscience, New York.
10. Hawley, J. W. 1978. Purification with Activated Carbon. Chemical Publishing Company, New York.
11. McGarry, J. J., and Kowalski, V. L. 1977. Granular Activated Carbon in water treatment. Journal American Water Works Association, 69(12):427-444 [Japan].
12. Matheson, D. W., and Buffet, L. S. 1979. Adsorption of Copper from Domestic Water Supplies. Journal American Water Works Association, 71(11):421-424 [1979:11:421].

13. Charminskoff, B.M., and Millerbach, P. Eds. 1979. Carbon Adsorption Handbook. Ann Arbor Science Publishers, Inc., Ann Arbor, Michigan.
14. Buffet, J.M. 1982. An Evaluation of Activated Carbon for Drinking Water Treatment. A National Academy of Science Report. Ground-Water Science and Technology. 18(1):44-54 (January).
15. Miller, B. 1980a. Adsorption on Carbon/ Theoretical Considerations. Environmental Science and Technology. 14(1):616-624 (July).
16. Miller, B. 1980b. Adsorption on Carbon. Balance Effects on Adsorption. Environmental Science and Technology. 14(9):1417-1421 (September).
17. Buffet, J.M., and McQuire, R.S. Eds. 1981. Activated Carbon Adsorption of Gases from the Atmosphere. Volume 1. Ann Arbor Science Publishers, Inc., Ann Arbor, Michigan.
18. Buffet, J.M., and McQuire, R.S. Eds. 1981. Activated Carbon Adsorption of Gases from the Atmosphere. Volume 2. Ann Arbor Science Publishers, Inc., Ann Arbor, Michigan.
19. Buffet, J.M., and McQuire, R.S. Eds. 1981. Treatment of Water by Granular Activated Carbon. American Chemical Society, Washington, D.C.
20. Weber, M.J., Jr., and Rao Vasth, S.M. 1980. Fundamental Concepts for Application of Activated Carbon in Water and Wastewater Treatment. In: Activated Carbon Adsorption of Gases from the Atmosphere. Volume 1. Edited by Buffet, J.M., and McQuire, R.S. Ann Arbor Science Publishers, Inc., Ann Arbor, Michigan. pp. 15-45.
21. Switzer, J.H., Ash, R.H., Muller, R.D., Weber, M.J., Jr., and Christensen, J.O. 1984. Surface Chemistry of Active Carbon: Specific Adsorption of Phenols. Journal of Colloid and Interface Science. 91(1): 154-168 (September).
22. Becke, C.J., and Fawcett, J.M. 1973. Adsorption of Organic Solutes from Aqueous Solution on Activated Carbon. Industrial Engineering and Chemistry Fundamentals. 12(4):445-451.

23. Forness, A.J., and Hutchins, R.A. 1968. Purifying Liquids with Activated Carbon. Chemical Engineering, 12:179-244 (April).
24. Hutchins, R.A. 1961. Activated Carbon. In: Activated Carbon Adsorption and Related Processes. Edited by Forness, J.A. Oak Press, Inc., Boca Raton, Florida. pp. 10-40.
25. Sahasran, S.P., Moreno-Castillo, C., and Walker, F.L., Jr. 1985. Surface-treated Activated Carbon for Removal of Phenol from Water. Separation Science and Technology, 11(11):1733-1751.
26. Paul, D.R. 1969. Carbon Adsorption of Pure Compounds and Mixtures from Solution Phase. In: Activated Carbon Adsorption of Gases from the Solution Phase. Volume 1. Edited by Seifert, J.B., and McQuinn, R.J. Oak Ridge Science Publishers, Inc., Ann Arbor, Michigan. pp. 353-378.
27. Mackin, W., and Ben-David, S. 1969. Adsorption of Non-ionic Surfactants on Activated Carbon and Mineral Clay. Water Research, 11(7):445-454.
28. Coakham, J.V., Jr. 1979. Adsorption Mechanisms: The Chemistry of Organic Adsorption on Activated Carbon. In: Carbon Adsorption Handbook. Edited by Chermantier, P.M., and Elmerich, F. Ann Arbor Science Publishers, Inc., Ann Arbor, Michigan. pp. 141-278.
29. Hill, W.A., and Noller, R.R. 1975. A New Model of Granular Activated Carbon Adsorption Kinetics. Water Research, 11(15):441.
30. Reinisch, T.M., and Garmann, R. 1973. Regeneration Modeling of Heterogeneous Systems in Continuous Columns for Wastewater Treatment. Clemson University, Clemson, South Carolina.
31. Wagner, R.J., and Jain, R.J. 1981. Activated Carbon Adsorption. In: Activated Carbon Adsorption for Wastewater Treatment. Edited by Forness, J.A. Oak Press, Inc., Boca Raton, Florida. pp. 41-82.
32. Sroogish, Y.L., and Weber, W.J., Jr. 1967. The Surface Chemistry of Active Carbon: Discussion of Structure and Surface Functional Groups. Environmental Science and Technology, 1(2):122-134 (March).

33. Coughlin, R.W., and Suen, P.S. 1968. Role of Surface Acidity in the Adsorption of Organic Pollutants on the Surface of Carbon. Environmental Science and Technology, 2:141-151-257 (April).
34. Coughlin, R.W., Suen, P.S., and Tan, S.S. 1968. Influence of Chlorinated Hydropn on Adsorption onto Carbon from Aqueous Solution. Journal of Colloid and Interface Science, 27:374-384-384 (November-December).
35. Graham, J.F., Jr. 1975. The Adsorption Chemistry of Gases on Water on Activated Carbon. Water Resources Research, 11:1011-1024-1024.
36. Mahajan, D.B., Tummel, A., and Walker, P.L., Jr. 1975. Surface-Treated Activated Carbon for Removal of Ammonia from Water. Separation Science and Technology, 12:481-487-488.
37. Schinski, C., Marti, L., and Ruiz, M. 1965. Effect of Surface Chlorination of Activated Carbon on the Adsorption of Chloroform from Aqueous Solution. In: Breakdown of Water by Spreading Activated Carbon. Edited by Modine, R.C., and Ruffin, J.R. American Chemical Society, Washington, D.C. pp. 15-20.
38. Suen, P.S. 1968. Chemical Identification of Surface Groups. In: Advances in Carcinoma and Related Subjects, Volume 15. Edited by Gray, P.W., Flann, M., and Brown, P.S. Academic Press, New York. pp. 175-185.
39. Graham, J.F. 1968. Physicochemical Concepts of Adsorption by OC WITHIN Carbon Adsorption Beds. In: Activated Carbon Adsorption of Gases from the Air. Edited by Ruffin, J.R., and Modine, R.C. Ann Arbor Science Publishers, Inc., Ann Arbor, Michigan. pp. 375-384.
40. Coughlin, R.W., and Tan, S.S. 1968. Role of Functional Groups in Adsorption of Organic Pollutants on Carbon. Chemical Characterized Polymers Symposium Series, 11:205-214.
41. Graham, J.F. 1975. Characterization of Physical Adsorption Systems. II. The Separate Effects of Bulk Size and Surface Acidity upon the Adsorbent Capacities of Activated Carbons. Journal of Physical Chemistry, 79:288-292.
42. Szymanski, J.S., and Hunt, P.S. 1976. Operational Parameters for Optimum Removal of Phenolic Compounds

From Polished Metals by Columns of Activated Carbon, In: Carbon Adsorption Handbook, Edited by CHARNOZHUKOFF, P.M., and KILGUSSEN, P. Also ARNOLD SOLEMAN PUBLISHERS, Inc., Ann Arbor, Michigan, pp. 257-277

43. LUTTMAN, R.B., GORE, J.B., and GUNNELL, R.G. 1974. Film Transport Coefficient in Aqueous Suspensions of Activated Carbon. Journal Water Pollution Control Federation, 48(11):2516-2518
44. ZIMMICH, F.R., and MEYER, R.J., Jr. 1969. A Predictive Model for the Design of Fixed-Bed Adsorbers. Journal Water Pollution Control Federation, 42(4):761-766.
45. SHARPLES, E.L., and BUCKMAN, R.B. 1987. Kinetics of Adsorption by Activated Carbons From Aqueous Organic Solutions. Chemical Engineering Progress Symposium Series, 62(70):48-58.
46. HARTON, R.D., and AL-MURSHIDI, R.B. 1979. Adsorption Studies Using Gas-Liquid Chromatography--CIS- Experimental Factors Influencing Adsorption. Water Research, 13:879-889.
47. SANDERS, S.J., and SANCYANSKY, V.L. 1943. Evaluating GAC Adsorptive Capacity. Journal American Water Works Association, 35(4):444-448.
48. HARTON, S.J. 1966. Activated Carbon Product Selection for Water and Wastewater Treatment. Industrial Engineering and Chemistry Analysis Research and Development, 12(7):437-441.
49. SANCYANSKY, V.L., MEYER, R.J., Jr., and KURT, R.B. 1947. Sorption of Phenol and Naphthol by Activated Carbon. Environmental Science and Technology, 21(6):618-626.
50. MCCREARY, J.M., and SANCYANSKY, V.L. 1965. Characterization and Activated Carbon Adsorption of Several Foreign Substances. Water Research, 1:131-148
51. MEYER, R.J., Jr., and HARTON, S.J. 1968. Adsorption in Heterogeneous Systems. Journal American Water Works Association, 60(4):449-457.
52. MEYER, R.J., Jr., and HARTON, S.J. 1966. Equilibria and Capacities for Adsorption on Carbon. Journal of the National Research Council, American Society of Civil Engineers, 57(16):1171-1177

37. Sidelis, L.D., and Sweeney, H.J. 1983. Evaluation of Activated Carbon by the Dynamic Monolayer Adsorption Technique. In: Treatment of Water by Granular Activated Carbon. Edited by McQuirk, H.J., and Suffet, I.B. American Chemical Society, Washington, D.C. pp. 213-249.
38. Weber, H.J., Jr., Velox, P.C., and Jendryas, A. 1983. Adsorption of Toxic Substances: The Effects of Heterogeneity and Spatial Characterization. Journal American Water Works Association. 23:121-125-128.
39. Smith, J.R. Ed. 1981. Activated Carbon Adsorption for Wastewater Treatment. Oak Press, Inc., New Britain, Florida. pp. 12-14.
40. McQuirk, A. 1979. Activated Carbon: Evaluation and Application. Weyss Data Corporation, Park Ridge, New Jersey.
41. Glaser, G.M., Conway, R.A., and Brown, C.T. 1979. Activated Carbon Adsorption of Phenanthrenes. Journal Water Pollution Control Federation. 48:943-949.
42. Al-Bahrani, H.S., and Martin, R.J. 1979. Adsorption Studies Using Gas-Liquid Chromatography--I. Effect of Molecular Structure. Water Research. 13:723-729.
43. Rogers, P.C., and Yen, C.T. 1979. Adsorption of Alkyl Phenols by Activated Carbon. In: Activated Carbon Adsorption of Organic from the Aqueous Phase, Volume 1. Edited by Suffet, I.B., and McQuirk, H.J. Ann Arbor Science Publishers, Inc., Ann Arbor, Michigan. pp. 187-195.
44. Martin, R.J., and Al-Bahrani, H.S. 1977. Adsorption Studies Using Gas-Liquid Chromatography--II. Competitive Adsorption. Water Research. 11:704-709.
45. McDale, R.A., and Sweeney, H.J. 1979. Adsorption of Soluble Aromatic Hydrocarbons on Granular Activated Carbon. Water Research. 13:191-199.
46. McQuirk, H.J., and Suffet, I.B. 1982. The Calculated Net Adsorption Energy Concept. In: Activated Carbon Adsorption of Organic from the Aqueous Phase, Volume 1. Edited by Suffet, I.B., and McQuirk, H.J. Ann Arbor Science Publishers, Inc., Ann Arbor, Michigan. pp. 31-43.
47. McQuirk, H.J., Suffet, I.B., and Bedard, J.V. 1979. Assessment of Data Procedures for the Removal of Trace

organic compounds from distilled water. Journal American Water Works Association, 78(11):545-552.

64. Mann, H. 1980. The Polymers Adsorption Potential Theory and Its Applications to Adsorption from Water Solutions onto Activated Carbons. In: Activated Carbon Adsorption of Organic from the Aqueous Phase, Volume 1. Edited by Ballal, I.R., and Kozicki, R.J. ACS Arbor Science Publishers, Inc., Ann Arbor, Michigan. pp. 43-54.
65. Krickla, R.J., and Kozicki, R.J. 1982. Prediction of the Preferentially Adsorbed Compound in Simplex Column Systems. American Institute of Chemical Engineers Preprint Series, 28, 17-21.
66. Su, C., and Rieger, F.C. 1984. Competitive Adsorption of Phenols on Activated Carbon. Journal of Environmental Engineering, 110(5):976-985.
67. Weston, R.D., and El-Hadrami, S.S. 1979. Adsorption Studies Using Gas-Liquid Chromatography. In: Adsorption from Aqueous Systems. Water Research, 13(12):1381-1391.
68. Isayaka, S.S., and Focht, S.O. 1974. The Effect of Phosphate Buffer on the Adsorption of 2,4-dichlorophenol and 2,4-dinitrophenol. Journal of Environmental Science and Health, 11(11):717-721-718.
69. McCreary, J.D., and Isayaka, S.L. 1980. Chelationism and Activated Carbon Adsorption of Several Metal Substances. Water Research, 15:181-189.
70. Oguma, F.A., and Weber, W.S., Jr. 1979. Sorption Kinetics in Solids Batch Experiments. Journal Water Pollution Control Federation, 52(4):752-755.
71. Hantke, S.J., and Jansen, C.P. 1982. Effects of Salts on Activated Carbon Adsorption of Polymers and Organic Acids. Journal American Water Works Association, 72(1):84-89.
72. Gelman, P.P., and Ward, T.R. 1948. A Model for the Adsorption of Weak Electrolytes on Solids as a Function of pH. Journal of Colloid and Interface Science, 2(4):447-452.
73. Kozicki, R.J., and Weber, W.S., Jr. 1983. Kinetics of the Hydrated Proton with Active Carbon. In: Advances in Chemistry Series, 79. Edited by Gould, I.F. American Chemical Society Publications, Washington, D.C. pp. 113-134.

73. Kozin, C.J., and Secorink, V.L. 1979. Competitive Adsorption of 2,6-Dichlorophenol and 2,4,6-Trichlorophenol to the Humiclike or Humiclike Colloidlike Ions. Environmental Science and Technology, 13(11):1017-1021.
74. Jain, J.B., and Secorink, V.L. 1979. Adsorption from Aqueous Systems at Active Carbon. Carbon 17(1): 101-112.
75. Sauer, J.C., and Seidman, C.W. 1976. Competitive Adsorption of Organic Materials by Activated Carbon. Proceedings of the 11th Carbon Chemistry International Conference, Edited by Wall, J. Ann Arbor Science Publishers, Inc., Ann Arbor, Michigan. pp. 127-131.
76. Tsai, W., and Sekimender, E.B. 1974. Simultaneous Adsorption Equilibria of Organic Solutes in Dilute Aqueous Solution on Activated Carbon. Chemical Engineering Science, 22:1277-1292.
77. Kozin, C.J., and Freeman, J.B. 1973. Thermodynamics of Multi-Solute Adsorption from Dilute Liquid Solutions. Research Institute of Chemical Engineering Journal, 11(4):363-369.
78. Weber, M.J., Jr., and Pirbarns, W. 1973. Removal of Carbon Trichloride from Water by Activated Carbon. In: Treatment of Water by Granular Activated Carbon. Edited by McCallum, W.J., and Suffet, I.B., Advances in Chemistry Series No. 102. American Chemical Society, Washington, D.C. pp. 123-144.
79. Gidde, A.A. 1982. Multicomponent Adsorption Column Parameter Studies. In: Activated Carbon Adsorption of Organic from the Aqueous Phase, Volume 1. Edited by Suffet, I.B., and Weber, M.J. Ann Arbor Science Publishers, Inc., Ann Arbor, Michigan. pp. 251-273.
80. Frick, E.B., and Sekimender, W. 1983. Adsorption Equilibria in Multisolute Mixtures of Known and Unknown Composition. In: Treatment of Water by Granular Activated Carbon. Edited by McCallum, W.J., and Suffet, I.B., Advances in Chemistry Series No. 203. American Chemical Society, Washington, D.C. pp. 247-249.
81. Joensuu, L., Freeman, J.B., Frick, E., Sekimender, E.B., and Myers, A.L. 1978. Thermodynamics of Multi-Solute Adsorption from Dilute Aqueous Solutions. Chemical Engineering Science, 33:1077-1090.

88. Soper, H.J., Jr., Veith, F.C., Parkhurst, R., Root, C.E., and Glasoff, D.R. 1961. Sorption of Hydrophobic Compounds by Sediments, Soils and Suspended Solids--II. Sorption Evaluation Studies. Water Research, 17(12):1427-1452.
89. Soderstedt, E.T. 1977. Physical-Chemical Removal of Dissolved Materials. In: Water and Environmental Treatment. McGraw-Hill Book Company, New York. pp. 52-71.
90. Stiller, R. 1966. Adsorption on Carbon: Theoretical Considerations. Environmental Science and Technology, 1(4):316-324.
91. Sumrell, L.D., Fulkner, J.P., and Wood, B.L. 1969. Process Chemistry for Water and Wastewater Treatment. Prentice-Hall Publishing, Inc., New York. pp. 772-784.
92. Tritz, W., and Schindler, A.G. 1960. Comparative Adsorption of Two Dissolved Organic onto Activated Carbon--I: Adsorption Equilibria. Canadian Chemical Science, 16:721-724.
93. Myers, A.L., and Freeman, J.R. 1962. Thermodynamics of Mixed-Gas Adsorption. American Institute of Chemical Engineering Journal, 10(1) 121-129.
94. Stumm, G., and Belfort, G. 1965. Selective Adsorption of Organic Molecules onto Activated Carbon from Dilute Aqueous Solutions. In: Equilibrium of Water on Synthetic Activated Carbon. Edited by Rodiere, H.J., and Belfort, G. Advanced in Chemistry Series No. 182. American Chemical Society, Washington, D.C. pp. 18-61.
95. Weber, P. 1966. Adsorption on Carbon: Solvent Effects on Adsorption. Environmental Science and Technology, 1(9):1817-1819.
96. Aronow, W.B. 1962. Adsorption Equilibria: Adsorption of Organic Compounds on Activated Carbon from Aqueous Solutions. Environmental Science and Technology, 1(7) 521-528.
97. Myers, W., and Weber, J.-D.E. 1969. Application of the Freundlich Adsorption Potential Theory to Adsorption from Solution on Activated Carbon. Journal of Physical Chemistry, 73(1):214-216.
98. Myers, W., and Greenberg, R. 1963. Adsorption of Multicomponent Liquids from Water onto Activated

Carbon: Comparison Selection Methods for Treatment of Water by Granular Activated Carbon. Edited by McQuire, R.J., and Saffert, L.R. American Chemical Society, Washington, D.C. p. 1-27

94. Voloshin, G.A., and Sauer, B. 1979. Application of the Solange Adsorption Potential Theory to Adsorption from Solution on Activated Carbon. II. Adsorption of Partially Miscible Organic Liquids from Water from Solvents. Journal of Physical Chemistry. 83(1):39-44.
95. Sauer, B.J., Jr. 1980. Micromedion I: Adsorption Models for Activated Carbon Adsorption of Gases from the Applied Phase, Volume 1. Edited by Sauer, B.J., and McQuire, R.J. Ann Arbor Science Publishers, Inc., Ann Arbor, Michigan. pp. 217-229.
96. Christensen, J.D., and Sauer, B.J., Jr. 1979. Model for Design of Multi-Component Adsorption Systems. Journal of the Environmental Engineering Division, American Society of Civil Engineers. 103(1987): 1179-1178.
97. Saffert, L. 1979. Selective Adsorption of Organic Homologues onto Activated Carbon from Binary Aqueous Solutions. Adsorption Potential Approach and Correlations of Solar Adsorptivity with Physicochemical Parameters. Environmental Science and Technology. 13(10):819-828.
98. Myers, A.L., and Freeman, J.M. 1943. Thermodynamics of Vapor-Gas Adsorption. American Institute of Chemical Engineers Journal. 35(1):121-128.
99. Geyman, F.A., Gidycz, G., Frank, R., and Smolenski, R. 1979. A Simplified Competitive Equilibrium Adsorption Model. Chemical Engineering Science. 32(12):1847-1873.
100. Kilham, A.J., and Myers, A.L. 1966. A Simplified Method for the Prediction of Multicomponent Adsorption Equilibria from Single Gas Isotherms. American Institute of Chemical Engineering Journal. 18(3): 581-586.
101. Fennell, J., Mueller, J.A., and Penick, A.B. 1980. Prediction of Carbon Values Performance from Four Solvent Data. Journal Water Pollution Control Federation. 52(7):2029-2033.
102. Tien, C. 1982. Recent Advances in the Calculation of Multicomponent Adsorption in Fixed Beds. In.

Treatment of Water by Granular Activated Carbon
 Edited by Melnick, R.J., and Saffar, I.R. American
 Chemical Society, Washington, D.C. pp. 147-195.

103. Eklund, P.A., Saldorf, G., Frick, R., and Bartholomew, R. 1980. Simplifying the Description of Competitive Adsorption for Practical Applications in Water Treatment. In: Activated Carbon Adsorption of Pollutants from the Aquatic Phase, Volume 1. Edited by Saffar, I.R., and Melnick, R.J. Ann Arbor Science Publishers, Inc., Ann Arbor, Michigan pp. 221-234.
104. Toppa, S.R. 1982. The Effects of Unequal Competition and Irreversible Adsorption on Multi-Component Adsorption Equilibria. Ph.D. Dissertation, Clemson University, Clemson, South Carolina.
105. Carl, R.L., and Kinsman, G.A. 1980. Explicit-Adsorbate Model for apparent Analogies with Organic Adsorption in Natural Adsorbents. Environmental Science and Technology, 14(12):924-927.
106. Toppa, S.R., Kinsman, G.A., Fomander, E., and Jang, J.P. 1983. Single-Phase Irreversible Adsorption on Granular Activated Carbon. Environmental Science and Technology, 17(10):619-621.
107. Melnick, R.J. Jr., McCreary, J.D., Spangler, R.W., Rhee, J.L., Jackson, J.A.G., Woodall, R.M., and Spangas, G.M. 1982. Trace Metals and Phenolic Greenhouse in the Upper Suwannee Creek Region. A Report to the Okech Corporation Foundation, Inc. Department of Environmental Engineering Sciences, University of Florida, Gainesville.
108. Kinsman, G. 1984. Solubility of Organic Mixtures in Water. Environmental Science and Technology, 18(7): 147-151.
109. Carl, R.L., and Kinsman, G. 1982. Attainment of Equilibrium in Activated Carbon Batchwise Studies. Environmental Science and Technology, 16(1):44-47.
110. Goryunova, A., Kuznetsov, A., and Sokolowski, S. 1973. Gel Permeation Chromatography Using Porous Glass. Investigations of the Influence of Eluent on Retention and Adsorption. Separation Science, 16(4):275-288.

BIOGRAPHICAL SKETCH

The author was born on December 14, 1918, in Richmond, Virginia. He received a Bachelor of Science Degree in June, 1941, from the Department of Chemical Engineering at the Massachusetts Institute of Technology, Cambridge, Massachusetts. He completed the Master of Science in Engineering Degree in sanitary engineering in May, 1943, at West Virginia University, Morgantown, West Virginia. He was commissioned a Second Lieutenant in the United States Army Medical Service Corps in August, 1943, with a sanitary occupational specialty of sanitary engineer. He served tours of duty in Maryland, West Germany, and Spain prior to beginning studies at the University of Florida in August, 1948. He currently holds the rank of major. He is married to the former Anna Evelyn Collins. Upon degree completion he will commence a three-year tour of duty with the United States Army Pacific Environmental Health and Engineering Agency in Tokyo, Japan.

I certify that I have read this study and that in my opinion it conforms to acceptable standards of scholarly presentation and is fully adequate, in scope and quality, as a dissertation for the degree of Doctor of Philosophy.


John E. H. H. H.
Professor of Environmental
Engineering Sciences

I certify that I have read this study and that in my opinion it conforms to acceptable standards of scholarly presentation and is fully adequate, in scope and quality, as a dissertation for the degree of Doctor of Philosophy.


John E. H. H. H.
Professor of Environmental
Engineering Sciences

I certify that I have read this study and that in my opinion it conforms to acceptable standards of scholarly presentation and is fully adequate, in scope and quality, as a dissertation for the degree of Doctor of Philosophy.


W. R. H. H. H.
Professor of Environmental
Engineering Sciences

I certify that I have read this study and that in my opinion it conforms to acceptable standards of scholarly presentation and is fully adequate, in scope and quality, as a dissertation for the degree of Doctor of Philosophy.


Kenneth O. Cook
Professor of Chemical
Engineering

I certify that I have read this study and that in my opinion it conforms to acceptable standards of scholarly presentation and is fully adequate, in scope and quality, as a dissertation for the degree of Doctor of Philosophy.


Benjamin L. Ingman
Associate Professor of
Environmental Engineering
Engineering

This dissertation was submitted to the Graduate Faculty of the College of Engineering and to the Graduate School and was accepted as partial fulfillment of the requirements for the degree of Doctor of Philosophy.

December 1988


Herb. College of Engineering

Dean, Graduate School